US Army Corps of Engineers

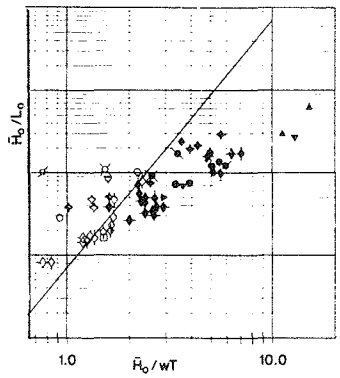

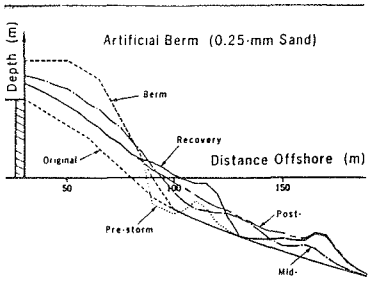

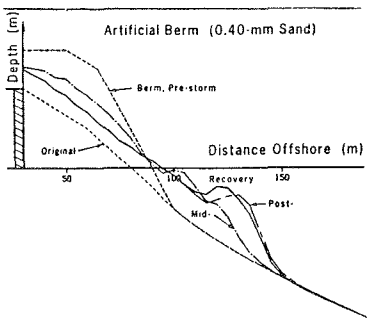

COASTAL ENGINEERING RESEARCH CENTER

TECHNICAL REPORT CERC-89-9

SBEACH: NUMERICAL MODEL FOR SIMULATING STORM-INDUCED BEACH CHANGE

Report 1
EMPIRICAL FOUNDATION AND MODEL DEVELOPMENT

by

Magnus Larson

Department of Water Resources Engineering
Institute of Science and Technology
University of Lund
Box 118, Lund, Sweden S-221 00

and

Nicholas C. Kraus

DEPARTMENT OF THE ARMY
Coastal Engineering Research Center
Waterways Experiment Station, Corps of Engineers
PO Box 631, Vicksburg, Mississippi 39181-0631

July 1989

Report 1 of a Series

Approved For Public Release; Distribution Unlimited

Prepared for DEPARTMENT OF THE ARMY
US Army Corps of Engineers
Washington, DC 20314-1000

Under Surf Zone Sediment Transport Processes
Work Unit 34321

Destroy this report when no longer needed. Do not return it to the originator.

The findings in this report are not to be construed as an official Department of the Army position unless so designated by other authorized documents.

This program is furnished by the Government and is accepted and used by the recipient with the express understanding that the United States Government makes no warranties, expressed or implied, concerning the accuracy, completeness, reliability, usability, or suitability for any particular purpose of the information and data contained in this program or furnished in connection therewith, and the United States shall be under no liability whatsoever to any person by reason of any use made thereof. The program belongs to the Government. Therefore, the recipient further agrees not to assert any proprietary rights therein or to represent this program to anyone as other than a Government program.

The contents of this report are not to be used for advertising, publication, or promotional purposes. Citation of trade names does not constitute an official endorsement or approval of the use of such commercial products.

SECURITY CLASSIFICATION OF THIS PAGE

REPORT DOCUMENTATION PAGE

Form Approved OMB No. 0704-0188

1a. REPORT SECURITY CLASSIFICATION: Unclassified	1b. RESTRICTIVE MARKINGS
2a. SECURITY CLASSIFICATION AUTHORITY	3. DISTRIBUTION/AVAILABILITY OF REPORT: Approved for public release; distribution unlimited.
2b. DECLASSIFICATION/DOWNGRADING SCHEDULE	
4. PERFORMING ORGANIZATION REPORT NUMBER(S): Technical Report CERC-89-9	5. MONITORING ORGANIZATION REPORT NUMBER(S)
6a. NAME OF PERFORMING ORGANIZATION: USAEWES, Coastal Engineering Research Center; 6b. OFFICE SYMBOL (If applicable)	7a. NAME OF MONITORING ORGANIZATION
6c. ADDRESS (City, State, and ZIP Code): 3909 Halls Ferry Road, Vicksburg, MS 39180-6199	7b. ADDRESS (City, State, and ZIP Code)
8a. NAME OF FUNDING/SPONSORING ORGANIZATION: US Army Corps of Engineers; 8b. OFFICE SYMBOL (If applicable)	9. PROCUREMENT INSTRUMENT IDENTIFICATION NUMBER
8c. ADDRESS (City, State, and ZIP Code): Washington, DC 20314-1000	10. SOURCE OF FUNDING NUMBERS: PROGRAM ELEMENT NO. / PROJECT NO. / TASK NO. / WORK UNIT ACCESSION NO. 34321

11. TITLE (Include Security Classification)
SBEACH: Numerical Model for Simulating Storm-Induced Beach Change; Report 1: Empirical Foundation and Model Development

12. PERSONAL AUTHOR(S)
Larson, Magnus; Kraus, Nicholas C.

13a. TYPE OF REPORT	13b. TIME COVERED	14. DATE OF REPORT (Year, Month, Day)	15. PAGE COUNT
Report 1 of a series	FROM Aug 86 TO Mar 89	July 1989	267

16. SUPPLEMENTARY NOTATION
Available from National Technical Information Service, 5285 Port Royal Road, Springfield, VA 22161.

17. COSATI CODES		
FIELD	GROUP	SUB-GROUP

18. SUBJECT TERMS (Continue on reverse if necessary and identify by block number)

Accretion	Cross-shore sand transport	Longshore bars
Beach erosion	Dune erosion	Numerical models
Berms	Erosion	Storm erosion

19. ABSTRACT (Continue on reverse if necessary and identify by block number)

A two-dimensional numerical model is presented for calculating dune and beach erosion produced by storm waves and water levels. The model is empirically based and was first developed from a large data set of net cross-shore sand transport rates and geomorphic change observed in large wave tanks, then verified using high-quality field data. The model is aimed to reproduce macroscale features of the beach profile, with focus on the formation and movement of longshore bars. The ultimate goal of the modeling effort is prediction of storm-induced beach erosion and post-storm recovery. Bars are simulated satisfactorily, but berm processes are less well reproduced, due in part to a lack of data for defining accretionary wave and profile processes. A new criterion is developed for predicting erosion and accretion, and the model uses this criterion to calculate net sand transport rates in four regions of the nearshore extending from deep water to the limit of wave runup. Wave height and setup across the profile are calculated to obtain the net cross-shore sand

(Continued)

20. DISTRIBUTION/AVAILABILITY OF ABSTRACT: ☒ UNCLASSIFIED/UNLIMITED ☐ SAME AS RPT. ☐ DTIC USERS	21. ABSTRACT SECURITY CLASSIFICATION: Unclassified
22a. NAME OF RESPONSIBLE INDIVIDUAL	22b. TELEPHONE (Include Area Code) / 22c. OFFICE SYMBOL

DD Form 1473, JUN 86 *Previous editions are obsolete.* SECURITY CLASSIFICATION OF THIS PAGE Unclassified

19. ABSTRACT (Continued).

transport rate. The model is driven by engineering data, with main inputs of time series of wave height and period in deep water, time series of water level, median beach grain size, and initial profile shape. Comprehensive sensitivity testing is performed, and example applications are made to evaluate the response of the profile to the presence of a vertical seawall and the behavior of different beach fill cross sections in adjustment to normal and storm wave action.

PREFACE

This study was conducted at the Coastal Engineering Research Center (CERC), US Army Engineer Waterways Experiment Station (WES), and the Department of Water Resources Engineering (DWRE), Institute of Science and Technology, University of Lund (UL), Lund, Sweden. The work described herein was authorized as a part of the Civil Works Research and Development Program by the US Army Corps of Engineers (USACE) and was performed under the Surf Zone Sediment Transport Processes Work Unit 34321 which is in the Shore Protection and Restoration Program, CERC. Messrs. John H. Lockhart, Jr., James E. Crews, Charles W. Hummer, and John G. Housley are USACE Technical Monitors. Dr. Charles L. Vincent is Program Manager for the Shore Protection and Restoration Program at CERC.

This study was performed and the report prepared over the period 1 August 1986 through 30 March 1989 by Dr. Magnus Larson, Assistant Professor, DWRE, and Dr. Nicholas C. Kraus, Senior Scientist, Research Division (CR), CERC. The content of this report is substantially the same as the thesis submitted to UL by Dr. Larson in partial fulfillment of the requirements for a Ph.D. degree in civil engineering. Dr. Kraus was a thesis committee member. The report updates and extends some material in the thesis.

Work at UL was performed under the general supervision of Dr. Gunnar Lindh, Head, DWRE, and was partially funded by Work Unit 34321 through the US Army Research, Development, and Standardization Group, UK, under contract No. DAJA-86-C-0046. Dr. Larson was in residence at CERC over the period 15 July 1986 through 30 August 1987. Work performed at CERC was under general administrative supervision of Dr. James R. Houston, Chief, CERC; Mr. Charles C. Calhoun, Jr., Assistant Chief, CERC; and Mr. H. Lee Butler, Chief, CR, CERC.

Dr. Kraus was the Principal Investigator of Work Unit 34321 during the technical phase of the study. Ms. Kathryn J. Gingerich, Coastal Processes Branch (CR-P), CERC, was Principal Investigator during the publication phase of the report and provided review and technical editing. Ms. Carolyn J. Dickson (CR-P) assisted in formatting and preparation of the final manuscript. Mr. Bruce A. Ebersole was Chief, CR-P. This report was edited by Ms. Shirley

A. J. Hanshaw, Information Products Division, Information Technology Laboratory, WES.

COL Dwayne G. Lee, CE, was Commander and Director of WES during the research and report preparation phases of this study. COL Larry B. Fulton was Commander and Director upon publication. Dr. Robert W. Whalin was Technical Director.

CONTENTS

	Page
PREFACE	1
CONTENTS	3
LIST OF TABLES	5
LIST OF FIGURES	6
PART I: INTRODUCTION	9
Problem Statement and Objectives	9
Procedure Used	11
Basic Terminology	13
Organization of This Report	16
PART II: LITERATURE REVIEW	18
Chronological Survey of Literature	18
Synthesis of Previous Work	40
PART III: DATA EMPLOYED IN THIS STUDY	44
Data Acquisition Approaches	44
Laboratory and Field Data Sets	46
PART IV: QUANTIFICATION OF MORPHOLOGIC FEATURES	55
Data Analysis Procedure	56
Concept of Equilibrium Beach Profile	59
Criteria for Distinguishing Profile Response	62
Form and Movement of Bars	77
Form and Movement of Berms	106
Summary	114
PART V: CROSS-SHORE TRANSPORT RATE	117
General Features of Cross-Shore Transport	119
Classification of Transport Rate Distributions	122
Approach to Equilibrium	129
Magnitude of Net Cross-Shore Transport Rate	136
Transport Regions	137
Summary	153
PART VI: NUMERICAL MODEL OF BEACH PROFILE CHANGE	155
Methodology	156
Wave Model	158
Transport Rate Equations	166
Profile Change Model	173

Calibration and Verification 175
Summary 181

PART VII: APPLICATIONS OF THE NUMERICAL MODEL 183

Sensitivity Analysis of Model Parameters 183
Effect of Time-Varying Water Level and Waves 193
Multiple Barred Profiles 199
Simulation of Field Profile Change 204
Comparison with the Kriebel Model 215
Simulation of Beach Profile Accretion 218
Influence of a Seawall and Beach Fill 223

PART VIII: SUMMARY AND CONCLUSIONS 231

REFERENCES 238

APPENDIX A: CORRELATION AND REGRESSION ANALYSIS A1

APPENDIX B: NOTATION B1

LIST OF TABLES

No.		Page
1	CE Experiments: Wave Height, Wave Period, and Water Depth in the Horizontal Section of the Tank and Deepwater Wave Steepness	51
2	CRIEPI Experiments: Wave Height, Wave Period, and Water Depth in the Horizontal Section of the Tank, Initial Beach Slope, and Deepwater Wave Steepness	52
3	Criteria for Classifying Bar and Berm Profiles Erosion and Accretion	63
4	CE Experiments: Values of Selected Quantities	115
5	CRIEPI Experiments: Values of Selected Quantities	116

LIST OF FIGURES

No.		Page
1	Definition sketch of the beach profile	14
2	Tank for Large Waves at Dalecarlia Reservation	48
3	View of the wave generator in the LWT	49
4	Notation sketch for beach profile morphology	58
5	Absolute sum of profile change for selected cases	61
6	Criterion for distinguishing profile type by use of wave steepness and dimensionless fall speed parameter	67
7	Criterion for distinguishing profile type by use of wave steepness and ratio of wave height to grain size	68
8	Criterion for distinguishing profile type by use of wave steepness and Dean parameter	68
9	Criterion for distinguishing profile type by use of ratio of breaking wave height and grain size, and Ursell number at breaking	70
10	Classification of erosion and accretion events in the field using deepwater wave steepness and dimensionless fall speed, with wave height taken as mean wave height	74
11	Criterion for distinguishing shoreline retreat and advance by use of wave steepness, dimensionless fall speed, and initial beach slope	76
12	Criteria for distinguishing profile type applied to small-scale laboratory data	78
13	Growth and movement of breakpoint bar with elapsed time and location of break point	80
14	Profile measured after 4.2 hr together with the initial profile and wave height distribution	81
15	Growth of bar volume with elapsed time	83
16	Measured equilibrium bar volume V_m and empirical prediction V_p	85
17	Evolution of depth-to-bar crest	87
18	Depth-to-bar crest h_c versus breaking wave height H_b	88
19	Ratio of depth-to-trough bottom and depth-to-bar crest h_t/h_c as a function of wave period	90
20	Evolution of maximum bar height	91
21	Comparison of measured equilibrium bar height $(Z_B)_m$ and empirical prediction $(Z_B)_p$	93
22	Horizontal movement of bar center of mass	95
23	Speed of bar movement with elapsed time	97
24	Comparison of measured and predicted nondimensional horizontal distance between break point and trough bottom	101
25	Evolution of shoreward slope of main breakpoint bars	102
26	Evolution of seaward slopes of main breakpoint bars	104
27	Evolution of representative step and terrace slopes	106
28	Relation between berm center of mass and wave runup	108
29	Growth of berm volume with elapsed time	110
30	Growth of maximum berm height with elapsed time	112
31	Growth of representative berm slopes with elapsed time	113
32	Evolution of beach profile under constant incident wave conditions for an erosional case (Case 300)	121

33 Calculated distributions of the net cross-shore sand transport rate for an erosional case (Case 300) 122
34 Evolution of beach profile under constant incident waves for an accretionary case (Case 101) 123
35 Calculated distributions of net cross-shore sand transport rate for an accretionary case (Case 101) 124
36 Net cross-shore sand transport rate distributions 126
37 Evolution of beach profile under constant incident wave conditions for a mixed accretionary and erosional case (Case 3-2) 128
38 Decay of net cross-shore sand transport rate 131
39 Evolution of peak offshore net sand transport rate for 16 CE cases 132
40 Decay of peak offshore sand transport rate and a best-fit empirical predictive expression 134
41 Evolution of peak onshore net sand transport rate for 16 CE cases 135
42 Decay of peak onshore sand transport rate and a best-fit empirical predictive equation 136
43 Definition sketch for four principal zones of cross-shore sand transport 138
44 Spatial decay rate coefficient seaward of the break point 141
45 Comparison of net offshore sand transport rates seaward of the break point and an empirical expression 141
46 Comparison of spatial decay rate coefficients and an empirical predictive expression 143
47 Comparison of net onshore sand transport rates seaward of the break point and an empirical predictive equation 144
48 Net cross-shore sand transport rate distributions between break point and plunge point 147
49 Net cross-shore sand transport rate versus calculated wave energy dissipation per unit volume in broken wave region 149
50 Time behavior of net cross-shore sand transport rate distribution on the foreshore 153
51 Distribution of breaker ratio for the CRIEPI data 160
52 Distribution of breaker ratio for small-scale laboratory data . . . 160
53 Comparison between measured and predicted breaker ratio 162
54 Ratio between breaking and deepwater wave height as a function of deepwater wave steepness 162
55 Measured and calculated wave heights 164
56 Definition sketch for describing avalanching 172
57 Calibration of numerical model 179
58 Net cross-shore transport rates at selected times 179
59 Optimization for model calibration 180
60 Verification of numerical model 182
61 Effect of K on bar volume 185
62 Effect of K on maximum bar height 185
63 Effect of ϵ on bar volume 186
64 Effect of κ on bar volume 187
65 Effect of Γ on bar volume 189
66 Effect of D on bar volume 190
67 Effect of D on bar center of mass 191

68 Effect of T on bar volume 192
69 Effect of runup height on bar volume 193
70 Verification for case of varying water level 194
71 Simulation with varying wave period 196
72 Simulation with varying water level 196
73 Effect of varying wave height 198
74 Transport rate distributions for varying wave height 198
75 Simulation with varying water level and wave height 199
76 Reproduction of the second breakpoint bar 202
77 Distribution of grain size across profile line 188 205
78 Field calibration, event 840403-840406 210
79 Field verification, event 821207-821215 211
80 Field verification omitting water level variation 213
81 Field verification with fixed wave height, wave period, and water level 213
82 Comparison of present model and Kriebel model for a surge case 217
83 Comparison of present model and Kriebel model for a step increase in water level 219
84 Simulation of berm formation and growth 222
85 Simulation with and without seawall 224
86 Wave height and water level for beach fill simulations 225
87 Response of original beach to the storm event 227
88 Response of artificial berm to the storm event 228
89 Response of the Bruun fill to the storm event 230

SBEACH: NUMERICAL MODEL FOR SIMULATING STORM-INDUCED BEACH CHANGE

EMPIRICAL FOUNDATION AND MODEL DEVELOPMENT

PART I: INTRODUCTION

Problem Statement and Objectives

1. The study of beach profile change in the broad sense encompasses nearshore processes that shape the beach on all spatial and temporal scales. Beach profile change is a phenomenon of fundamental interest and, as such, has been studied by geologists, oceanographers, and coastal engineers.

2. In coastal engineering, quantitative understanding of beach profile change is pursued mainly to allow prediction of beach evolution in the vicinity of planned or existing engineering projects. Two types of coastal engineering problems of particular importance for which predictive tools are needed are beach and dune erosion that occurs under storm waves and high water levels and adjustment of beach fill to long-term wave action. The time scale associated with storm-induced beach erosion is on the order of 1 to 3 days and depends on the level and duration of the storm surge as well as the wave characteristics, whereas the time scale of beach fill adjustment is several weeks to several months and depends on season of placement, fill material, and wave climate at the coast.

3. It is often convenient to separate nearshore sediment movement into two components, longshore sediment transport and cross-shore sediment transport, although this separation is not always valid in a strict sense because it is implicitly based on the assumption of plane and parallel profile contours. Longshore sediment transport figures prominently in situations involving loss of sediment supply, such as damming of rivers, and in impoundment at structures such as groins and jetties. In these cases longshore transport is the major process governing nearshore topography change and cannot be neglected.

4. For beaches located away from structures, inlets, and river mouths, it may be appropriate to neglect longshore transport as a first approximation, i.e., assume the gradient of the longshore transport rate is negligibly small

at the site. In this case, cross-shore transport will determine the change in beach profile contours. This assumption will be made in this investigation: longshore sediment transport is neglected and profile change produced solely by cross-shore sediment transport is considered.

5. The ultimate goal of this investigation is development of a numerical model to predict beach profile change produced by wave action. Numerous such models have been reported in the literature; however, apart from the present work only one highly schematized numerical model has been considered sufficiently accurate to be of engineering use. Most efforts appear to have failed because the level of detail attempted was beyond the state of knowledge of the physical processes involved. At present, knowledge is very limited on the collective motion of sediment particles in spatially varying flows of oscillatory currents, wave-induced mean current, and turbulence fields of breaking waves. Numerous other complicating factors, such as the complex fluid motion over an irregular bottom and absence of rigorous descriptions of broken waves and sediment-sediment interaction, also make the problem of computing sediment transport and resultant beach profile change essentially impossible if a first-principles approach at the microscale is taken.

6. On the other hand, despite the incredibly complex and diverse processes and factors involved, beach profile change, if viewed on the macroscale (spatial scale on the order of meters, and temporal scale on the order of hours), is remarkably smooth and simple. Certain prominent features, such as bars, troughs, and berms go through cycles of formation, growth, movement, and erasure with a morphodynamic pattern that has been reasonably well described by a number of qualitative conceptual models. The question can then be asked whether it is possible to develop a quantitative (numerical) model of beach profile change based on empirically determined global relations for the wave-induced net cross-shore sediment (sand) transport rate that can be inferred from the smooth and regular change observed to occur during beach profile evolution. Development of such a model is the subject of this investigation. Consideration is limited to sediment in the sand range of grain size (particle diameters in the range of 0.062 - 2.00 mm).

Procedure Used

7. The principal physical mechanisms which determine beach profile change must be quantitatively described to model the profile response numerically. For this purpose it is necessary to study profile evolution under varying waves, sand characteristics, and profile shape. However, to establish cause and effect relationships between the governing factors and the profile response, it must be possible to clearly delineate these relationships. Laboratory facilities provide an environment where such investigations may be carried out efficiently, while allowing for data sampling at almost any spatial or temporal scale. The difficulty of transforming observations made under scale distortion is eliminated if experiments are performed at the scale of the prototype, i.e., at a sufficiently large scale as to satisfactorily represent the interaction between fluid forces and sand grains that produces significant sand transport in the field.

8. Use of field profile data as a basis for developing a numerical model is extremely difficult due to the complexity and randomness of naturally occurring conditions and cost of data collection. Ultimately a numerical model must be verified against field data, but, in the process of model development, laboratory data can provide considerably more insight into the relative influence of the factors producing the profile change. Study of these individual factors implicitly assumes the validity of the superposition principle for application of the model to the general case. For example, examination of the effect of water level variation on profile evolution under fixed incident waves isolates the influence of this factor and allows understanding of the related physical processes involved. A combination of such observations constitutes the foundation for a numerical model which is used in a predictive mode for varying water level and wave conditions, even though these factors have been evaluated separately. Consequently, careful data analysis is the basis for many assumptions and empirical relationships employed in the numerical model developed here and the first logical step toward understanding beach profile change by this procedure.

9. From an engineering point of view it is of considerable importance to quantify the various properties related to beach profile change. This

regards both geometric parameters such as bar volume and depth-to-bar crest, as well as more complex quantities such as the net cross-shore sand transport rate. Any structure or activity extending into the nearshore region is influenced by and exerts influence on the evolution of the beach profile, thus requiring quantitative estimates of profile change under various environmental and design conditions. A thorough analysis of various geometric characteristics of the profile and their dependence on the wave and sand properties is in this respect valuable. Through this analysis the important processes shaping the beach and generating various topographic features may be clarified, forming the conceptual framework for a numerical model.

10. A fundamental assumption of this study is that beach profile change is mainly governed by breaking of short-period waves (periods in the approximate range of 3-20 sec). No attempt has been made to include the effect of long-period waves, such as partially standing waves or infragravity waves, in the driving force of profile evolution, because no adequate data on profile change are available that permit firm conclusions to be made. Recent field investigations have indicated that, in some cases, infragravity or long-period wave energy can be more energetic near the shoreline than that of the existing short-period waves. This dominance of the wave energy spectrum in very shallow water by long-period waves is expected to play an important role in beach profile processes on the beach face and, possibly, the inner surf zone. However, no relationship between beach profile change and infragravity waves exists at present due to lack of data. When such data become available, superposition should allow calculation of profile change under both short- and long-period waves.

11. The main purpose of the data analysis is not to derive widely applicable relationships for geometric properties of the profile, but to identify the important factors governing profile change. These factors will be integral parts in the conceptual foundation underlying the numerical model development. In some cases, however, empirical relationships derived from the data are used directly in the model if general conclusions about the behavior of the quantity can be made.

Basic Terminology

12. Nomenclature associated with the beach profile and nearshore region which is used throughout the report is presented in this section. Terms defined in the Shore Protection Manual (SPM 1984) have been adopted to a large extent. However, for some quantities, slightly different descriptions are employed that are better suited for nearshore processes as related to beach profile change. Figures 1a and 1b are definition sketches pertaining to beach profile morphology and nearshore wave dynamics, respectively. The portion of the beach profile of interest spans across the shore from the dunes to the seaward limit of the nearshore zone.

Profile morphology

13. As waves approach the beach from deep water, they enter the nearshore zone. The seaward boundary of the nearshore zone is dynamic and for our purpose is considered to be the depth at which incident waves begin to shoal. The shoreward boundary of wave action is also dynamic and is at the limit of wave runup located at the intersection between the maximum water level and the beach profile. A gently sloping bottom will cause a gradual shoaling of the waves, leading to an increase in wave height and finally to breaking at a point where the wave height is about equal to the water depth. The region seaward of wave breaking is denoted as the offshore; the inshore encompasses the surf zone, i.e., that portion of the profile exposed to breaking and broken waves. The broken waves both propagate and dissipate with large energy through turbulence, initiating and maintaining sand movement. At the beach face, the remaining wave energy is expended by a runup bore as the water rushes up the profile.

14. The flat area shoreward of the beach face is called the backshore and is only wetted during severe (storm) wave conditions or when the water level is unusually high. On the backshore, one or several berms may exist; these are accretionary features formed of material which has been deposited by wave runup. The term "accretionary" refers to features generated by sand transport directed onshore. A step often develops immediately seaward of a

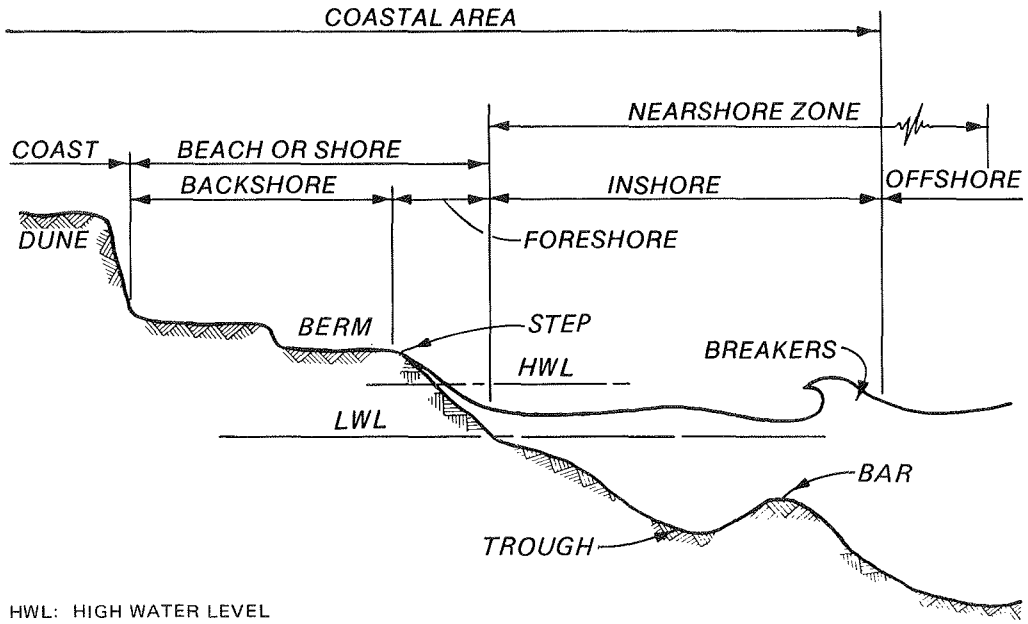

a. Morphology

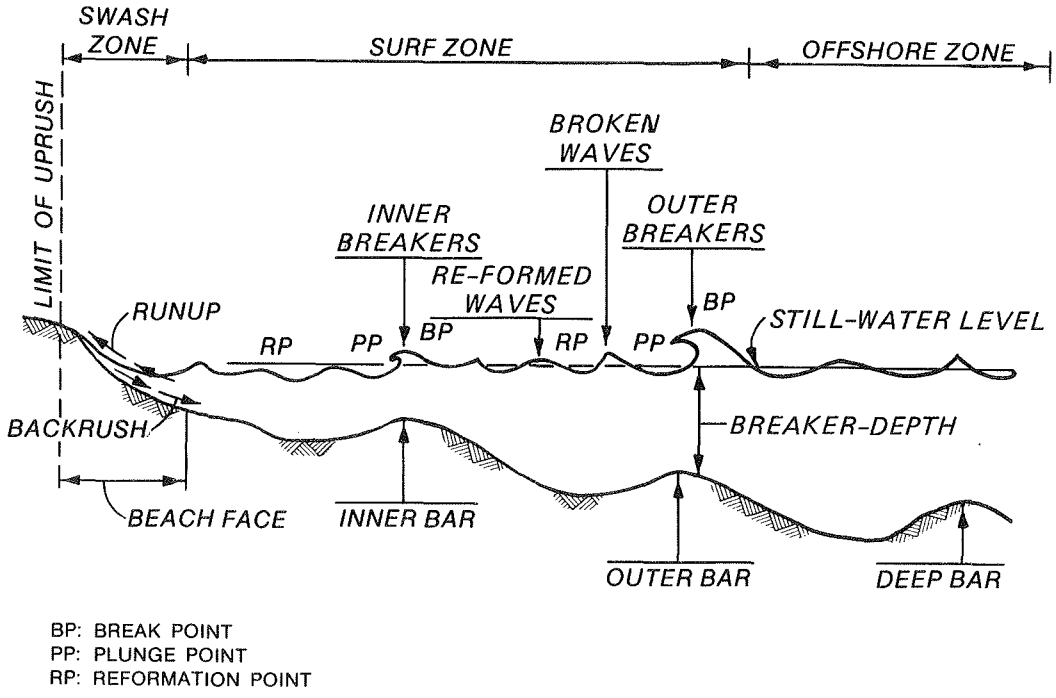

b. Nearshore wave dynamics

Figure 1. Definition sketch of the beach profile (after SPM (1984))

berm, and the slope of the step depends on the properties of the runup bore and the sand grains. Under storm wave action a scarp may also form; here, the term "step" will sometimes be used to denote both a scarp and a step. On many beaches a line of dunes is present shoreward of the backshore. Dunes consist of large ridges of unconsolidated sand that has been transported by wind from the backshore.

15. A bar is a depositional feature formed by sand transported from neighboring areas. Several bars may appear along a beach profile, often having a distinct trough on the shoreward side. Bars are highly dynamic features that respond to the existing wave climate by changing form and translating across-shore, but at the same time bars influence the waves incident upon them. If a bar was created during an episode of high waves, it may be located at such great depth that very little or almost no sand transport activity takes place until another period of high waves occurs. Some transport from the bar caused by shoaling waves may take place, but the time scale of this process is considerably longer than if the bar is located close to the surf zone and the breaking or broken waves.

Nearshore waves

16. The above-discussed terminology is related mainly to the various regions and features of the beach profile. Nearshore waves are also described by a specialized terminology (Figure 1b). Again, some definitions are not unique and describe quantities that change in space and time. The region between the break point and the limit of the backrush, where mainly broken waves exist, is called the surf zone. The swash zone extends approximately from the limit of the backrush to the maximum point of uprush, coinciding with the region of the beach face. As waves break and propagate toward shore, reformation may occur depending on the profile shape; that is, the translatory broken wave form reverts to an oscillatory wave. This oscillatory wave will break again as it reaches sufficiently shallow water, transforming into a broken wave with considerable energy dissipation. A region where broken waves have reformed to oscillatory waves is called a reformation zone, and the point where this occurs is the wave reformation point. Depending on the regularity of the incident waves and shape of the beach profile, wave breaking and reformation may occur several times.

17. The break point is located where the maximum particle velocity of the wave exceeds the wave celerity and the front face of the wave becomes vertical. As a wave breaks, the crest falls over into the base of the wave accompanied by large amount of energy dissipation. If the breaking waves are of the plunging type, the point of impingement is easily recognized and denoted as the plunge point. For spilling breakers, however, the plunge point concept is not commonly used, but such a point could be defined using the location of maximum energy dissipation. This definition is in accordance with the conditions prevailing at the plunge point for a plunging breaker.

18. A beach profile exposed to constant wave and water level conditions over a sufficiently long time interval, as can be done in the laboratory, will attain a fairly stable shape known as the equilibrium profile. On a beach in nature, where complex wave and water level variations exist, an equilibrium profile may never develop or, if so, only for a short time before the waves or water level again change. However, the equilibrium concept remains useful since it provides information on the amount of sand that has to be redistributed within the profile to attain the natural shape for a specific set of wave conditions. The equilibrium profile is in general considered to be a function of sand and wave characteristics.

Organization of This Report

19. Part I is an introduction and gives a statement of the problem and objectives of the investigation. Part II reviews the literature of beach profile change, covering laboratory, field, and theoretical studies, and ends with a synthesis of results considered to be of particular relevance to the present investigation. Since the approach taken relies extensively on measurements, the data sets used are discussed in detail in Part III.

20. The main portion of the original work in this investigation was performed in a logical progression of three substudies. The first substudy, presented in Part IV, quantifies the morphology of the beach profile and the dynamics of its change under wave action. Based on these results, general features of cross-shore transport and empirically-based transport rate formulas needed for the development of the predictive numerical model are

derived in Part V. The profile change numerical model and the required wave model are described in Part VI. Part VII presents the results of extensive testing of the model, including sensitivity analyses, application to describe profile change in the field, and examples of its use to predict the adjustment of beach fill to storm wave action, together with the subsequent recovery process.

21. Part VIII gives conclusions and summarizes results. A summary of statistical procedures and terminology used is given in Appendix A, and mathematical notation is listed in Appendix B. The second report in the SBEACH series (Larson, Kraus, and Byrnes in prep) presents a detailed discussion of the numerical solution procedure used in both the wave and profile change models. It also gives additional examples of field verification and refinements in model usage.

PART II: LITERATURE REVIEW

22. From the earliest investigations of beach morphology, the study of profile change has focused to a large extent upon the properties of bars. A wide range of morphologic features has been classified as bar formations by various authors, and different terminology has been used to denote the same feature. The literature on beach profile change is vast, and this chapter is intended to give a chronological survey of results relevant to the present work.

Chronological Survey of Literature

23. Many of the first contributions to the study of bars were made by German researchers around the beginning of this century. Lehmann (1884) noted the role of breaking waves in suspending sand and found that profile change could occur very rapidly with respect to offshore bar movement. Otto (1911) and Hartnack (1924) measured geometric properties of bars in the Baltic Sea, such as depth-to-bar crest, distance from shoreline to bar crest, and bar slopes. Hartnack (1924) pointed out the importance of breaking waves in the process of bar formation and noted that the distance between bar crests increased with distance from shore for multiple bars, with the depth-to-bar crest increasing correspondingly.

24. Systematic laboratory modeling of beach profile evolution appears to have been first performed by Meyer (1936) who mainly investigated scaling effects in movable bed experiments. He also derived an empirical relationship between beach slope and wave steepness. Waters (1939) performed pioneering work on the characteristic response of the beach profile to wave action and classified profiles as ordinary or storm type. He concluded that wave steepness can be used to determine the type of beach profile that developed under a set of specific wave conditions. The process of sediment sorting along the profile was demonstrated in the experiments in which the coarser material remained near the plunge point and finer material moved offshore.

25. Bagnold (1940) studied beach profile evolution in small-scale laboratory experiments using rather coarse material (0.5-7.0 mm), resulting in

accretionary profiles with berm buildup. He found that the foreshore slope was independent of the wave height and mainly a function of grain size. However, the equilibrium height of the berm was linearly related to wave height. The effect of a seawall on the beach profile was investigated by allowing waves to reach the end of the tank. By varying the water level, a tide was simulated; in other experiments, a varying wave height was employed.

26. Evans (1940) studied bars and troughs (named balls and lows by Evans) along the eastern shore of Lake Michigan and concluded these features to be the result of plunging breakers. He regarded the bar and trough to form a unit, with the trough always located shoreward of the bar. If the profile slope was mild so that several break points appeared, a series of bars and troughs would develop. Also, a change in wave conditions could result in a change in bar shape and migration of the bar seaward or shoreward. A decreasing water level would cause the innermost bar to migrate onshore and take the form of a subaqueous dune, whereas an increase in water level would allow a new bar system to develop inshore. The most seaward bars would then become inactive.

27. In support of amphibious landing operations during World War II, Keulegan (1945) experimentally obtained simple relations for predicting the depth-to-bar crest and the trough depth. He found the ratio between trough and crest depths to be approximately constant and independent of wave steepness. Important contributions to the basic understanding of the physics of beach profile change were also made through further laboratory experiments by Keulegan (1948). The objective of the study was to determine the shape and characteristics of bars and the process through which they were molded by the incident waves. He recognized the surf zone as being the most active area of beach profile change and the breaking waves as the cause of bar formation. The location of the maximum sand transport rate, measured by traps, was found to be close to the break point, and the transport rate showed a good correlation with the wave height envelope. Keulegan (1948) noted three distinct regions along the profile where the transport properties were different from a morphologic perspective. A gentler initial beach slope implied a longer time before the equilibrium profile was attained for fixed wave conditions. For a constant wave steepness, an increase in wave height moved the bar seaward,

whereas for a constant wave height, an increase in wave steepness (decrease in wave period) moved the bar shoreward. He noted that bars developed in the laboratory experiments were shorter and more peaked than bars in the field and attributed this difference to variability in the wave climate on natural beaches.

28. King and Williams (1949), in work also connected with the war effort, distinguished between bars generated on nontidal beaches and bars occurring on beaches with a marked tidal variation (called ridge and runnel systems by them). They assumed that nonbreaking waves moved sand shoreward and broken waves moved sand seaward. Field observations from the Mediterranean confirmed the main ideas of this conceptualization. In laboratory experiments the cross-shore transport rate was measured with traps, showing a maximum transport rate located around the break point. Furthermore, the term "breakpoint bar" was introduced, whereas berm formations were denoted as "swash bars." The slope of the berm was related to the wavelength, where a longer wave period produced a more gentle slope. King and Williams hypothesized that ridge and runnel systems were not created by breaking waves but were a result of swash processes.

29. Johnson (1949) gave an often cited review of scale effects in movable bed modeling and referenced the criterion for distinguishing ordinary and storm profiles discovered by Waters (1939).

30. Shepard (1950) made profile surveys along the pier at Scripps Institution of Oceanography, La Jolla, California, in 1937 and 1938, and discussed the origin of troughs. He suggested that the combination of plunging breakers and longshore currents was the primary cause. He also showed that the trough and crest depths depended on breaker height. Large bars formed somewhat seaward of the plunge point of the larger breakers, and the ratios for the trough-to-crest depth were smaller than those found by Keulegan (1948) in laboratory experiments. Shepard (1950) also observed the time scale of beach profile response to the incident wave climate and concluded that the profile change was better related to the existing wave height than to the greatest wave height from the preceding 5 days.

31. Bascom (1951) studied the slope of the foreshore along the Pacific coast and attempted to relate it to grain size. A larger grain size implied a

steeper foreshore slope. He also determined a trend in variation in grain size across the profile that is much cited in the literature. A bimodal distribution was found with peaks at the summer berm and at the step of the foreshore. The largest particles were found on the beach face close to the limit of the backrush, and the grain size decreased in the seaward direction.

32. Scott (1954) modified the wave steepness criterion of Waters (1939) for distinguishing between ordinary (summer) and storm profiles, based on his laboratory experiments. He also found that the rate of profile change was greater if the initial profile was farther from equilibrium shape, and he recognized the importance of wave-induced turbulence for promoting bar formation. Some analysis of sediment stratification and packing along the profile was carried out.

33. Rector (1954) investigated the shape of the equilibrium beach profile in a laboratory study. Equations were developed for profile shapes in two sections separated at the base of the foreshore. Coefficients in the equilibrium profile equation were a function of deepwater wave steepness and grain size normalized by the deepwater wavelength. An empirical relationship was derived for determining the maximum depth of profile adjustment as a function of the two parameters. These parameters were also used to predict net sand transport direction.

34. Watts (1954) and Watts and Dearduff (1954) studied the effect on the beach profile of varying wave period and water level, respectively. A varying wave period reduced the bar and trough system as compared to waves of constant period but only slightly affected beach slope in the foreshore and offshore. The influence of the water level variation for the range tested (at most 20 percent variation in water level with respect to the tank depth in the horizontal portion) was small, producing essentially the same foreshore and offshore slopes. However, the active profile translated landward for the tidal variation, allowing the waves to attack at a higher level and thus activating a larger portion of the profile.

35. Bruun (1954) developed a predictive equation for the equilibrium beach profile by studying beaches along the Danish North Sea coast and the California coast. The equilibrium shape (depth) followed a power curve with distance offshore, with the power evaluated as 2/3.

36. Ippen and Eagleson (1955) experimentally and theoretically investigated sorting of sediments by wave shoaling on a plane beach. The movement of single spherical particles was investigated and a "null point" was found on the beach where the particle was stable for the specific grain size.

37. Saville (1957) was the first to employ a large wave tank capable of reproducing near-prototype wave and beach conditions, and he studied equilibrium beach profiles and model scale effects. Waves with very low steepness were found to produce storm profiles, contrary to results from small-scale experiments (Waters 1939, Scott 1954). Comparisons were made between the large wave tank studies and small-scale experiments, but no reliable relationship between prototype and model was obtained. The data set from this experiment is used extensively in the present work.

38. Caldwell (1959) presented a summary of the effects of storm (northeaster) and hurricane wave attack on natural beach profiles for a number of storm events.

39. McKee and Sterrett (1961) investigated cross-stratification patterns in bars by spreading layers of magnetite over the sand.

40. Kemp (1961) introduced the concept of "phase difference," referring to the relation between time of uprush and wave period. He assumed the transition from a step (ordinary) to a bar (storm) profile to be a function of the phase difference and to occur roughly if the time of uprush was equal to the wave period.

41. Bruun (1962) applied his empirical equation (Bruun 1954) for an equilibrium beach profile to estimate the amount of erosion occurring along the Florida coast as a result of long-term sea level rise.

42. Bagnold (1963, 1966) developed formulas for calculating sediment transport rates, including cross-shore transport, based on a wave energy approach, and distinguishing between bed load and suspended load. This work has been refined and widely applied by others (e.g., Bailard and Inman 1981, Bailard 1982, Stive 1987). Bed-load transport occurs through the contact between individual grains, whereas in suspended load transport the grains are supported by the diffusion of upward eddy momentum. A superimposed steady current moves the grains along the bed. Inman and Bagnold (1963) derived an expression for the local equilibrium slope of a beach based on wave energy

considerations. The equilibrium slope was a function of the angle of repose and the ratio between energy losses at the bed during offshore- and onshore-directed flow.

43. Eagleson, Glenne, and Dracup (1963) studied equilibrium profiles in the region seaward of the influence of breaking waves. They pointed out the importance of bed load for determining equilibrium conditions and used equations for particle stability to establish a classification of beach profile shapes.

44. Iwagaki and Noda (1963) derived a graphically presented criterion for predicting the appearance of bars based on two nondimensional parameters, deepwater wave steepness, and ratio between deepwater wave height and median grain size. The change in character of breaking waves due to profile evolution in time was discussed. The potential importance of suspended load was recognized and represented through the grain size, this quantity emerging as a significant factor in beach profile change.

45. Zenkovich (1967) presented a summary of a number of theories suggested by various authors for the formation of bars.

46. Wells (1967) proposed an expression for the location of a nodal line of the net cross-shore sand transport based on the horizontal velocity skewness being zero, neglecting gravity, and derived for the offshore, outside the limit of breaking waves. Seaward of the nodal line material could erode and shoreward-moving sand could accumulate, depending on the sign of the velocity skewness.

47. Berg and Duane (1968) studied the behavior of beach fills during field conditions and suggested the use of coarse, well-sorted sediment for the borrow material to achieve a more stable fill. The mean diameter of the grains in the profile roughly decreased with depth, with the coarsest material appearing at the waterline (Bascom 1951, Scott 1954).

48. Mothersill (1970) found evidence through grain size analysis that longshore bars are formed by plunging waves and a seaward-directed undertow (Dally 1987). Sediment samples taken in troughs were coarser, having the properties of winnowed residue, whereas samples taken from bars were finer grained, having the characteristics of sediments that had been winnowed out and then redeposited.

49. Sonu (1969) distinguished six major types of profiles and described beach change in terms of transitions between these types.

50. Edelman (1969, 1973) studied dune erosion and developed a quantitative predictive procedure by assuming that all sand eroded from the dune was deposited within the breaker zone. On the basis of a number of simplifying assumptions, such as the shape of the after-storm profile being known together with the highest storm surge level, dune recession as produced by a storm could be estimated.

51. Sonu (1970) discussed beach change caused by the 1969 hurricane Camille, documenting the rapid profile recovery that took place during the end of the storm itself and shortly afterward (see also, Kriebel 1987).

52. Nayak (1970, 1971) performed small-scale laboratory experiments to investigate the shape of equilibrium beach profiles and their reflection characteristics. He developed a criterion for the generation of longshore bars that is similar to that of Iwagaki and Noda (1963) but included the specific gravity of the material. The slope at the still-water level for the equilibrium profile was controlled more by specific gravity than by grain size. Furthermore, the slope decreased as the wave steepness at the beach toe or the dimensionless fall speed (wave height divided by fall speed and period) increased. The dimensionless fall speed was also found to be a significant parameter for determining the reflection coefficient of the beach.

53. Allen (1970) quantified the process of avalanching on dune slopes for determining the steepest stable slope a profile can attain. He introduced the concepts of angle of initial yield and residual angle after shearing to denote the slopes immediately before and after the occurrence of avalanching.

54. Dyhr-Nielsen and Sorensen (1971) proposed that longshore bars were formed from breaking waves which generated secondary currents directed toward the breaker line. On a tidal beach with a continuously moving break point, a distinct bar would not form unless severe wave conditions prevailed.

55. Saylor and Hands (1971) studied characteristics of longshore bars in the Great Lakes. The distance between bars increased at greater than linear rate with distance from the shoreline, whereas the depth to crest increased linearly. A rise in water level produced onshore movement of the bars (cf. Evans 1940).

56. Davis and Fox (1972) and Fox and Davis (1973) developed a conceptual model of beach change by relating changes to barometric pressure. They reproduced complex nearshore features by schematizing the beach shape and using empirical relationships formed with geometric parameters describing the profile. Davis et al. (1972) compared development of ridge and runnel systems (King and Williams 1949) in Lake Michigan and off the coast of northern Massachusetts where large tidal variations prevailed. The tides only affected the rate at which onshore migration of ridges occurred and not the sediment sequence that accumulated as ridges.

57. Dean (1973) assumed suspended load to be the dominant mode of transport in most surf zones and derived on physical grounds the dimensionless fall speed as governing parameter. Sand grains suspended by the breaking waves would be transported onshore or offshore depending on the relation between the fall speed of the grains and the wave period. A criterion for predicting the cross-shore transport direction based on the nondimensional quantities of deepwater wave steepness and fall speed divided by wave period and acceleration of gravity (fall speed parameter) was proposed. The criterion of transport direction was also used for predicting profile response (normal or storm profile).

58. Carter, Liu, and Mei (1973) suggested that longshore bars could be generated by standing waves and associated reversal of the mass transport in the boundary layer, causing sand to accumulate at either nodes or antinodes of the wave. In order for flow reversal to occur, significant reflection had to be present. Lau and Travis (1973), and Short (1975a, b) discussed the same mechanism for longshore bar formation.

59. Hayden et al. (1975) analyzed beach profiles from the United States Atlantic and gulf coasts to quantify profile shapes. Eigenvector analysis was used as a powerful tool to obtain characteristic shapes in time and space. The first three eigenvectors explained a major part of the variance and were given the physical interpretation of being related to bar and trough morphology. The number of bars present on a profile showed no dependence on profile slope, but an inverse relationship between slopes in the inshore and offshore was noted.

60. Winant, Inman, and Nordstrom (1975) also used eigenvector analysis to determine characteristic beach shapes and related the first eigenvector to mean beach profile, the second to the bar/berm morphology, and the third to the terrace feature. The data set consisted of 2 years of profile surveys at Torrey Pines, California, performed at monthly intervals.

61. Davidson-Arnott (1975) and Greenwood and Davidson-Arnott (1975) performed field studies of a bar system in Kouchibouguac Bay, Canada, and identified conditions for bar development; namely, gentle offshore slope, small tidal range, availability of material, and absence of long-period swell. They distinguished between the inner and outer bar system and described in detail the characteristics of these features. The break point of the waves was located on the seaward side of the bar in most cases and not on the crest. Greenwood and Davidson-Arnott (1972) did textural analysis of sand from the same area, revealing distinct zones with different statistical properties of the grain size distribution across the profile (Mothersill 1970).

62. Exon (1975) investigated bar fields in the western Baltic Sea which were extremely regular due to evenly distributed wave energy alongshore. He noted that the presence of engineering structures reduced the size of the bar field.

63. Kamphuis and Bridgeman (1975) performed wave tank experiments to evaluate the performance of artificial beach nourishment. They concluded that the inshore equilibrium profile was independent of the initial slope and a function only of beach material and wave climate. However, the time elapsed before equilibrium was attained, as well as the bar height, depended upon the initial slope.

64. Sunamura and Horikawa (1975) classified beach profile shapes into three categories distinguished by the parameters of wave steepness, beach slope, and grain size divided by wavelength. The criterion was applied to both laboratory and field data, only requiring a different value of an empirical coefficient to obtain division between the shapes. The same parameters were used by Sunamura (1975) in a study of stable berm formations. He also found that berm height (datum not given) was approximately equal to breaking wave height.

65. Swart (1975, 1977) studied cross-shore transport properties and characteristic shapes of beach profiles. A cross-shore sediment transport equation was proposed where the rate was proportional to a geometrically-defined deviation from the equilibrium profile shape. A numerical model was developed based on the derived empirical relationships and applied to a beach fill case.

66. Wang, Dalrymple, and Shiau (1975) developed a computer-intensive three-dimensional numerical model of beach change assuming that cross-shore transport occurred largely in suspension. The transport rate was related to the energy dissipation across shore.

67. Van Hijum (1975, 1977) and Van Hijum and Pilarczyk (1982) investigated equilibrium beach profiles of gravel beaches in laboratory tests and derived empirical relationships for geometric properties of profiles. The net cross-shore sand transport rate was calculated from the mass conservation equation, and a criterion for the formation of bar/step profiles was proposed for incident waves approaching at an angle to the shoreline.

68. Hands (1976) observed in field studies at Lake Michigan that plunging breakers were not essential for bar formation. He also noted a slower response of the foreshore to a rising lake level than for the longshore bars. A number of geometric bar properties were characterized in time and space for the field data.

69. Dean (1976) discussed equilibrium profiles in the context of energy dissipation from wave breaking. Various causes of beach profile erosion were identified and analyzed from the point of view of the equilibrium concept. Dean (1977) analyzed beach profiles from the United States Atlantic and gulf coasts and arrived at a 2/3 power law as the optimal function to describe the profile shape, as previously suggested by Bruun (1954). Dean (1977) proposed a physically-based explanation for the power shape assuming that the profile was in equilibrium if the energy dissipation per unit water volume from wave breaking was uniform across shore. Dean (1977b) developed a schematized model of beach recession produced by storm activity based on the equilibrium profile shape (Edelman 1969, 1973).

70. Owens (1977) studied beach and nearshore morphology in the Gulf of St. Lawrence, Canada, describing the cycles of erosion and accretion resulting from storms and post-storm recovery.

71. Chiu (1977) mapped the effect of the 1975 Hurricane Eloise on the beach profiles along the Gulf of Mexico (Sonu 1970). Profiles with a gentle slope and a wide beach experienced less erosion compared with steep slopes, whereas profiles in the vicinity of structures experienced greater amounts of erosion.

72. Dalrymple and Thompson (1977) related foreshore slope to the dimensionless fall speed using laboratory data and presented an extensive summary of scaling laws for movable-bed modeling.

73. Felder (1978) and Felder and Fisher (1980) divided the beach profile into various regions with specific transport relationships and developed a numerical model to simulate bar response to wave action. In the surf zone, the transport rate depended on the velocity of a solitary wave.

74. Aubrey (1978) and Aubrey, Inman, and Winant (1980) used the technique of eigenvector analysis (Hayden et al. 1975) in beach profile characterization to predict beach profile change. Both profile evolution on a daily and weekly basis were predicted from incident wave conditions where the weekly mean wave energy was found to be the best predictor for weekly changes. Aubrey (1979) used measurements of beach profiles in southern California spanning 5 years to investigate temporal properties of profile change. He discovered two pivotal (fixed) points, one located at 2 to 3-m depth and one at 6-m depth. Sediment exchange across the former point was estimated at 85 m^3/m and across the latter at 15 m^3/m per year.

75. Hunter, Clifton, and Phillips (1979) studied nearshore bars on the Oregon coast which attached to the shoreline and migrated alongshore. A seaward net flow (undertow) along the bottom was occasionally observed shoreward of the bar during field investigations (Mothersill 1970).

76. Greenwood and Mittler (1979) found support in the studies of sedimentary structures of the bar system being in dynamic equilibrium from sediment movement in two opposite directions. An asymmetric wave field moved the sand landward and rip currents moved the material seaward.

77. Greenwood and Davidson-Arnott (1979) presented a classification of wave-formed bars and a review of proposed mechanisms for bar formation (Zenkovich 1967).

78. Hallermeier (1979, 1984) studied the limit depth for intense bed agitation and derived an expression for this depth based on linear wave shoaling. He also proposed an equation for the yearly limit depth for significant profile change involving wave conditions which exceeded 12 hours per year (see also Birkemeier 1985b).

79. Hattori and Kawamata (1979) investigated the behavior of beach profiles in front of a seawall by means of laboratory experiments. Their conclusion was that material eroded during a storm returned to the seawall during low wave conditions to form a new beach (cf. reviews of Kraus 1987, 1988).

80. Chappell and Eliot (1979) performed statistical analyses of morphological patterns from data obtained along the southern coast of Australia. Seven inshore states were identified which could be related to the current, the antecedent wave climate, and the general morphology (Sonu 1969).

81. Nilsson (1979) assumed bars to be formed by partially reflected Stokes wave groups and developed a numerical model based on this mechanism. Sediment transport rates were calculated from the bottom stress distribution, and an offshore directed mean current was superimposed on the velocity field generated by the standing waves.

82. Short (1979) conducted field studies along the southeast Australian coast which formed the basis for proposing a conceptual three-dimensional beach-stage model. The model comprised ten different stages ranging from pure erosive to pure accretive conditions. Transitions between stages were related to the breaking wave height and breaker power. Wright et al. (1979) discussed the characteristics of reflective and dissipative beaches as elucidated from Australian field data. The surf scaling parameter (Guza and Bowen 1977) was considered an important quantity for determining the degree of reflectivity of a specific profile. Long-period waves (infragravity waves, edge waves) were believed to play a major role in the creation of three-dimensional beach morphology.

83. Bowen (1980) investigated bar formation by standing waves and presented analytical solutions for standing waves on plane sloping beaches. He also derived equilibrium slopes for beach profiles based on Bagnold's (1963) transport equations and assuming simple flow variations.

84. Dally (1980) and Dally and Dean (1984) developed a numerical model of profile change based on the assumption that suspended transport is dominant in the surf zone. The broken wave height distribution across-shore determined by the numerical model supplied the driving mechanism for profile change. An exponential-shaped profile was assumed for the sediment concentration through the water column.

85. Davidson-Arnott and Pember (1980) compared bar systems at two locations in southern Georgian Bay, the Great Lakes, and found them to be very similar despite large differences in fetch length. The similarity was attributed to the same type of breaking conditions prevailing, with spilling breakers occurring at multiple break points giving rise to multiple bar formations (Hands 1976).

86. Hashimoto and Uda (1980) related beach profile eigenvectors for a specific beach to shoreline position. Once the shoreline movement could be predicted, the eigenvectors were given from empirical equations and the three-dimensional response obtained.

87. Shibayama and Horikawa (1980a, 1980b) proposed sediment transport equations for bed load and suspended load based on the Shields parameter (Madsen and Grant 1977). A numerical beach profile model was applied using these equations which worked well in the offshore region but failed to describe profile change in the surf zone.

88. Davidson-Arnott (1981) developed a numerical model to simulate multiple longshore bar formation. The model was based on the mechanism proposed by Greenwood and Mittler (1979) for bar genesis, and the model qualitatively produced offshore bar movement; but no comparison with measurements was made.

89. Bailard and Inman (1981) and Bailard (1982) used Bagnold's (1963) sediment transport relationships to develop a model for transport over a plane sloping beach. They determined the influence in the model of the longshore current on the equilibrium profile slope. The beach profile was flattened in

the area of the maximum longshore current and the slope increased with sand fall velocity and wave period.

90. Hughes and Chiu (1981) studied dune recession by means of small-scale movable-bed model experiments. The amount of dune erosion was found by shifting the barred profile horizontally until eroded volume agreed with deposited volume (Vellinga 1983). Geometric properties of the equilibrium bar profile were expressed in terms of dimensionless fall speed.

91. Sawaragi and Deguchi (1981) studied cross-shore transport and beach profile change in a small wave tank and distinguished three transport rate distributions. They developed an expression for the time variation of the maximum transport rate and discussed the relation between bed and suspended load.

92. Gourlay (1981) emphasized the significance of the dimensionless fall speed (Gourlay 1968) in describing equilibrium profile shape, relative surf zone width, and relative uprush time.

93. Hattori and Kawamata (1981) developed a criterion for predicting the direction of cross-shore sediment transport similar to Dean (1973), but including beach slope. The criterion was derived from the balance between gravitational and turbulent forces keeping the grains in suspension.

94. Watanabe, Riho, and Horikawa (1981) calculated net cross-shore transport rates from the mass conservation equation (van Hijum 1975, 1977) and measured profiles in the laboratory, arriving at a transport relationship of the Madsen and Grant (1977) type. They introduced a critical Shields stress below which no transport occurred and assumed a linear dependence of the transport rate on the Shields parameter.

95. Moore (1982) developed a numerical model to predict beach profile change produced by breaking waves. He assumed the transport rate to be proportional to the energy dissipation from breaking waves per unit water volume above an equilibrium value (Dean 1977). An equation was given which related this equilibrium energy dissipation to grain size. The beach profile calculated with the model approached an equilibrium shape in accordance with the observations of Bruun (1954) if exposed to the same wave conditions for a sufficiently long time.

96. Kriebel (1982, 1986) and Kriebel and Dean (1984, 1985a) developed a numerical model to predict beach and dune erosion using the same transport relationship as Moore (1982). The amount of erosion was determined primarily by water-level variation, and breaking wave height entered only to determine the width of the surf zone. The model was verified both against large wave tank data (Saville 1957) and data from natural beaches taken before and after Hurricane Eloise (Chiu 1977). The model was applied to predict erosion rates at Ocean City, Maryland, caused by storm activity and sea level rise (Kriebel and Dean 1985b).

97. Holman and Bowen (1982) derived idealized three-dimensional morphologic patterns resulting from interactions between edge waves and reflected waves, assuming that drift velocities associated with these waves caused bar formation.

98. Watanabe (1982, 1985) introduced a cross-shore transport rate which was a function of the Shields parameter to the 3/2 power in a three-dimensional model of beach change. The model simulated the effects of both waves and nearshore currents on the beach profile. The transport direction was obtained from an empirical criterion (Sunamura and Horikawa 1975).

99. Vellinga (1982, 1986) presented results from large wave tank studies of dune erosion and discussed scaling laws for movable-bed experiments (Hughes and Chiu 1981). The dimensionless fall speed proved to provide a reasonable scaling parameter in movable-bed studies. He also emphasized the dependence of the sediment concentration on wave breaking.

100. Dolan (1983) and Dolan and Dean (1984) investigated the origin of the longshore bar system in Chesapeake Bay and concluded that multiple breaking was the most likely cause (Hands 1976). Other possible mechanisms discussed were standing waves, edge waves, secondary waves, and tidal currents, but none of these could satisfactorily explain the formations.

101. Kajima et al. (1983a, b) discussed beach profile evolution using data obtained in a large wave tank with waves of prototype size. Beach profile shapes and distributions of the net cross-shore transport rates were classified according to the criterion developed by Sunamura and Horikawa (1975). A model of beach profile change was proposed based on a schematized

transport rate distribution which decayed exponentially with time. The data set given by Kajima et al. (1983b) is used in the present work.

102. Sasaki (1983) developed a conceptual three-dimensional beach stage model based on extensive field measurement from two beaches in Japan (see also Sonu 1969, Short 1979). Transition between the different stages was determined as a function of the average deepwater wave steepness and the average breaker height divided by the median grain size. A larger breaker height and deepwater wave steepness caused greater shoreline recession during storms, whereas a coarser grain size gave reduced shoreline retreat.

103. Sunamura (1983) developed a simple numerical model of shoreline change caused by short-term cross-shore events and described both erosional and accretional phases of a field beach. Exponential response functions were used to calculate the magnitude of shoreline change, and direction was given by the criterion proposed by Sunamura and Horikawa (1975).

104. Vellinga (1983, 1986) presented an empirically based mathematical model for calculating dune erosion during high surge-short duration storm events. The amount of dune recession was determined from the significant wave height, storm surge level, and beach profile shape during storm conditions. Van de Graaff (1983) discussed a probabilistic approach for estimating dune erosion. Distribution functions for a number of important parameters regarding dune erosion were suggested such as maximum storm surge level, significant wave height, median grain size, and profile shape. Visser (1983) applied a probability-based design scheme to the dunes in the Delta area of The Netherlands (Verhagen 1985).

105. Seelig (1983) analyzed large wave tank data from Saville (1957) and developed a simple prediction method to estimate beach volume change above the still-water level.

106. Balsillie (1984) related longshore bar formation to breaking waves from field data and developed a numerical model to predict profile recession produced by storm and hurricane activity.

107. Davidson-Arnott and Randall (1984) performed field measurements of the spatial and temporal characteristics of the surface elevation and cross-shore current spectra on a barred profile at St. Georgian Bay, Lake Ontario.

The greatest portion of the energy was found in the frequencies of the incident short-period waves.

108. Sunamura (1984a) derived a formula to determine the cross-shore transport rate in the swash zone taken as an average over 1 hour. The transport rate was related to the near-bottom orbital velocity, and the transport equation predicted the net direction of sand movement.

109. Takeda (1984) studied the behavior of beaches during accretionary conditions. Based on field investigations from Naka Beach, Japan, he derived predictive relationships for determining if onshore movement of bars occurs, average speed of onshore bar migration, and berm height. He pointed out the rapid formation of berms in the field where the buildup may be completed in one or two days (cf. Kriebel, Dally, and Dean 1986).

110. Greenwood and Mittler (1984) inferred the volume flux of sediment over a bar by means of rods driven into the bed on which a freely moving fitting was mounted to indicate changes in bed elevation. Their study indicated an energetics approach in accordance with Bagnold (1963) to be reasonable for predicting equilibrium slopes seaward of the break point.

111. Sunamura (1984b) obtained empirical expressions for the beach face slope involving the breaking wave height, wave period, and grain size. Equations were developed and applied for laboratory and field conditions.

112. Shibayama (1984) investigated the role of vortices in sediment transport and derived transport formulas for bed and suspended load based on Shields parameter. The generation of vortices was not confined to plunging breakers but could occur under spilling breakers as well.

113. Sunamura and Takeda (1984) quantified onshore migration of bars from a 2-year series of profile data from a beach in Japan. They derived a criterion to determine the occurrence of onshore bar movement and an equation to estimate the migration speed (Takeda 1984). Onshore transport typically took place in the form of bed load carried shoreward in a hydraulic bore.

114. Wright and Short (1984) used the dimensionless fall speed, based on the breaking wave height, in a classification process of three-dimensional beach stages.

115. Mei (1985) mathematically analyzed resonant reflection from nearshore bars that can enhance the possibility for standing waves to generate bars.

116. Shimizu et al. (1985) analyzed data obtained with a large wave tank to investigate the characteristics of the cross-shore transport rate. Transport rate distributions were classified in three categories, and the criterion of Sunamura and Horikawa (1975) was used to delineate between different types. The transport rate distribution was modeled by superimposing three separate curves representing the transport rate on the foreshore, in the surf zone, and in the offshore zone (cf. Kajima et al. 1983a).

117. Aubrey and Ross (1985) used eigenvector and rotary component analysis to identify different stages in the beach profile and the corresponding frequency of change. A frequency of one year related to exchange of sediment between bar and berm was the dominant mode found in the analysis.

118. Deguchi and Sawaragi (1985) measured the sediment concentration at different locations across the beach profile in a wave tank. Both the bed load and suspended load were determined, and sediment concentration decayed exponentially with distance above the bed (Kraus and Dean 1987).

119. Mason et al. (1985) summarized a field experiment conducted at Duck, North Carolina, where a nearshore bar system was closely monitored during a storm. Bar dynamics showed a clear dependence on wave height, the bar becoming better developed and migrating offshore as the wave height increased. Birkemeier (1985a) analyzed the time scale of beach profile change from a data set comprising 3-1/2 years of profile surveying at Duck, North Carolina. Large bar movement occurred with little change in the depth to crest. If low-wave conditions prevailed for a considerable time, a barless profile developed.

120. Jaffe, Sternberg, and Sallenger (1985) measured suspended sediment concentration in a field surf zone with an optical back-scattering device. The concentration decreased with elevation above the bed, and an increase in concentration was found over the nearshore bar.

121. Birkemeier (1985b) modified parameter values in an equation proposed by Hallermeier (1979) to describe the seaward limit of profile change at Duck, North Carolina.

122. Gourlay (1985) identified four different kinds of profile response related to dominant breaker type. The dimensionless fall speed (sediment mobility parameter) was decisive for describing both profile response and profile geometry (Hughes and Chiu 1981). The effect of beach permeability was discussed with respect to wave setup and berm height.

123. Sallenger, Holman, and Birkemeier (1985) observed the rapid response of a natural beach profile at Duck, North Carolina, to changing wave conditions. Both offshore and onshore bar movement occurred at much higher speeds than expected, and the ratio between trough and crest depth was approximately constant during offshore bar movement but varied during onshore movement. Since bars appeared to be located well within the surf zone, they concluded that wave breaking was not directly responsible for bar movement.

124. In a numerical model developed by Stive and Battjes (1985), offshore sand transport was assumed to occur through the undertow and as bed load only. They verified the model against laboratory measurements of profile evolution produced by random waves. Stive (1987) extended the model to include effects of asymmetry in the velocity field from the waves in accordance with the transport relations of Bailard (1982).

125. Verhagen (1985) developed a probabilistic technique for estimating the risk of breakthrough of dunes during storm surge and wave action. A main part of this technique was the use of a model to calculate expected dune erosion during a storm (Vellinga 1983) modified by statistical distributions of the factors influencing dune erosion (van de Graaff 1983, Visser 1983).

126. Wood and Weishar (1985) made profile surveys at monthly intervals on the east shore of (tideless) Lake Michigan. They found a strong temporal correlation between berm undulation and the annual lake-level variation.

127. Kriebel, Dally, and Dean (1986) studied beach recovery after storm events both during laboratory and field conditions, noting the rapid process of berm formation. They could not find evidence for breakpoint bars moving onshore and welding onto the beach face during the recovery process; instead, the berm was built from material originating farther inshore. Beach recovery following the 1985 Hurricane Elena was also discussed by Kriebel (1987), who concluded that the presence of a seawall did not significantly affect the process of beach recovery at the site.

128. Wright et al. (1986) concluded from field measurements that bar-trough morphology was favored by moderate breaker heights combined with small tidal ranges. Short-period waves were the main cause of sediment suspension in the surf zone, although long period waves were believed to be important in the overall net drift pattern.

129. Rushu and Liang (1986) proposed a criterion for distinguishing between beach erosion and accretion involving a number of dimensionless quantities. A new parameter consisting of the bottom friction coefficient, critical velocity for incipient motion of the grains, and the fall speed of the grains was introduced.

130. Thomas and Baba (1986) studied berm development produced by onshore migration of bars for a field beach at Valiathura, at the southwest coast of India, and related the conditions for onshore movement to wave steepness.

131. Dette (1986), Uliczka and Dette (1987), and Dette and Uliczka (1987a, b) investigated beach profile evolution generated in a large wave tank under prototype-scale conditions. The tests were carried out with both monochromatic and irregular waves for a dunelike foreshore with and without a significant surf zone. For one case starting from a beach without "foreshore," monochromatic waves produced a bar, whereas irregular waves of significant height and peak spectral period of the monochromatic waves did not. The incident wave energy was different between the cases, however. Sediment concentration and cross-shore velocity were measured through the water column at selected points across the profile.

132. Wright et al. (1987) investigated the influence of tidal variations and wave groupiness on profile configuration. Higher values of the wave groupiness factor tended to correlate with beach states of more dissipative character.

133. Howd and Birkemeier (1987) presented 4 years of profile data obtained at four different shore normal survey lines at Duck, North Carolina. Corresponding wave and water level data were also published, making this data set one of the most complete descriptions available of beach profile response to wave action in the field.

134. Seymour (1987) summarized results from the Nearshore Sediment Transport Study (NSTS) 6-year program in which nearshore sediment transport conditions were investigated. He pointed out the importance of bar formation for protecting the foreshore against wave action and the resulting rapid offshore movement of the bar on a beach exposed to storm waves.

135. Takeda and Sunamura (1987) found from field studies in Japan the great influence of bar formation on the subaerial response of beaches with fine sand.

136. Dally (1987) tested the possibility of generating bars by long period waves (surf beat) in a small wave tank, but he found little evidence for this mechanism. Instead, breaking waves in combination with undertow proved to be the cause of bar formation in the studied cases, whether spilling or plunging breakers prevailed.

137. Hallermeier (1987) stressed the importance of large wave tank experiments for providing valuable information of the beach response to storm conditions. He compared results from a large wave tank experiment (Case 401 in Kraus and Larson 1988a) with a natural erosion episode at Bethany Beach, Delaware, and found similar erosive geometry.

138. Sunamura and Maruyama (1987) estimated migration speeds for seaward moving bars as given by large wave tank experiments using monochromatic waves. The bars were generated by breaking waves and located somewhat shoreward of the break point (Greenwood and Davidson-Arnott 1975). They emphasized that spilling breakers could also form bars, although the approach to equilibrium was much slower than for bars formed by plunging breakers.

139. Kobayashi (1987) presented analytical solutions to idealized cases of dune erosion simplifying the governing equations to result in the heat diffusion equation (cf. Edelman 1969, 1973).

140. Hughes and Cowell (1987) studied the behavior of reflective beaches in southern Australia, in particular, changes in the foreshore step. The height of the beach step was correlated to the breaking wave height and the grain size where a larger wave height and a coarser grain size both produced a higher step.

141. Kriebel, Dally, and Dean (1987) performed laboratory experiments using a small wave tank and beach shapes designed with the dimensionless fall

speed as the scaling parameter. They found marked differences in profile response depending on the initial shape being planar or equilibrium profile type (Bruun 1954, Dean 1977). An initially plane beach produced a more pronounced bar and steeper offshore slopes. The fall speed parameter (Dean 1973) and the deepwater wave steepness were used to distinguish erosional and accretionary profiles using large wave tank data.

142. Mimura, Otsuka, and Watanabe (1987) performed a laboratory experiment with a small wave tank to investigate the effect of irregular waves on the beach profile. They addressed the question of which representative wave height to use for describing profile response. The mean wave height represented macroscopic beach changes such as bar and berm development most satisfactorily, whereas microscopic phenomena such as threshold of transport and ripple formation were better described by use of significant wave height.

143. Nishimura and Sunamura (1987) applied a numerical model to simulate a number of test cases from the large wave tank experiments by Kajima et al. (1983a). The cross-shore transport rate expression employed the Ursell number and a mobility parameter proposed by Hallermeier (1982). The numerical model had the capability of generating bars but failed to predict bar location.

144. Boczar-Karakiewicz and Davidson-Arnott (1987) proposed the non-linear interaction between shallow-water waves as a possible cause of bar formation. A mathematical model was developed to predict the generation of bars, and model results were compared with field data.

145. Kraus and Larson (1988a) described the large wave tank experiments on beach profile change performed by Saville (1957) and a similar experiment performed by the US Army Corps of Engineers, giving a listing of all the data.

146. Nairn (1988) developed a cross-shore sediment transport model involving random wave transformation. Two different methods of wave height transformation were investigated, namely using the root mean square wave height as a representative measure in the wave height calculations and the complete transfer of the probability density function based on the response of individual wave components.

147. Möller and Swart (1988) collected data on beach profile change on a natural beach at Oranjemund on the South West African coast during a severe

storm event. Artificial beach nourishment was carried out during the storm to prevent beach recession, and the event involved some of the highest loss rates recorded.

148. Seymour and Castel (1988) evaluated a number of cross-shore models (the concept of a model taken in a very general sense), focusing on their possibility of predicting transport direction. Of the models studied, the one proposed by Hattori and Kawamata (1981) proved to have the highest predictive capability when applying it to three different field sites. Most models were not considered successful at predicting transport direction.

149. Fenaish, Overton, and Fisher (1988) and Overton and Fisher (1988) studied dune erosion induced by swash action and developed a numerical model based on laboratory and field measurements. The amount of dune erosion during an event was linearly related to the summation of the impact force from the individual swashes.

150. Sunamura (in press) gave a comprehensive summary of beach profile morphology presenting quantitative relationships for many of the geometric parameters of the beach profile. Laboratory data were mainly used to derive the predictive equations. Furthermore, a descriptive model of three-dimensional beach change was proposed consisting of eight topographic stages delineated by a dimensionless quantity (breaking wave height squared to the product of gravitational acceleration, median grain size, and wave period squared).

Synthesis of Previous Work

151. This section summarizes findings from previous work of particular relevance to this study. The role of breaking waves in bar formation was pointed out in pioneering field studies by Lehmann (1884), Hartnack (1924), Evans (1940), King and Williams (1949), and Shepard (1950). Numerous early laboratory investigations also showed that breaking waves were a main cause of bar genesis, e.g., Waters (1939), Keulegan (1948), Rector (1954), and Saville (1957). Wave breaking generates turbulent motion and provides the necessary mechanism for suspending and keeping sediment in suspension, thus mobilizing the grains for transport by mean currents. The importance of transport as

suspended load in the surf zone was emphasized by Dean (1973) and verified through measurements under prototype-scale laboratory conditions by Dette (1986) and under field conditions by Kraus and Dean (1987) among others.

152. Although profile change is highly stochastic on a microscale involving turbulence, movement of individual and collective grains, and various types of organized flows, if viewed on a macroscale, changes in the profile are surprisingly regular and consistent with respect to large features such as bars and berms. Several landmark studies, such as Keulegan (1945), Shepard (1950), Hands (1976), and Sunamura (in press) have characterized the geometry of morphologic features of beach profiles in the field. The possibility of successfully describing morphologic features under complex wave and water level conditions, as indicated by the above studies, formed much of the early foundation of the present study in the development of a numerical model of beach profile change.

153. It was shown by Sonu (1969), Short (1979), Sasaki (1983), Wright and Short (1984), and Sunamura (in press) that even very complex three-dimensional beach changes may be described by a small number of schematized beach states characterized by different values of one or two nondimensional parameters. Consequently, if the main processes of beach profile change are identified, response of the profile to wave and water level variations may be predicted based on semi-empirical relationships developed from relevant data.

154. Several criteria for delineating bar and berm profile response expressed in terms of wave and sediment properties have been proposed. The first criterion involved only wave steepness (Waters 1939, Scott 1954), whereas later-developed criteria included nondimensional quantities characterizing the beach sediment (Kemp 1961; Iwagaki and Noda 1963; Nayak 1970; Dean 1973; Sunamura and Horikawa 1975; Rushu and Liang 1986; Kriebel, Dally, and Dean 1987). The formation of bar and berm profiles is closely related to the direction of cross-shore transport. Criteria similar to those used to distinguish between bar and berm formation have been applied to determine transport direction (Rector 1954, Hattori and Kawamata 1979).

155. The existence of an equilibrium profile, a profile of constant shape which is approached if exposed to fixed wave and water level conditions, was proven to be a valid concept under laboratory conditions by Waters (1939),

Rector (1954), and Swart (1977). Bruun (1954) proposed a power law to relate water depth to distance offshore, which was given support by Dean (1977) on theoretical grounds. The empirical shape parameter in this simple power equation was related to grain size by Moore (1982).

156. Characteristics of cross-shore sand transport were studied first by Keulegan (1948) and King and Williams (1949) through trap measurements in laboratory wave tanks. By integrating the mass conservation equation between consecutive profiles in time, the net cross-shore transport rate distribution can be obtained, as discussed by van Hijum (1975, 1977); Watanabe, Riho, and Horikawa (1981); Kajima et al. (1983a, b); and Shimizu et al. (1985). Classification of the cross-shore transport rate distributions has been performed by Sawaragi and Deguchi (1981), Kajima et al. (1983a), and Shimizu et al. (1985).

157. Various formulas for predicting the cross-shore sand transport rate have been expressed in terms of local fluid velocity (Bagnold 1963, 1966; Bailard and Inman 1981); local shear stress (Madsen and Grant 1977, Shibayama and Horikawa 1980a, Watanabe 1982); and local energy dissipation per unit volume (Moore 1982, Kriebel 1982, Kriebel and Dean 1985a). A cross-shore transport equation based on energy dissipation per unit volume under breaking and broken waves was successfully applied in engineering numerical models for predicting beach profile change (Moore 1982, Kriebel 1982, Kriebel and Dean 1985a).

158. Several numerical models for predicting beach profile change have been developed, although few have been used for engineering predictions. Many of the earlier models included mechanisms for bar generation that did not explicitly assume breaking waves as the primary factor (Felder 1978, Nilsson 1979). Numerical models of profile change based on breaking waves as the cause of bar formation were developed by Dally (1980), Dally and Dean (1984), Moore (1982), Kriebel (1982), and Kriebel and Dean (1985a). At present, the most successful and widely used numerical model is that developed by Kriebel (1982) and Kriebel and Dean (1985a), and it has been applied to a number of sites along the U.S. coast (Kriebel and Dean 1985b, Kraus et al. 1988). However, this model does not incorporate bar formation and movement, nor does it simulate beach accretion.

159. In the present work, an empirically-based model of beach profile change is developed with the express aim of replicating the dynamics of macroscale features of bars and berms by using standard data available in most engineering applications.

PART III: DATA EMPLOYED IN THIS STUDY

Data Acquisition Approaches

160. Three approaches can be used to obtain data for studying beach profile change and the underlying physical processes; laboratory experiments using small wave tanks, field measurements, and experiments employing large wave tanks. For reference, a small wave tank is considered to generate wave heights on the order of 0.1 m, whereas wave heights on the order of 1 m can be generated in large wave tanks.

Small-scale laboratory approach

161. Numerous laboratory studies of beach profile change have been performed with small wave tanks (for example, Waters 1939, Bagnold 1940, Keulegan 1945, 1948, Nayak 1970, Rector 1954, Scott 1954, Watts 1954, Watts and Dearduff 1954, McKee and Sterrett 1961, Iwagaki and Noda 1963, Sunamura 1975, Sunamura and Horikawa 1975, Hughes and Chiu 1981, van Hijum and Pilarczyk 1982, Shibayama 1984). Such experiments have proven valuable for identifying potential parameters controlling beach change and qualitatively describing profile features. However, as demonstrated in a landmark paper by Saville (1957), in which profile change generated in small and large wave tanks was compared, a large scale effect is introduced through the magnitude of the wave height. Other independent variables may also produce a scaling distortion, and generally applicable scaling laws for interpreting results of small-scale movable bed models of beach change have yet to be determined (Hughes 1983, 1984, Sayao 1984, Vellinga 1984). Thus, data sets from laboratory experiments performed with small-scale facilities are of limited value for establishing quantitative understanding of profile change in nature.

Field approach

162. Field data sets useful for quantitative study of beach profile change are extremely rare because of the required high resolution in time and space of morphology and associated wave climate and water level. Because of the great spatial and temporal variability of waves and the three-dimensional character of nearshore bathymetry in the field, it is difficult to extract conclusive cause and effect relationships between waves and profile change

resulting solely from the wave-induced, cross-shore component of sediment transport. Recently, Birkemeier (1985a), Sallenger, Holman, and Birkemeier (1985), and Howd and Birkemeier (1987) have reported results from repetitive concurrent field measurements of the beach profile, waves, and water level. However, horizontal spacing between measurements along the profile was typically tens of meters, and the time interval between surveys was on the order of a half day to a week, during which wave conditions and water level varied substantially. Hands (1976) quantified several geometric properties of a longshore bar system in Lake Michigan but could not make direct correlations with the waves and water level due to a lack of measurements. Wright, Short, and Green (1985) made daily observations over 6-1/2 years of Narrabeen Beach, Australia, and related gross change in nearshore morphology to a single parameter, the dimensionless fall speed, discussed further below.

163. Several descriptive models of beach profile change have been developed based on field observations and measurements, but these are primarily statistical or conceptual and are not capable of quantitative prediction (e.g., Evans 1940; King and Williams 1949; Shepard 1950; Bascom 1951; Sonu 1969; Davis and Fox 1972; Davidson-Arnott 1975; Aubrey, Inman, and Nordstrom 1977; Owens 1977; Short 1979; Sasaki 1983; Takeda 1984; Wright and Short 1984; Wright, Short, and Green 1985; Wright et al. 1986; Sunamura in press).

Prototype-scale laboratory approach

164. The third approach available for quantitative investigation of beach profile change is use of large wave tanks (LWT). Such facilities enable controlled reproduction of near-prototype conditions of beach slope, wave height and period, turbulence induced by wave breaking, and resultant sediment transport and beach change. The problem of scaling is eliminated, and the required high resolution measurement of the profile can also be attained. Disadvantages associated with wave tanks include contamination by reflection from the beach and wave generator and formation of wave harmonics (Buhr Hansen and Svendsen 1975). Experience suggests that these factors are negligibly small under reasonable experiment design.

165. Experiments using LWTs have been performed with monochromatic waves (Saville 1957; Caldwell 1959; Kajima et al. 1983a, b; Dette and Uliczka 1987a; Kraus and Larson 1988a) and irregular waves with random heights and

periods (Vellinga 1986, Dette and Uliczka 1987b, Uliczka and Dette 1987). Irregular waves will most closely reproduce naturally occurring profile change. Mimura, Otsuka, and Watanabe (1987) compared beach change produced in a small laboratory wave tank by irregular waves and corresponding representative monochromatic waves. They found that macroscale patterns of profile change, such as bar and berm development, were similar if representative monochromatic waves were chosen as the mean wave height and period of the irregular wave train. On the other hand, microscale features, such as initiation of sand motion and ripple size, were best described by the significant wave height. Properties compared included profile morphology, cross-shore sand transport rate, and critical depth for sediment motion.

166. Irregular waves introduce additional independent parameters associated with the wave spectrum, whereas in monochromatic wave tests the effects produced by the basic parameters of wave height and period can be isolated and systematically investigated. Hughes and Chiu (1981) discuss theoretical and practical problems associated with use of irregular waves in movable bed modeling. At this first stage of quantification of prototype beach change, it is probably most fruitful to examine the response of the profile to elemental, monochromatic waves.

167. Recently, two independent data sets on beach profile change have become available from experiments performed using LWTs and monochromatic waves (Kajima et al. 1983a, 1983b, Kraus and Larson 1988a). These experiments involved combinations of waves, water levels, beach slopes, and sands of the scale that exist in the field, but with the advantages of true two-dimensionality, control of the external (wave) force, and an optimized measurement schedule. These data sets formed the core data for this study and are described next.

Laboratory and Field Data Sets

Laboratory data

168. Two data sets on beach profile change generated in experiment programs using LWTs were employed. These independent data sets allowed systematic examination of profile evolution through time for a wide range of

realistic incident wave heights and periods, water levels, initial beach slopes, and sand grain sizes. The LWT facilities generated monochromatic waves, so that phenomena associated with random waves as occur in nature, such as wave grouping and long period wave motion, were absent. This simplification is viewed as an asset in the present study, allowing focus on transport produced solely by short-period incident waves without ambiguities.

169. One data set was obtained in experiments performed by the US Army Corps of Engineers (CE) in the years 1956-1957 and 1962 (Saville 1957, Caldwell 1959, Kraus and Larson 1988a) at Dalecarlia Reservation, Washington, DC. The second data set pertains to experiments performed at the Central Research Institute of Electric Power Industry (CRIEPI) in Chiba, Japan (Kajima et al. 1983a, b).

CE experiments

170. The CE experiments were performed using American customary units. Conversion is made here to metric units to achieve generality, but customary units are retained for equipment specifications. The concrete tank used was 193.5 m long, 4.6 m wide, and 6.1 m deep (635 x 15 x 20 ft). The standard operating depth of the tank was 4.6 m (15 ft), which required a water volume of approximately 3,800 m^3. A mobile instrument carriage mounted on rails on top of the tank carried equipment and personnel for making measurements. A picture of the CE tank is displayed in Figure 2, in which the wave generator and instrument carriage are seen at the far end of the tank.

171. The wave generator consisted of a vertical bulkhead 4.6 m (15 ft) wide and 7.0 m (23 ft) high mounted on a carriage which moved back and forth on rails to create the wave motion. The carriage was given oscillatory movement by arms 13 m in length (42 ft 9 in.), connected to two driving discs. Each disc was 5.8 m (19 ft) in diameter, weighed 12.7 tons, and was driven through a train of gears by a 510-hp variable speed electric motor. Wave periods between 2.6 and 24.8 sec could be generated by a gearing mechanism, and the maximum usable wave height at the standard operating depth was approximately 1.8 m (6 ft). Figure 3 gives a view of the wave generator, where the bulkhead is seen in the front of the picture and the two rotating discs are distinguished in the back. The experimental facility is further described by Raynor and Simmons (1964) and Kraus and Larson (1988a).

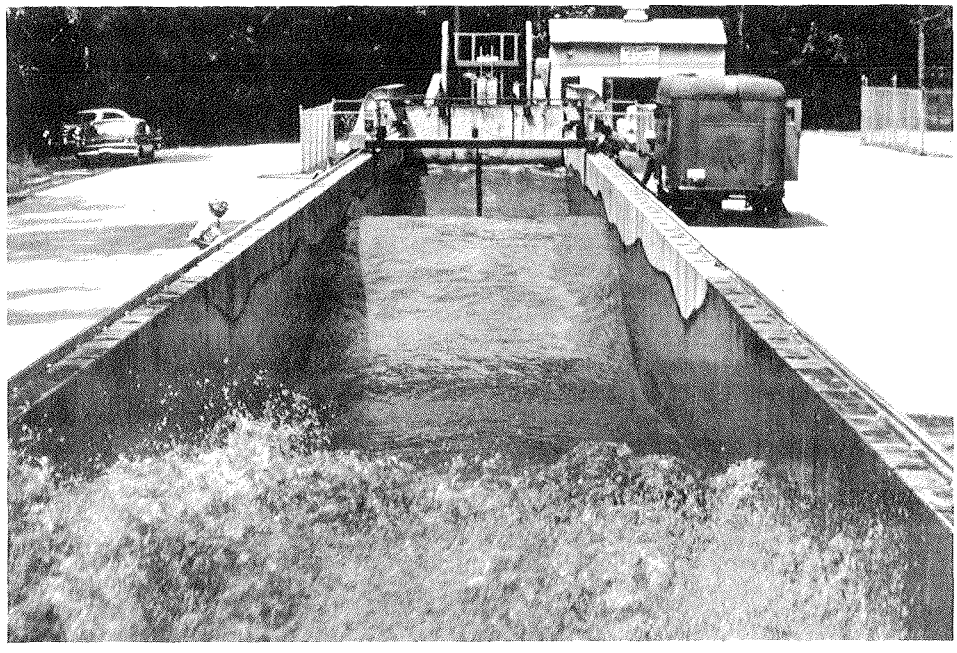

Figure 2. Tank for Large Waves at Dalecarlia Reservation

172. Eighteen distinct cases have been documented (see Kraus and Larson 1988a) of which all but two were started from a plane slope of 1:15. Approximately 1,500 m^3 of sand were needed to grade the plane initial slope, which was done with a small bulldozer. The wave parameters ranged from periods between 3.75 and 16.0 sec and generated wave heights between 0.55 and 1.68 m in the horizontal part of the tank. The wave height, wave period, and water depth were held constant during a run, except in one case for which the water level was varied to simulate a tide. The water depth ranged from 3.5-4.6 m in the different cases, and two grain sizes were used with median diameters of 0.22 and 0.40 mm. The 0.22-mm grain size was employed in the 1956-57 experiments, and the 0.40-mm grain size was used in the 1962 experiments. The specific gravity of the sand grains was 2.65. Waves were run until a stable beach profile had developed and no significant changes were detected, which normally occurred after 40-60 hr. The term "case" will be used to describe a

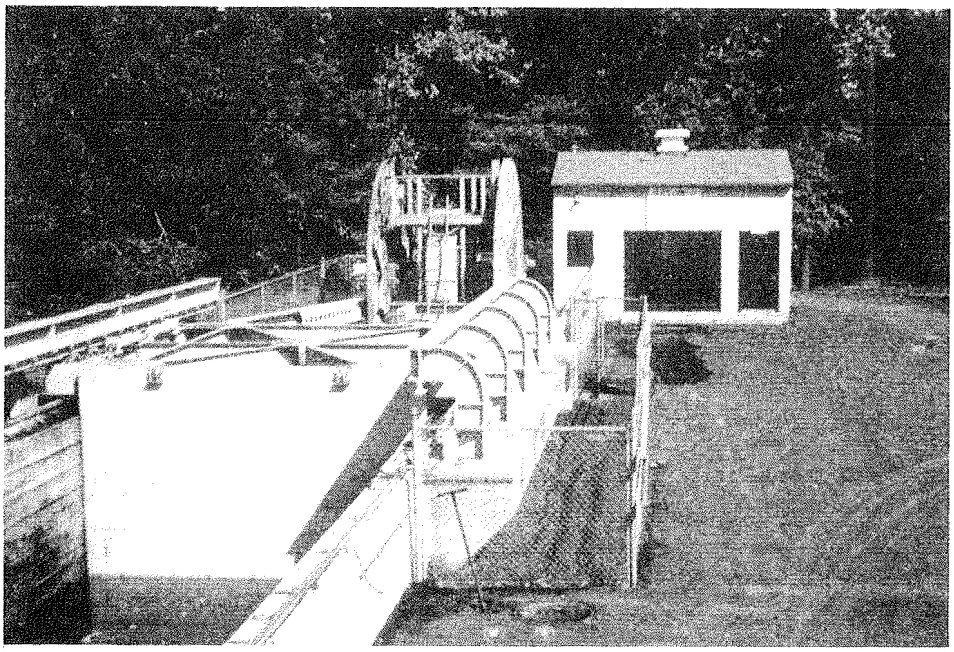

Figure 3. View of the wave generator in the LWT

collection of profile surveys for a unique combination of incident waves, beach slope, and grain size. A "run" is more loosely used to refer to either a case or an interval of wave action between two profile surveys.

173. Profile surveys were made intermittently during a run with shorter time increments in the beginning when large profile changes where expected. On the order of 10-15 profile surveys were made during a typical case, and the survey interval was 1.2 m (4 ft). For the initial cases with the 0.22-mm sand and all cases with the 0.40-mm sand, profiles were surveyed along three different lines in the tank*. Corresponding differences in depth between the three lines were small, and for the 0.22-mm sand only the survey along the center line was retained. However, for the 0.40-mm sand, although the cross-tank depth difference was small, surveys along three lines were made through

* Personal Communication, 1986, George W. Simmons, Former Engineering Technician, Beach Erosion Board, Dalecarlia Reservation, Washington, DC.

the entire experiment series, and the profile depths used in this report are an average of the three lines.

174. The numbering of the CE cases is discussed by Kraus and Larson (1988a) and essentially agrees with the system used by Hallermeier (1987). Table 1 summarizes the CE cases which started from a plane slope of 1:15, giving the wave and water level conditions. The deepwater wave steepness is also listed and was calculated using linear wave theory. Two cases not given in Table 1 were conducted from an initial profile that was irregular (Cases 510 and 610). Also, a repetition run was performed for Case 100 (Case 110), and satisfactory agreement was achieved between the two cases (Saville 1957). In Case 911 the water level varied stepwise in a sinusoidal manner, but the wave and sand parameters were identical to those in Case 901. The period of the water level variation was approximately 12 hr, the amplitude 0.45 m, and the mean water level 3.96 m.

175. The wave height was measured with a step resistance gage placed in a fixed position at the toe of the beach during the experiments. The incident wave was measured before any reflection occurred against the wave paddle. The accuracy of the wave measurements was about 3 cm (0.1 ft), and the wave period was quite accurately set due to the large stroke length of the wavemaker and fixed gear ratio. For most of the cases the breaking wave height and breaker location were estimated visually at specific times during a run.

CRIEPI experiments

176. The CRIEPI LWT is similar in size to the CE LWT, except that it is somewhat narrower (205 x 3.4 x 6 m). The experiment program consisted of 24 cases with wave periods ranging between 3.0 and 12.0 sec and generated wave heights between 0.3 and 1.8 m. A summary of the CRIEPI cases is given in Table 2, in which the numbering is identical to that used by Kajima et al. (1983b). All CRIEPI cases were performed with monochromatic waves and fixed water level. Many of the cases started from a plane beach slope (17 of the 24), but the initial slope was varied, ranging from 1:50 to 1:10 in individual cases.

177. As in the CE experiments, two different grain sizes were used, 0.27 mm and 0.47 mm. For the present study the CRIEPI profile survey was digitized from charts enlarged from those given by Kajima et al. (1983b) with

Table 1

CE Experiments: Wave Height, Wave Period, and Water Depth in the Horizontal Section of the Tank and Deepwater Wave Steepness

Case No.	Wave Height m	Wave Period sec	Water Depth m	Deepwater Wave Steepness
		0.22-mm Sand		
100	1.28	11.33	4.57	0.0054
200	0.55	11.33	4.57	0.0023
300	1.68	11.33	4.27	0.0070
400	1.62	5.60	4.42	0.0351
500	1.52	3.75	4.57	0.0750
600	0.61	16.00	4.57	0.0011
700	1.62	16.00	4.11 (3.81)*	0.0028
		0.40-mm Sand		
101	1.28	11.33	4.57	0.0054
201	0.55	11.33	4.57	0.0023
301	1.68	11.33	4.27	0.0070
401	1.62	5.60	4.42	0.0351
501	1.52	3.75	4.57	0.0750
701	1.62	16.00	3.81	0.0028
801	0.76	3.75	4.57	0.0377
901	1.34	7.87	3.96	0.0129
911	1.34	7.87	3.96**	0.0129

* Water level decreased after 10 hr.
** Mean of variable water level.

Table 2

CRIEPI Experiments: Wave Height, Wave Period, and Water Depth in the Horizontal Section of the Tank, Initial Beach Slope, and Deepwater Wave Steepness

Case No.	Wave Height m	Wave Period sec	Depth m	Beach Slope	Deepwater Wave Steepness
			0.47-mm Sand		
1-1	0.44	6.0	4.5	1/20	0.0082
1-3	1.05	9.0	4.5	1/20	0.0075
1-8	0.81	3.0	4.5	1/20	0.0607
2-1	1.80	6.0	3.5	3/100	0.0313
2-2	0.86	9.0	3.5	3/100	0.0058
2-3	0.66	3.1	3.5	3/100	0.0473
			0.27-mm Sand		
3-1	1.07	9.1	4.5	1/20	0.0074
3-2	1.05	6.0	4.5	1/20	0.0196
3-3	0.81	12.0	4.5	1/20	0.0029
3-4	1.54	3.1	4.5	1/20	0.108
4-1	0.31	3.5	3.5	3/100	0.0178
4-2	0.97	4.5	4.0	3/100	0.0335
4-3	1.51	3.1	4.0	3/100	0.107
5-1	0.29	5.8	3.5	1/50	0.0057
5-2	0.74	3.1	3.5	1/50	0.0533
6-1	1.66	5.0	4.0	1/10	0.0456
6-2	1.12	7.5	4.5	1/10	0.0125

a length increment of 0.5 or 1.0 m depending on the resolution necessary to distinguish principal features of the profile shape. The accuracy of the digitization is judged to be compatible with the profile surveys of the CE data, which is on the order of ± 1.5 cm in the vertical coordinate. No attempt was made to distinguish small-scale profile features such as ripples.

178. In the CRIEPI experiments wave height along the profile was measured from a vehicle mounted on rails on top of the tank. To confirm the two-dimensionality of the experiment, profiles were surveyed along three lines in the tank during the first few runs. Because the depth difference was small between the three survey lines, only the center line was surveyed in later cases (Kajima et al. 1983a). Wave measurements were usually carried out between profile surveys, and wave setup was determined. Plunging, spilling, and surging breaking waves were observed, although plunging breakers occurred in the majority of cases. Cases started from nonplanar bottom (in most cases the beach profile that remained from the previous test case) are not included in Table 2, namely Cases 1-2, 1-4, 1-5, 1-6, 1-7, 4-4, and 6-3.

Field data

179. At the Field Research Facility (FRF) of the Coastal Engineering Research Center (CERC) located at Duck, North Carolina, profile surveys are made regularly together with measurements of the wave and water level climate. During the period 1981-1984, four shore-normal profile lines (Lines 58, 62, 188, and 190) were surveyed approximately every 2 weeks with a typical spacing between survey points of 10 m (Howd and Birkemeier 1987).

180. Wave data are tabulated at 6-hr intervals based on a 20-min record at a wave gage (Gage 620) located at the end of the research pier, and data are simultaneously collected by a Waverider buoy off the end of the pier in 18 m of water (Gage 625). Water level is measured at 6-min intervals by a tide gage mounted at the end of the pier, and the record consists of the total change, including both tide and storm surge. Water level measurements used in the present study are averages over 1-hr intervals.

181. The profile change data set from the FRF is the most detailed known, encompassing profile surveys, water level, and wave data, and showing both seasonal and short-term changes in the beach profile. The FRF data set was primarily used for verifying the numerical model of beach profile change.

Summary

182. Use of two independent data sets from LWT studies is expected to increase reliability of relationships derived between the incident waves and features of the beach profile. Also, by restricting consideration to data from LWT experiments (as opposed to small-scale experiments), it is believed that scaling effects are eliminated and that the processes occurring during bar and berm formation in the field are closely reproduced in the wave tanks. Relationships developed from the LWT experiments can then be assessed for their applicability to the field by use of the quality FRF data set.

PART IV: QUANTIFICATION OF MORPHOLOGIC FEATURES

183. The literature review presented in Part II revealed the remarkable fact that relatively few studies have been made to quantitatively characterize the shape of the beach profile. Even fewer studies have attempted to deterministically describe the response of the profile to the waves incident upon it. Development of a quantitative description of the observed dynamics of the profile in terms of the incident waves, therefore, appeared to be a valuable approach with which to begin this investigation, as well as a logical and necessary one in the path toward development of a predictive model of profile change. Precise knowledge of the morphology and dynamics of the profile is necessary both for understanding of the subject being studied and development of the predictive model.

184. As discussed in Part I, at this first stage of developing a quantitative deterministic description of the beach profile and its change, use of data obtained in experiments performed with large wave tanks was judged to be the best approach. The experiment condition of regular waves is considered an advantage for isolating the effect of breaking waves on the beach. The authors believe this to be the dominant process producing bar formation and much of the change in the beach profile under most environmental conditions. Solid understanding of profile change produced by breaking waves will further understanding of other possible contributing processes, since in nature all forcing agents act concurrently and their individual contributions are difficult to distinguish. Firm knowledge of one will aid in understanding the others.

185. The main purpose of the analysis described in this chapter is to establish the most important parameters governing beach profile evolution in terms of the wave and sediment characteristics. This procedure is expected to provide fundamental information on the response of the profiles and facilitate a physically based approach for development of the numerical model. The results are of interest in themselves in understanding beach profile response as well as for computation of cross-shore sand transport rates and profile change. Clear connections between cause (waves) and effect (profile change) as elucidated in the large wave tanks is expected to provide guidance for

applying a similar approach in analysis of field data where profile change is produced by the combination of a number of different forcing agents and is prone to ambiguity.

Data Analysis Procedure

186. In this study, morphologic profile features of interest are formations created by wave action, directly or indirectly, during time scales much greater than the wave period. To numerically evaluate properties of morphologic features, the survey data were approximated by a set of cubic spline polynomials, producing on the order of 75-250 polynomials per profile. This representation allowed geometric properties such as volumes, distances, depths, and slopes to be determined analytically once the spline coefficients were calculated. Also, by using the interpolation polynomials, a continuous and accurate description of the profile depth with distance offshore was obtained from the discrete depth values at survey points.

187. A fundamental problem immediately encountered in quantitative analysis of a morphologic feature is specification of an unambiguous definition that will preserve the characteristics intuitively associated with it. For example, a bar is normally considered to be a subaqueous accretionary feature formed of sand redistributed and deposited along the profile. From observation of a natural barred beach profile it is easy to determine the crest of a bar and hence the approximate location of the bar, whereas it is much more difficult to define or agree upon the exact cross-shore length of a bar, a quantity which is needed if a volume calculation is to be done. Keulegan (1945) used the concept of a barless beach profile to which bar properties could be referenced. The barless profile is constructed by drawing lines joining maximum trough depths along the profile with the point of zero depth. Apart from the arbitrary nature of this definition, it is sometimes difficult to determine the seaward limit of the bar by this method.

188. Use of points where the second derivative (radius of curvature) is zero to define a bar is found to be convenient if applied on the shoreward side of a bar, where the curvature of the profile changes sign going from

trough to crest. However, often no such point exists on the seaward side of a bar since an immediate trough may not be present.

189. In the present study, it was found most natural and productive to define morphologic features with respect to the initial profile, since a time sequence of profiles was available. This procedure is, of course, not directly applicable to the field. Areas where sand accretes with respect to the initial profile constitute bar- or berm-like features, whereas areas where material erodes are trough-like in appearance. Figure 4a shows a definition sketch for a beach profile with representative bar and trough features, and Figure 4b illustrates the corresponding berm case. Nomenclature describing the geometric properties is given in the figures, and a typical wave height envelope is outlined in Figure 4a.

190. As a result of relating bar properties to the initial profile, some properties, such as bar volume, will depend on the initial profile slope. For example, two erosional profiles formed of sand of the same grain size and exposed to the same wave climate will show different equilibrium bar properties if the initial slopes differ. However, the inshore slopes of the equilibrium profile will still be similar (Kamphuis and Bridgeman 1975), but different amounts of material will be redistributed within the profile. In this respect, bar volume is a function of initial profile slope, which makes such a definition less useful in field data analysis for some bar properties.

191. Definition of morphologic features with respect to the initial profile does not affect net sand transport rate distributions, which only depend upon two consecutively surveyed profiles in time, as will be shown. Furthermore, the main objective of the data analysis is to identify the dominant factors of beach profile change, supporting development of the numerical model. These factors can be distinguished with any reasonable if arbitrary definition of the profile features if it is consistently applied through time. For example, the aforementioned bar definition of Keulegan (1945) would give different values of bar volume with time, but the trend of bar development toward equilibrium and the factors controlling its growth would be similar to those determined by the definition employed here.

192. Only those cases in the data base with an initially plane profile slope were used in calculation of morphologic features to more easily allow

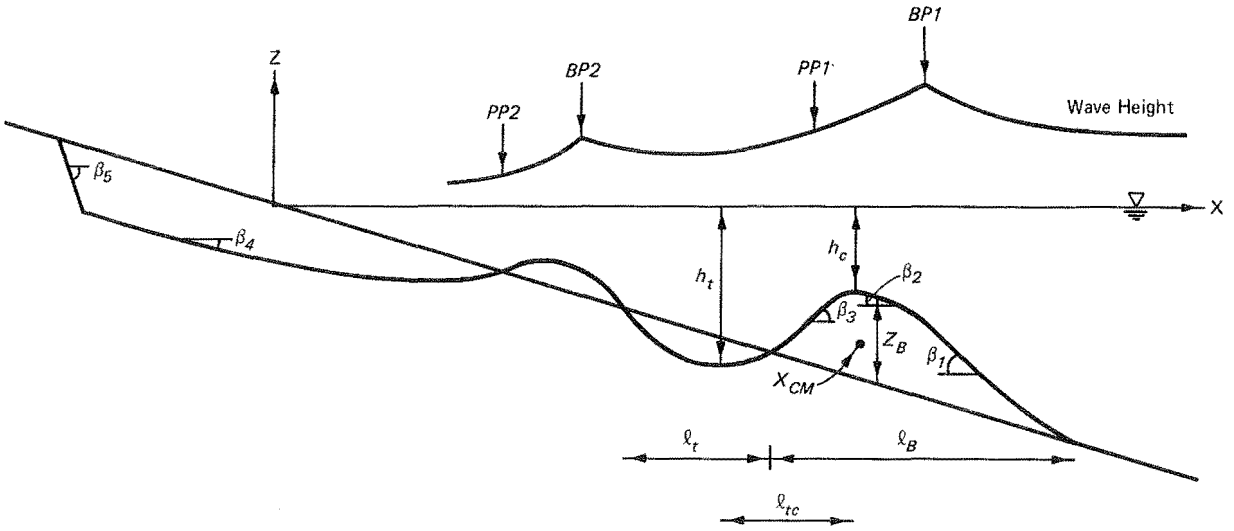

a. Bar profile

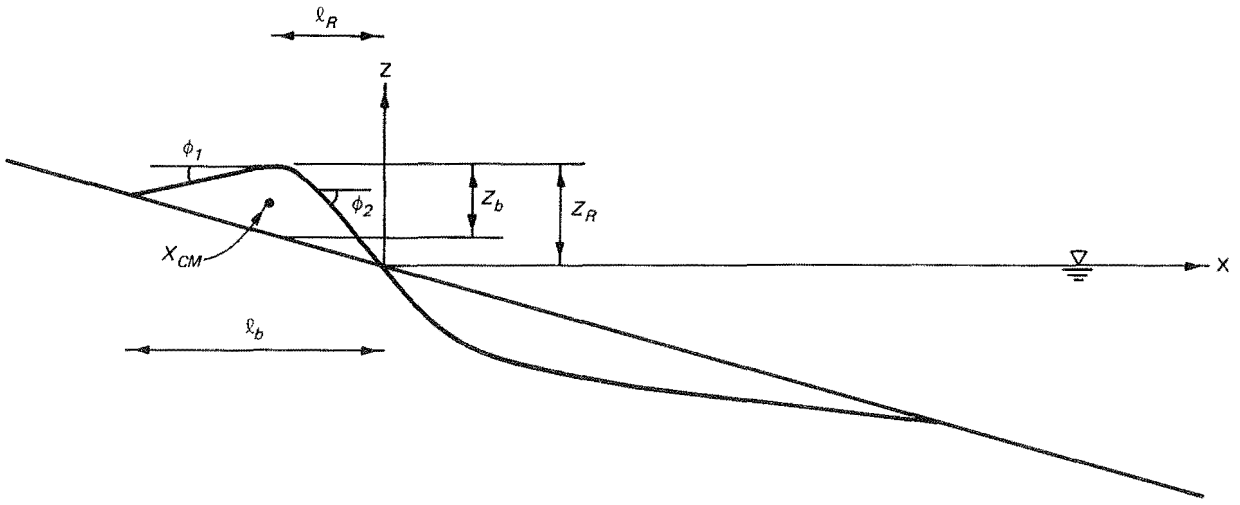

b. Berm profile

Figure 4. Notation sketch for beach profile morphology

comparison among various cases and to more clearly identify relationships between wave parameters and beach profile evolution. Definition of morphologic features with respect to the initial profile involves no limitations in characterizing the behavior of the features or understanding the fundamentals of profile response to wave action. Rather, a clear definition allows strict interpretation of where a bar, berm, or trough is located. Definition of a morphologic feature related to a specific profile has no meaning if a single profile is studied. The objective here is not to advocate a general definition of a bar or other feature applicable to an arbitrary beach profile but to employ a useful definition as a means for understanding the process of beach profile change and facilitating a quantitative description of the dynamic response of morphologic features.

193. An extensive correlation and regression analysis was carried out to investigate relations between geometric properties of the various morphologic features of the profile and the wave and sand characteristics. An overview of the statistical procedures used is given in Appendix A. The primary parameters used were: wave period T or deepwater wavelength L_o, deepwater wave height H_o, breaking wave height H_b, water depth h, median grain size D, sand fall speed w, and beach slope $\tan\beta$. Also, various nondimensional quantities were formed, both for deepwater and breaking wave conditions, such as H/L, H/wT, $\tan\beta/(H/L)^{1/2}$, D/H, and D/L, in which H and L are the local wave height and wavelength, respectively.

Concept of Equilibrium Beach Profile

194. A fundamental assumption in the study of beach profile change is the existence of an equilibrium profile which a beach will attain if exposed to constant wave conditions for a sufficiently long time. The idea is that the beach profile in its equilibrium state dissipates incident wave energy without significant net change in shape. If an equilibrium profile did not exist, the beach would continue to erode (or accrete) indefinitely if exposed to the same wave conditions and with no restrictions in the sand supply.

195. The concept of an equilibrium profile is an idealization that cannot be fully achieved in practice, since waves, water level, water tempera-

ture, and other conditions cannot be held perfectly fixed. Also, wave breaking and turbulence formed at the bottom and injected from the surface by wave breaking introduce randomness in the microscale sand motion, with resultant small continuous adjustments of the profile. Nevertheless, at a macroscale level, it has been demonstrated that an equilibrium profile can be approached, in which no significant systematic net sand transport occurs, although small perturbations still remain. Numerous laboratory studies (e.g., Rector 1954, Nayak 1970, Swart 1975) as well as the data used in this study support the equilibrium beach profile concept, since profile changes diminish with time and the beach profile approaches a stable shape.

196. From a theoretical viewpoint, it is of minor importance if the equilibrium profile is never realized in the field due to variable waves and water level, and complex three-dimensional hydrodynamic processes, as long as the concept is verified by experiment. Of course, from a practical point of view, it is of great significance if a natural beach of a certain representative grain size has a preferred shape under a given wave climate.

197. As an indicator of the approach of the beach to an equilibrium shape, cumulative change along the profile was calculated. Cumulative change was defined as the sum of the absolute differences in bottom elevation between initial profile and profile at a specific time (see also Shimizu et al. 1985). This quantity is plotted in Figure 5 for selected CE and CRIEPI cases.

198. The cumulative profile change will ideally approach a constant value under constant applied waves as the beach profile attains the equilibrium shape. The decrease in slope of the curves in Figure 5 is a measure of the rate at which equilibrium is approached. Some transport activity will always exist because of unsteadiness in experiment conditions, fluid turbulence, and random character of sand motion, and thus profile change will fluctuate about the equilibrium shape. Some cases exhibited cumulative change which had not completely leveled off at the end of the run, but the rate of change was still an order of magnitude smaller than the initial rate. Decreasing rates of accumulated profile change indicate an increasingly stable shape since less material was redistributed along the profile at later times.

199. A greater difference between initial profile and equilibrium profile for a specific wave climate and grain size implies that a greater

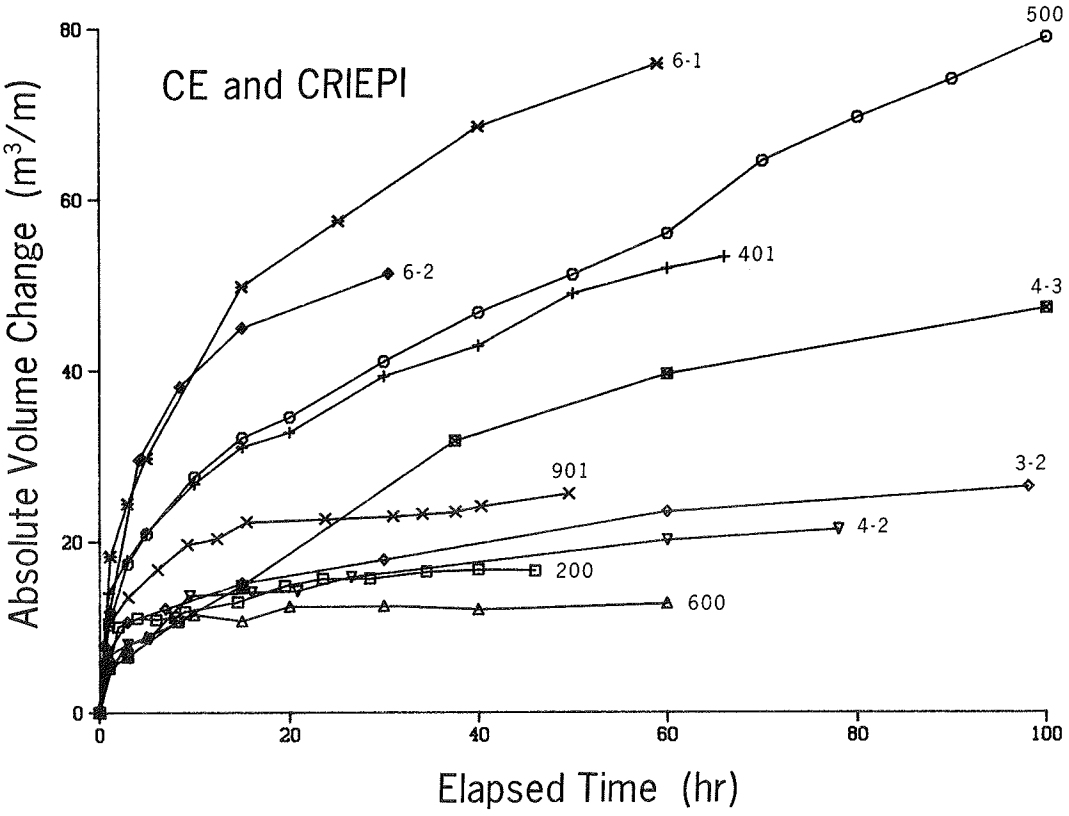

Figure 5. Absolute sum of profile change for selected cases

amount of sand must be redistributed in the process of reaching equilibrium. Dean (1977) derived a simple analytical expression for the beach profile shape in the surf zone based on the concept of a constant dissipation of wave energy per unit water volume. This expression agrees well with the relationship established by Bruun (1954) on empirical grounds from field data. The equilibrium beach profile shape may be written

$$h = Ax^{2/3} \tag{1}$$

where

h = water depth

A = shape parameter

x = cross-shore coordinate (directed positive in the seaward direction)

The shape parameter is mainly a function of grain size, in which a coarser grain size gives a larger value of A and a steeper beach (Dean 1977, Moore 1982). Dean (1987) recently reexpressed the curve of Moore (1982) in terms of

the dimensionless sediment fall speed H/wT, in which H is the local wave height, w is the sand fall speed, and T is the wave period.

200. For an equilibrium profile developed during a storm, during which a bar normally forms in the vicinity of the break point, Equation 1 is expected to apply only to the portion of the surf zone shoreward of the bar, where strong turbulence is present and energy dissipation is related to the breaking wave height and water volume. If wave reformation occurs, several areas along the profile may exist in which profile change is controlled by energy dissipation per unit volume, and the profile in these areas is expected to be well approximated by Equation 1.

Criteria for Distinguishing Profile Response

201. If a beach profile is not in equilibrium with the waves incident upon it, sand will be redistributed as the beach adjusts toward equilibrium shape. Depending on the wave conditions, existing profile shape, and sand properties, the cross-shore sand transport rate will be predominantly directed either offshore or onshore. Offshore transport results in erosion on the upper part of the profile and formation of a notable bar at the break point(s), whereas onshore transport leads to accretion of sand on the foreshore and berm buildup. These two types of profile response forming two distinctly different beach shapes are commonly known as bar/berm profiles (other descriptions are: winter/summer profile, storm/normal profile, erosional/accretionary profile, bar/step profile, bar/nonbarred profile, dissipative/reflective profile).

202. Criteria to distinguish bar and berm profiles have been developed by various authors, and Table 3 gives a summary of several criteria developed for distinguishing beach erosion and accretion or bar/berm profile response which will be discussed below. Note that the criteria of Rector (1954), Dean (1973), and Hattori and Kawamata (1981) originally referred to the direction of cross-shore transport.

Table 3

Criteria for Classifying Bar and Berm Profiles
Erosion and Accretion

Author	Parameters*	Comments
Waters (1939)	H_o/L_o	$H_o/L_o > 0.025$, bar $H_o/L_o < 0.025$, berm
Rector (1954)	H_o/L_o, D/L_o	$D/L_o < 0.0146(H_o/L_o)^{1.25}$, bar $D/L_o > 0.0146(H_o/L_o)^{1.25}$, berm
Iwagaki and Noda (1963)	H_o/L_o, H_o/D	Graphically determined
Nayak (1970)	H_o/L_o, H_o/SD	Graphically determined
Dean (1973) Kriebel, Dally, and Dean (1987)	H_o/L_o, $\pi w/gT$	$H_o/L_o > A\pi w/gT$, bar $H_o/L_o < A\pi w/gT$, berm A = 1.7, mainly lab scale A = 4-5, prototype scale
Sunamura and Horikawa (1975) Sunamura (1980)	H_o/L_o, D/L_o, $\tan\beta$	$H_o/L_o > C(\tan\beta)^{-0.27}(D/L_o)^{0.67}$ (bar) $H_o/L_o < C(\tan\beta)^{-0.27}(D/L_o)^{0.67}$ (berm) (C = 4, small-scale lab. regular waves; C = 18, field)
Hattori and Kawamata (1981)	$(H_o/L_o)\tan\beta$, w/gT	$(H_o/L_o)\tan\beta > 0.5\ w/gT$, bar $(H_o/L_o)\tan\beta < 0.5\ w/gT$, berm
Wright and Short (1984)	H_b/wT	$H_b/wT > 6$, bar H_b/wT = 1-6, mixed bar and berm $H_b/wT < 1$, berm
Present Work	H_o/L_o, H_o/wT	$H_o/L_o < M\ (H_o/wT)^3$, bar $H_o/L_o > M\ (H_o/wT)^3$, berm (M = 0.0007 regular waves in lab., or mean wave height in field)

* Notation: H_o , deepwater wave height; L_o , deepwater wavelength; D , median grain size; S , specific gravity of sand; w , sand fall speed; g , acceleration of gravity; T , wave period; $\tan\beta$, beach slope; H_b , breaking wave height.

Regular waves

203. Examination of cross-shore transport rate distributions inferred from successive profile change (Part V) shows that development of a bar or a berm profile is closely related to the direction of net transport as offshore or onshore, respectively. Thus, a criterion for predicting bar or berm development can also be applied to predict the principal direction of net cross-shore transport. Typically, if a bar forms, the main direction of transport is offshore even if the bar receives a net contribution from the shoreward transport of material originating from areas seaward of the bar (in the situation of a relatively mild wave climate). A criterion which refers to onshore/offshore transport will, in most cases, predict offshore-directed sand movement if a bar is present and onshore-directed movement if a berm is present. However, profiles between bar and berm type may have complex transport distributions where a clear trend for onshore or offshore transport is not apparent. This more complex transport pattern and resultant profile change are left for future study and not pursued further here.

204. From his laboratory experiments performed at small scale, Waters (1939) (summarized in Johnson 1949) found that deepwater wave steepnesses H_o/L_o greater than 0.025 produced a bar profile, whereas values less than 0.025 produced a berm profile. (Waters (1939) used the terminology storm/ordinary profile.) This convenient rule of thumb is still commonly applied to the field situation, but it is known to be incorrect for waves of prototype scale, as first pointed out by Saville (1957). Rector (1954) recognized the occurrence of a transition zone between bar and berm profiles defined by wave steepness values in the range of 0.016-0.025 (for small laboratory waves). Rector (1954) also developed an empirical equation for predicting cross-shore transport direction based on wave steepness and the ratio of median grain size to deepwater wavelength D/L_o .

205. Kemp (1961) defined a "phase difference" parameter in terms of the uprush time (time for the wave to travel from the break point to the limit of uprush) and the wave period. The transition from a berm to a bar profile was considered to occur if the uprush time equalled the wave period. (Kemp (1961) used the terminology bar/step profile.)

206. Iwagaki and Noda (1963) used a combination of two nondimensional parameters, H_o/L_o , and the ratio between deepwater wave height and median grain diameter, H_o/D , to predict erosion and accretion (bar/berm formation). Nayak (1970) approached the problem in a fashion similar to that of Iwagaki and Noda (1963) but included the specific gravity in the denominator of H_o/D .

207. Dean (1973) developed a popular heuristic model of sand transport in which most of the cross-shore transport in the surf zone is assumed to occur as suspended load, by which the sediment fall speed emerges as a significant parameter. The bar/berm predictive criterion developed by Dean (1973) is expressed in terms of H_o/L_o and $\pi w/gT$, in which g is the acceleration due to gravity. Dean (1973) also introduced the dimensionless fall speed parameter H/wT in a conceptual model of suspended sediment movement and developed it as an indicator of cross-shore transport direction. Gourlay (1968), Nayak (1970), and Kohler and Galvin (1973) also used the fall speed parameter as a descriptor of beach profile processes, based mainly on dimensional considerations.

208. Sunamura and Horikawa (1975) and Sunamura (1980) used three parameters in their criterion to predict erosion and accretion, H_o/L_o , D/L_o , and beach slope, $\tan\beta$. Different values of the empirical coefficient in the equation delineating erosion and accretion (bar/berm profiles) were obtained for laboratory and field conditions, and it is of interest that the same functional form of the equation proved valid for both situations.

209. Hattori and Kawamata (1981) developed a criterion for onshore and offshore sand transport based on parameters essentially identical to those used by Dean (1973), except that the initial beach profile slope was combined with the wave steepness parameter.

210. In a milestone experiment using the first LWT in the world, Saville (1957) recognized that the deepwater wave steepness criterion of 0.025 was not accurate for distinguishing bar and berm profiles as produced by large waves in the field. For his LWT experiments, which used regular waves, bar profiles occurred at much smaller values of wave steepness (as small as 0.0028 in the CE experiments), whereas corresponding cases scaled down to 1:10 experienced marked berm buildup.

211. In a study of criteria for the occurrence of bar/berm profiles performed as part of the present work, the deepwater wave steepness H_o/L_o and the dimensionless fall speed parameter H_o/wT were found to be the most reliable parameters. Figure 6 is a plot of the LWT data on profile response as bar or berm (erosion or accretion) together with a line drawn by inspection to best separate the erosional and accretionary cases. This line defines an empirical criterion in terms of the two parameters given by the following equation:

$$\frac{H_o}{L_o} = M \left[\frac{H_o}{wT} \right]^3 \tag{2}$$

in which the empirical coefficient $M = 0.00070$.

212. In classification of the different cases, only prominent features of the profile were considered. For example, a small berm which formed on the foreshore was ignored if a large bar also formed, since the main transport direction during the run was obviously offshore. In such a case, the profile was considered to be a bar profile. Similarly, a small bar may have formed close to the break point in a case where the main trend of transport was onshore by which large berm buildup occurred. The classification of the beach profile response determined here coincides with that used by Kriebel, Dally, and Dean (1987), except for two cases which were designated as mixed response by those authors but as berm type in this study. Similarity in classification indicates that results were not strongly influenced by subjectivity.

213. As an alternative to use of the dimensionless fall speed parameter, the parameter H_o/D suggested by Iwagaki and Noda (1963) and formulated based on small-scale laboratory data was combined with the deepwater wave steepness to yield a criterion for bar and berm profiles for the prototype-scale data. Figure 7 shows that a clear distinction results between bar and berm profiles. The line of delineation between bar and berm profiles is given by

$$\frac{H_o}{L_o} = 4.8\ 10^8 \left[\frac{H_o}{D} \right]^{-3.05} \tag{3}$$

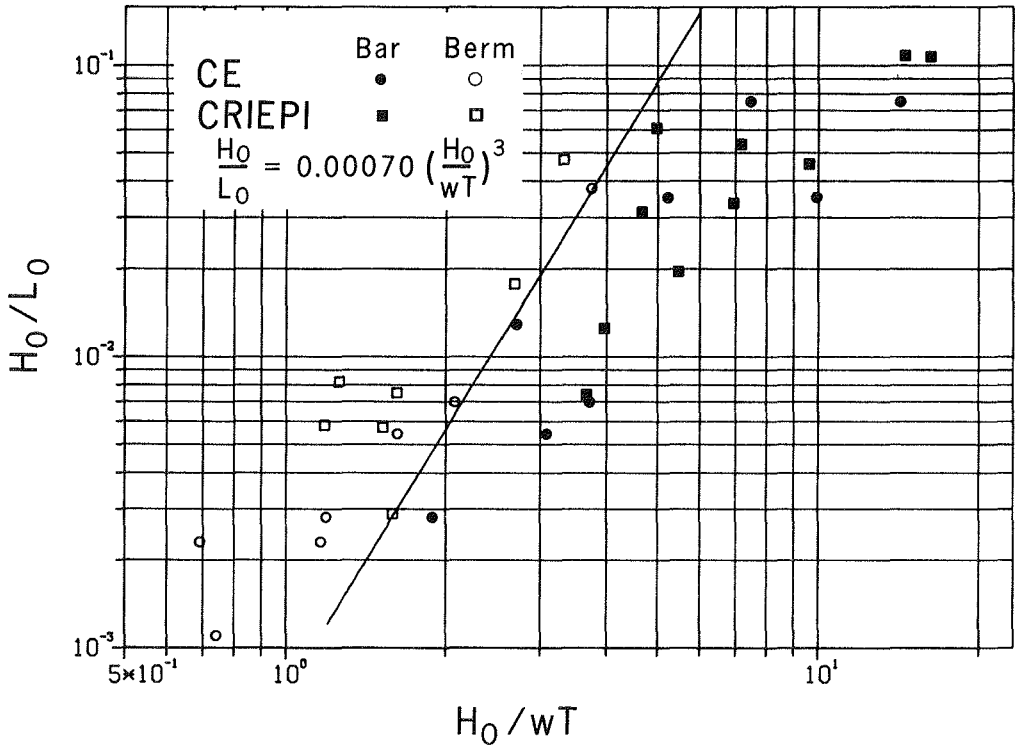

Figure 6. Criterion for distinguishing profile type by use of wave steepness and dimensionless fall speed parameter

214. Starting from the dimensionless fall speed parameter, Dean (1973) derived a criterion using H_o/L_o and the parameter $\pi w/gT$ (Dean parameter). Figure 8 shows the CE and CRIEPI data classified according to these parameters. The equation of the separation line (Line B) is

$$\frac{H_o}{L_o} = 5.5 \frac{\pi w}{gT} \tag{4}$$

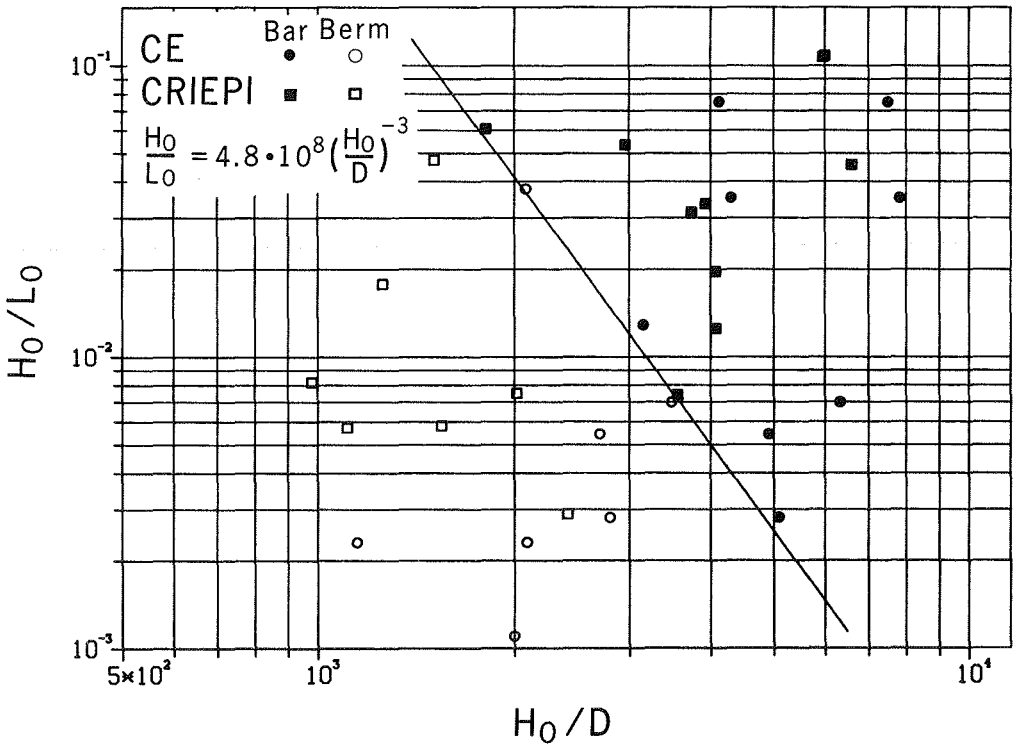

Figure 7. Criterion for distinguishing profile type by use of wave steepness and ratio of wave height to grain size

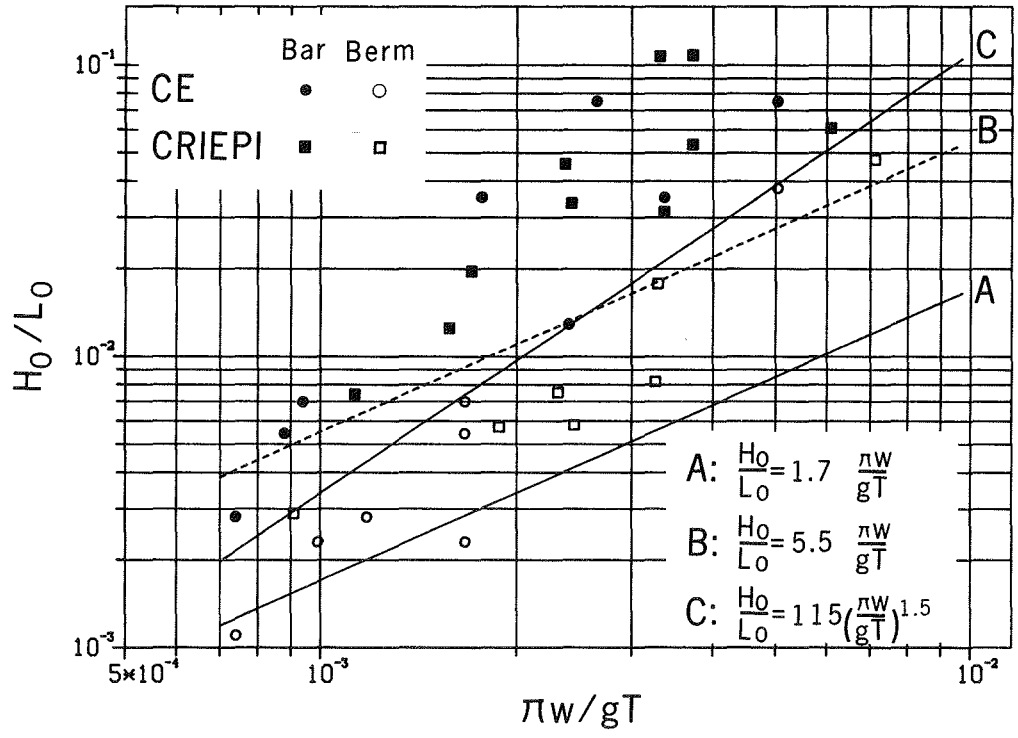

Figure 8. Criterion for distinguishing profile type by use of wave steepness and Dean parameter

215. The value of the empirical coefficient is 5.5 (Line B) and differs from the value of 1.7 (Line A) originally given by Dean (1973) as determined mainly from small-scale laboratory data. Kriebel, Dally, and Dean (1987) reevaluated this coefficient and obtained a band of values in the range of 4-5 using a portion of the CE and CRIEPI data set. It is, however, possible to achieve even a better delineation between bar/berm profiles if the Dean parameter is raised to an exponent (Line C) according to

$$\frac{H_o}{L_o} = 115\left[\frac{\pi w}{gT}\right]^{1.5} \tag{5}$$

Since $L_o \sim T^2$, Equation 5 indicates a relatively weak dependence on wave period.

216. Sunamura (in press) proposed two somewhat different dimensionless quantities for classifying beach profile response involving breaking wave properties instead of deepwater wave conditions, namely D/H_b and H_b/gT^2 . The second parameter is basically the inverse of the Ursell parameter $U = HL^2/h^3$ evaluated at breaking with linear wave theory. By using these two parameters, it was possible to obtain a good classification of profile type (Figure 9), although one point in the data set is located in the wrong area. The equation of the line separating bar/berm profiles is

$$\frac{D}{H_b} = 0.014\left[\frac{H_b}{gT^2}\right]^{0.68} \tag{6}$$

217. In summary, it is possible to obtain a clear distinction between bar profiles and berm profiles and, thereby, a predictor of overall erosion and accretion if the dimensionless quantities chosen to compose the criterion consist of parameters characterizing both sand and wave properties. Significant differences occur, however, in the values of the empirical coefficients in the criteria, depending on whether data from small-scale or prototype-scale experiments are used. Deepwater wave steepness appears in most criteria together with a parameter involving a quantity describing the sediment, such as the fall speed or grain size. In a theoretical sense, the sediment fall

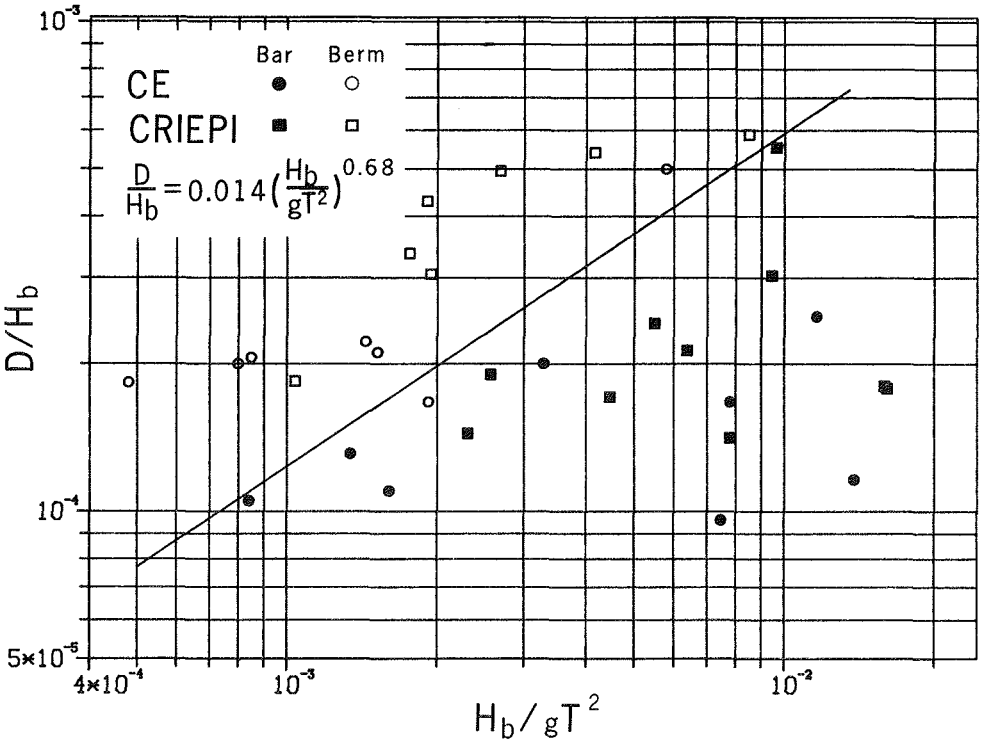

Figure 9. Criterion for distinguishing profile type by use of ratio of breaking wave height and grain size, and Ursell number at breaking

speed is superior to the grain size in development of profile classifications, as it incorporates both grain shape and fluid viscosity (water temperature).

218. An attempt was made to incorporate initial beach slope in the criteria for bar/berm profile classification using the LWT data set, but addition of this parameter did not increase predictability. In practice, determination of a representative beach slope on an irregular profile introduces some ambiguity, and a transitional slope would not be known in a predictive field application. A representative beach slope is implicitly contained in the fall speed (or grain size) because the equilibrium beach profile depends on this quantity (Moore 1982, Dean 1987). This implies that the existing beach profile should not be far from equilibrium for Equations 2-6 to be applicable, a condition expected to be satisfied at locations on the open coast and far from structures such as large jetties.

219. In the present study, use of the dimensionless fall speed as the sediment-related parameter gave a good delineation between bar/berm profiles, and this parameter has a sound physical basis, as first explained by Gourlay

(1968) and Dean (1973). Furthermore, in the process of quantifying morphologic features as described below, the dimensionless fall speed emerged in many of the developed empirical relationships. In most cases, the value of the dimensionless fall speed varies over the same order of magnitude for a wide range of sand and wave conditions, making it more appealing to use than, for instance, the parameter H_o/D . Thus, it is concluded that the parameters H_o/L_o and H_o/wT are the most basic and general for prediction of cross-shore beach change caused directly by large incident breaking waves. (Some researchers use the breaking wave height instead of the deepwater wave height in beach morphology descriptors, but this requires application of a breaking wave criterion to be useful in a predictive mode.)

220. The dimensionless parameters H_o/L_o and H_o/wT have distinct physical meanings. The wave steepness H_o/L_o is a measure of the wave asymmetry, which influences the direction of fluid flow in the water column. The dimensionless fall speed H_o/wT is a measure of the time that a sediment grain remains suspended in the water column (Dean 1973). Also, the wave height entering in the dimensionless fall speed directly introduces the magnitude of the wave height into the description of sediment motion (which is lacking in the wave steepness, as demonstrated by Saville 1957). The same argument is suggested for the wave period. Thus, although mathematically one power of H_o could be cancelled in the numerators of both sides of Equation 2 (and, similarly, for T in the denominators, since $L_o \sim T^2$), physically, the variables H and T enter on both sides of the equation for different reasons, on the left side for the wave asymmetry and the right side for the magnitudes of the wave height and wave period.

Irregular (field) waves

221. The criteria investigated above were developed for predicting tendencies for bars or berms to form (or for the profile to erode or accrete) under idealized laboratory conditions of regular waves and constant water levels in small and large wave tanks. The utility of such criteria has been questioned for applicability to the field situation (Seymour and King 1982, Seymour and Castel 1988). In the field, waves have a spread in height and period, implying potential differences in cross-shore sand transport produced directly by regular and irregular waves. Irregular waves may also be accom-

panied by long-period wave motion as surf beat and edge waves, modifying the transport regime that exists under purely regular waves. Other complicating factors include the change in water level with the tide and the ambiguity in specifying a representative grain size for the profile.

222. The literature provides guidance on the problem of the difference in transport under regular and irregular waves (see Kraus and Horikawa (1989) for a more complete discussion). Hattori (1982) found better correlation between the predicted cross-shore transport rate and the rate inferred from his field measurements if mean wave height was used in the predictive expressions instead of significant wave height. Mimura, Otsuka, and Watanabe (1987) compared profile change and transport direction and rate produced in a small wave tank in separate cases using regular and irregular waves. Among the many interesting results, they found that the Sunamura and Horikawa (1975) (Table 3) criterion of erosion and accretion was successful (with modified value of the empirical coefficient C) if mean wave height and period were used. Profile change also proceeded at a slower rate for the irregular waves, attributed to the presence of both "constructive" (accretionary) and "destructive" (erosional) wave components in the wave train.

223. To examine the applicability of Equation 2 for expressing profile type or erosion and accretion in the field, data sets published by Seymour (1985) and Sunamura (1980) were used. Seymour (1985) provides plots of the daily time history of contour movement between the berm and the approximately 1- to 2-m depth (relative to mean sea level) on three beaches--Santa Barbara and Scripps Beach, California, and Virginia Beach, Virginia--together with data on the significant wave height H_s and peak spectral wave period T_p at a nominal depth of 10 m, tidal range, and median sand size at the respective beaches. (It is noted that Figures 1 and 2 of Seymour (1985) should be interchanged.) Sunamura (1980) provides wave and sediment data on major erosion and accretion events in the literature and from his own field studies for a total of 10 beaches located on various coasts around the world.

224. The data of Seymour (1985) were censored to exclude days of minor contour change as based on the rate of change of the deeper contours. Deeper contours were used as the reference since the tidal range along the California beaches (approximately 1.5-2 m) and Virginia Beach (approximately 0.5-1 m)

indicates that large portions of the surveyed profiles were above water or in the swash zone most of the time. Criteria such as Equation 2 are applicable to the total surf zone profile extending from the berm to the main breakpoint bar and to prediction of major changes in it. In a strict sense, wading depth profiles do not provide a suitable data base for investigating beach erosion and accretion predictions since it is not known if sediment volume is conserved. Wave heights given by Seymour (1985) were shoaled to deep water using linear wave theory to provide a better estimate of the significant deepwater wave height H_{so} than the value at the gage. Water temperatures, needed to calculate sand fall speed, were obtained from tables given in a University of California (1982) publication for the California beaches and from data available at the US Army Engineer District Norfolk, for Virginia Beach*. The data of Sunamura (1980) were used directly, with the given wave height interpreted as significant deepwater wave height.

225. The total field data set was tested using Equation 2, with the deepwater wave height taken as either the root mean square H_{rms}, mean $\bar{H}$, or significant wave height H_{so}. These wave heights were calculated using the relationships $H_{rms} = 0.706\ H_{so}$ and $\bar{H} = 0.626\ H_{so}$, derived under the assumption of a narrow banded wave frequency spectrum, for which the wave height follows a Rayleigh distribution (Longuet-Higgins 1952). Plots made using the three statistical wave heights showed that the data separated into two approximately distinct groups, similar to Figure 6 for regular waves. For the wave heights H_{rms} and H_{so}, the values of M in Equation 2 were different from 0.00070 found for regular waves. However, when $\bar{H}$ was used, Equation 2 with $M = 0.00070$ was found to separate the eroding and accreting cases reasonably well, as shown in Figure 10. The lines drawn in Figures 6 and 10 are identical, indicating that mean wave height is the appropriate statistical wave height to use in comparisons of erosion and accretion occurring in the field with that generated by prototype-scale regular waves.

226. As previously mentioned, the data of Seymour (1985) were censored to restrict analysis to times of larger rates of change of the profile. In the censored data set, some points remained which appear anomalous if viewed

---

* Personal Communication, 1988, Paul Bowen, Geologist, US Army Engineer District, Norfolk, VA.

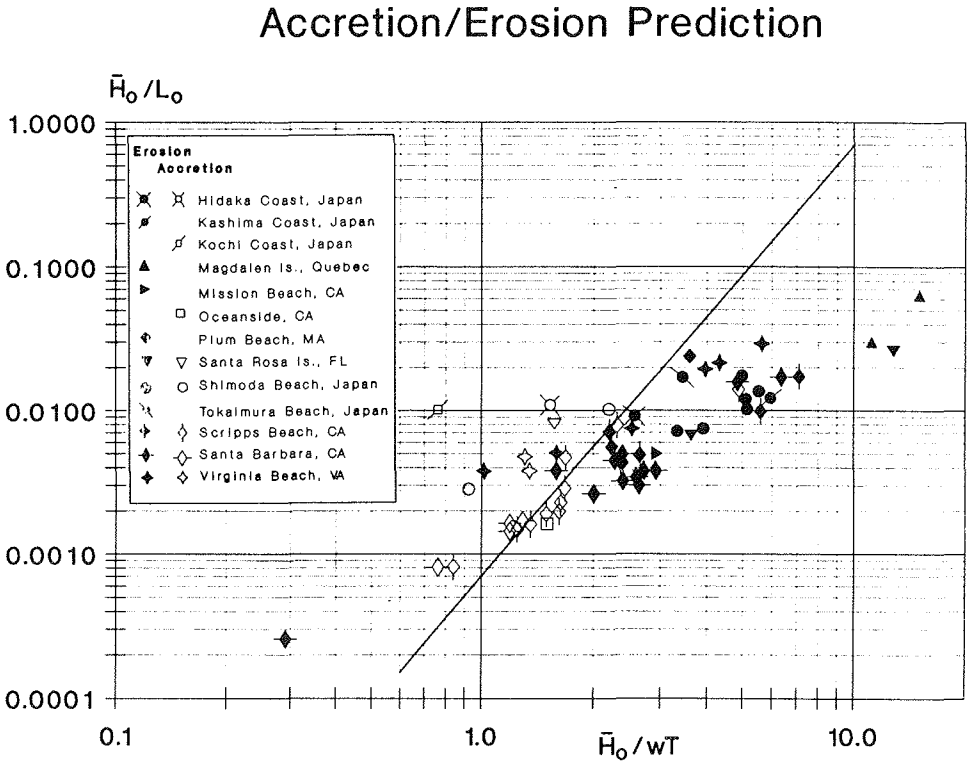

Figure 10. Classification of erosion and accretion events in the field using deepwater wave steepness and dimensionless fall speed, with wave height taken as mean wave height

within the context of the other plotted points. For example, day 1 of the Santa Barbara data described what would be considered as recovery waves with H_{so} = 0.21 m and T_p = 18 sec, yet the profile eroded. This point plotted at the bottom left side of Figure 10, far from other erosional events. Several mild accretionary events from the Scripps Beach data set plot on or near the erosion side of the separation line, suggesting that factors other than direct wave action contributed to produce the profile change and that the profile change may have been mixed. Kriebel, Dally, and Dean (1987) used a finite-width band rather than a single separation line to denote possible areas of mixed or ambiguous transport. In general, however, it is judged that the criterion given by Equation 2 is applicable to distinguish erosion and accretion events in nature for the more extreme events. Since engineering applications involving cross-shore sand transport, such as beach fill design, must consider extreme and not weak or mixed events, Figure 10 appears to be suitable as a first-order estimator for such purposes.

227. It is interesting to note that the erosion and accretion events plotted in Figure 10 are well separated by the simple criterion $\bar{H}/wT = 2$. This value is of the same order of magnitude as that found by Wright and Short (1984) in use of their large field data set and the fall speed parameter evaluated at the breaker line (Table 3). The LWT data do not separate well (Figure 6) by use of only this single parameter, however, and additional unambiguous field data are required to further investigate this point. The profile surveys should encompass the full active profile to allow checking of sand conservation.

228. In succeeding sections, discussion and analysis are again directed toward profile change produced by regular waves in LWTs, unless noted otherwise.

Shoreline movement

229. If shoreline retreat/advance is analyzed instead of bar/berm profile type or global erosion/accretion, a less clear distinction is obtained when only dimensionless fall speed and deepwater wave steepness are used. In this case, incorporation of the initial beach slope increases predictability of the criterion because the initial slope is closely related to the amount of material that moves before equilibrium is attained. Also, a gentler slope dissipates more incident wave energy because the waves travel a greater distance in the surf zone before reaching the shoreline. Some CRIEPI cases showed that shoreline advance occurred for situations with a gentle initial slope even if considerable erosion took place in the surf zone to produce a distinct barred profile.

230. Figure 11 plots shoreline retreat and advance that occurred in the CE and CRIEPI experiments, together with a line distinguishing the two types of response. The initial profile slope was included in the numerator of the nondimensional fall speed to increase predictability. The equation of the line in Figure 11 is $H_o/L_o = 0.44\ (\tan\beta\ H_o/wT)^{2.08}$.

Application to small-scale data

231. The dimensionless sediment fall speed and the deepwater wave steepness were also used to classify the data pertaining to small-scale laboratory profile change found in the experiments performed by Rector (1954), Iwagaki and Noda (1963), and Nayak (1970). As seen from Figure 12a, the

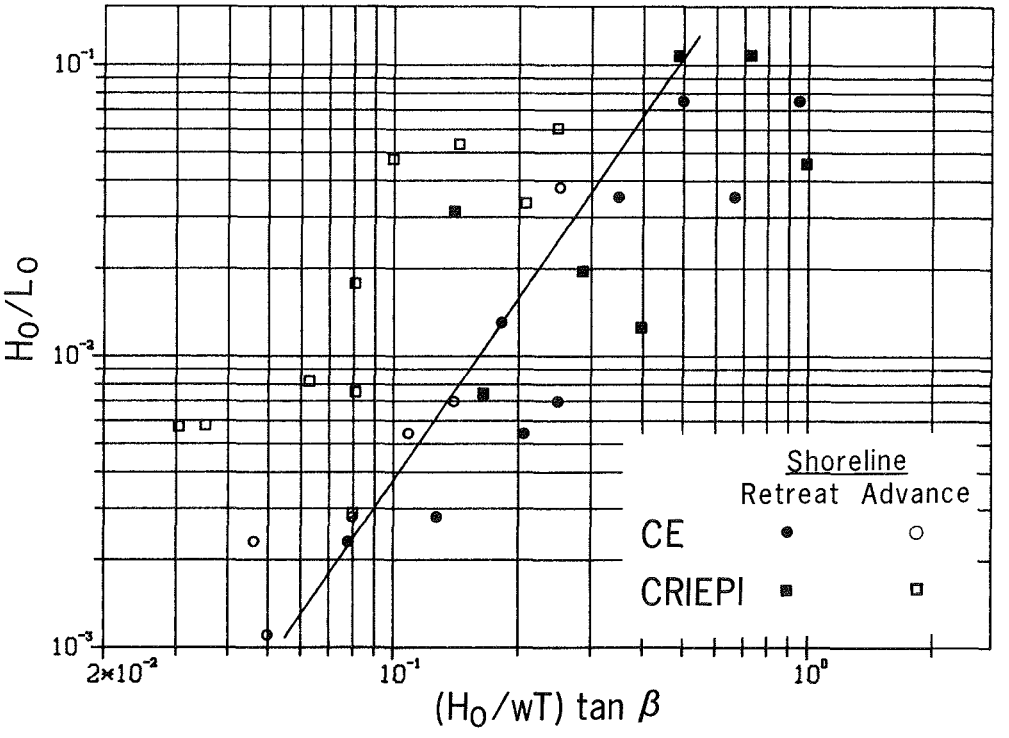

Figure 11. Criterion for distinguishing shoreline retreat and advance by use of wave steepness, dimensionless fall speed, and initial beach slope

criterion derived from the large-scale tests is not applicable to the small-scale data using the coefficients given in Equation 2. By modifying these coefficients it would be possible to obtain a crude delineation with the quantities in Equation 2. However, the dimensionless fall speed is probably of less significance in distinguishing bar/berm profile response in small-scale laboratory experiments than in prototype-scale experiments. This is attributed in great part to the mode of transport, the main transport mode probably being bed load in these types of experiments, with less significant contributions from suspended load as under higher waves as occur in the field.

232. Therefore, in small-scale laboratory experiments, use of the parameter H_o/D instead of H_o/wT should provide a better basis for profile classification since it expresses a relationship between the force exerted by the waves and the resistance offered by the grains (Nayak 1970). This interpretation is closely connected with the mechanism of bed load transport, where the main driving force is the horizontal component of the water particle

velocity near the bed. In contrast, in suspended mode, the upward transport of eddy momentum keeps sediment particles in the water column and available for transport by any current. Figure 12b illustrates the improvement obtained by using H_o/D for classifying beach profile change produced in small-scale experiments. Although the points denoting bar and berm profile response overlap to some extent, the delineation obtained is somewhat better than in Figure 12a.

233. The effect of wave period in scaling is also emphasized through the significant difference between small-scale and prototype-size experiments in classifying beach response using the dimensionless fall speed.

Form and Movement of Bars

Bar genesis

234. Several theories have been advanced to explain the formation of longshore bars. Since a wide variety of bed forms has been classified as a bar-like feature by various authors, various mechanisms may presumably prevail in the formation process. Here, bar generation by depth-limited breaking waves is investigated, the "classical" viewpoint of bar genesis. As waves break near shore, energy is dissipated producing a turbulent fluid environment where sediment is entrained and maintained in suspension. Depending on the vertical profile of both the cross-shore fluid velocity field and the sediment concentration, the sediment will experience net onshore or offshore movement, resulting in a berm or bar profile. Sediment transported in the offshore direction will drop out of the water column to be deposited where the turbulence begins to decrease, somewhat seaward of the plunge point, where breaking waves undergo maximum energy dissipation (Miller 1976, Skjelbreia 1987). A berm is formed as material is transported onshore and deposited on the foreshore, for which the force of gravity and properties of the uprush bore determine the berm height (Bagnold 1940, Sunamura 1975). In the field, long-period (infragravity) wave motions, if present, may also influence and perhaps dominate foreshore development, since the energy of these waves is not depth limited, as is the case for short-period waves. However, no direct evidence

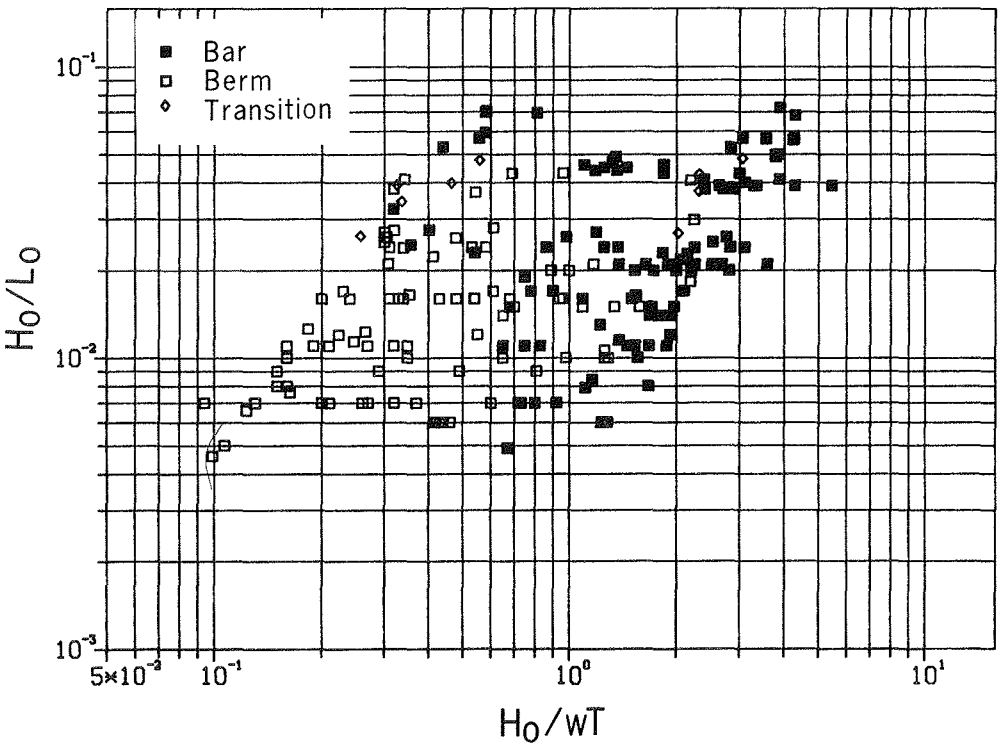

a. Dimensionless fall speed

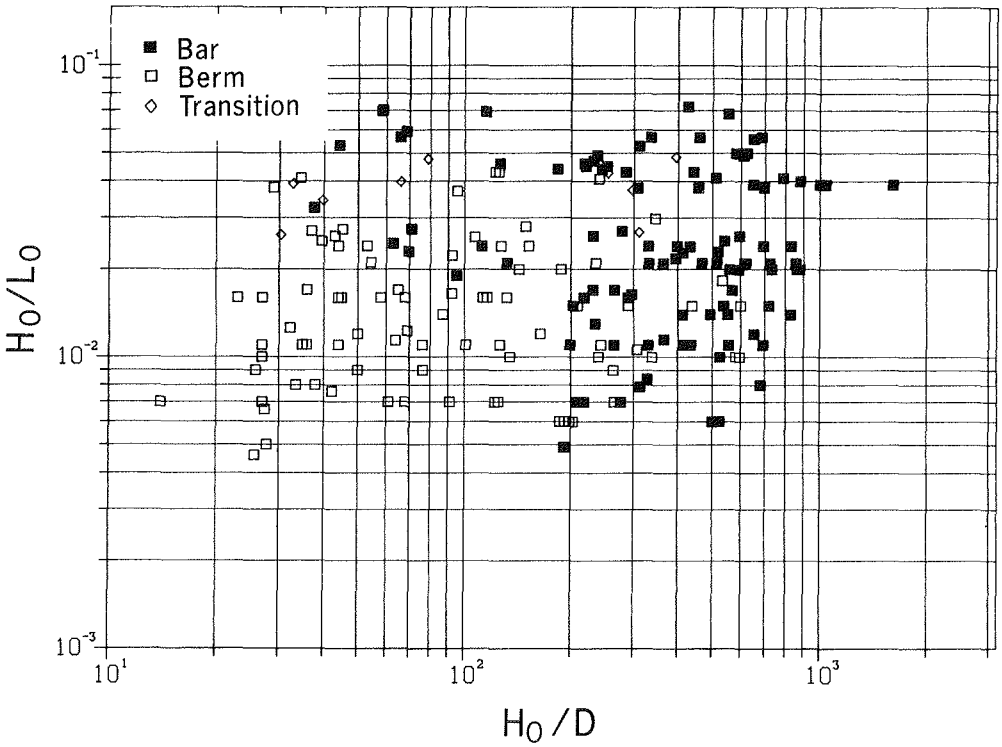

b. Ratio of wave height to grain size

Figure 12. Criteria for distinguishing profile type applied to small-scale laboratory data

of major bar or berm development by infragravity waves was found in the literature review.

235. The type of bars empirically investigated in this study are those formed by waves breaking on beaches exposed to moderate or high wave energy conditions with a moderate tidal variation (For a bar classification, see Greenwood and Davidson-Arnott 1979.) Waves approaching shore on a sloping beach increase in height due to shoaling until depth-limited breaking occurs. The condition for incipient breaking is a function of the local beach slope and the wave steepness (e.g., Weggel 1972, Singamsetti and Wind 1980). As breaking occurs, energy dissipation in the waves increases sharply, producing the necessary work to intensively entrain and transport sediment in the surf zone. The maximum in the cross-shore transport rate appears to be located in the vicinity of the plunge point where maximum energy dissipation occurs. Seaward of the point of maximum energy dissipation, the transport rate decreases, leading to deposition of sediment in this region and bar formation. As the bar grows, the waves break farther offshore and the break point and plunge point translate seaward, causing the location of the maximum transport rate and the bar to move offshore. Material needed to supply the bar is mainly taken from the region of the inner surf zone, resulting in erosion of the subaerial beach. This process continues until a stable beach profile is achieved which dissipates wave energy without significant changes in shape.

236. A broken wave may, after further travel, reach a stable wave height and reform, depending on the shape of the profile. Dissipation of energy decreases in the reformed waves, implying a corresponding decrease in the transport rate. Eventually, the reformed waves may shoal and break again closer to shore, resulting in a second but smaller bar in the same manner in which the more seaward main breakpoint bar was formed. The described mechanism is valid for both plunging and spilling breakers, both producing a trough in the profile shoreward of the break point (Sunamura in press), although the time scale of bar development will be longer under spilling breakers (Sunamura and Maruyama 1987). Figure 13 displays consecutive profiles in time for one of the CE cases (Case 500), showing a typical example of beach profile evolution with a main breakpoint bar and another smaller bar farther inshore.

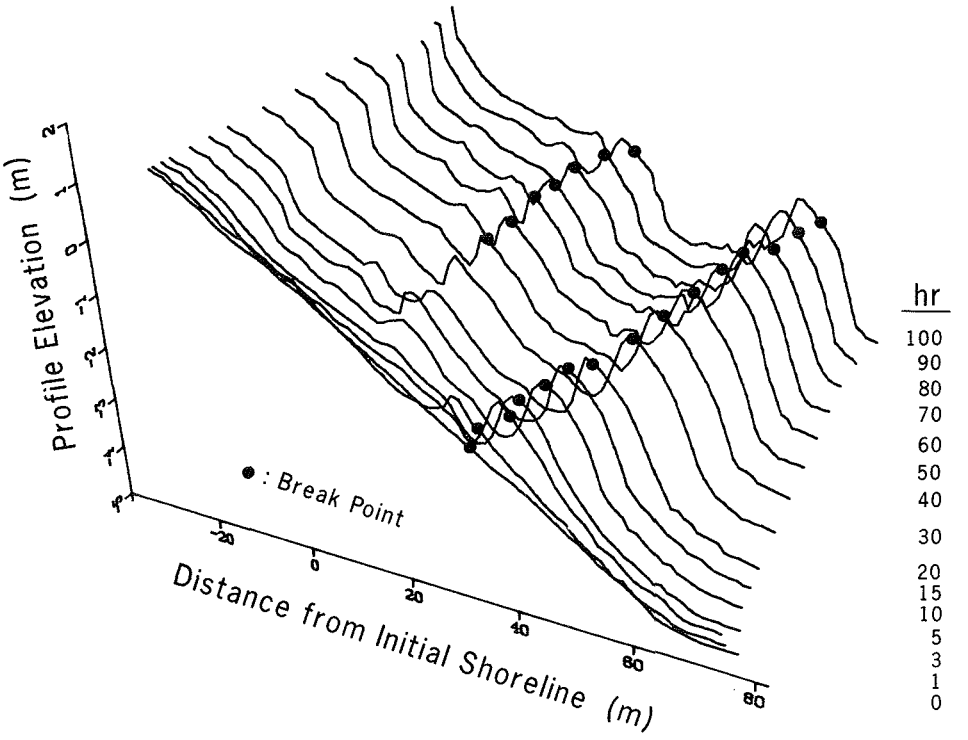

Figure 13. Growth and movement of breakpoint bar with elapsed time and location of break point

Average breaker locations are indicated in the figure for the profiles where such information was available.

237. Another mechanism for bar formation is long-period wave motion generated, for example, by reflection from the beach (Bowen 1980). Standing waves as a possible mechanism for bar formation have been investigated by Carter, Liu, and Mei (1973), Lau and Travis (1973), Short (1975a, b), and Mei (1985). An oscillating velocity field induces a steady mean current in the boundary layer close to the bed. If the oscillations are produced by purely progressive waves, the mean drift in the boundary layer will always be in the direction of the propagating waves. Partial reflection of the incident wave may cause the direction of mass transport in the lower part of the boundary layer to reverse if reflection is sufficiently large. (Theoretically the reflection coefficient should exceed 0.414, according to Carter, Liu, and Mei 1973.) A complete standing wave induces mass transport toward the nodes in the lower part of the boundary layer and toward the antinodes in the upper part of the boundary layer. Depending on the height to which the grains are

lifted in the water column when transported, the grains will experience a net drift and accumulate under the nodes or antinodes. This should depend on grain size to some extent (De Best and Bijker 1971). Holman and Bowen (1982) assumed that suspended sediment transport was dominant and used the average mass transport in the upper part of the boundary layer to calculate equilibrium shapes of beaches based on a Bagnold-type transport formula. Complex three-dimensional geometries were derived by superimposing progressive waves to obtain standing wave patterns alongshore and cross-shore.

238. In some of the CRIEPI cases which started from the steep plane slope of 1:10, considerable reflection was present (a reflected wave height of 0.4 m superimposed on the wave height distribution), but the effect of the reflected wave on the profile shape appeared to be very small (see Figure 14).

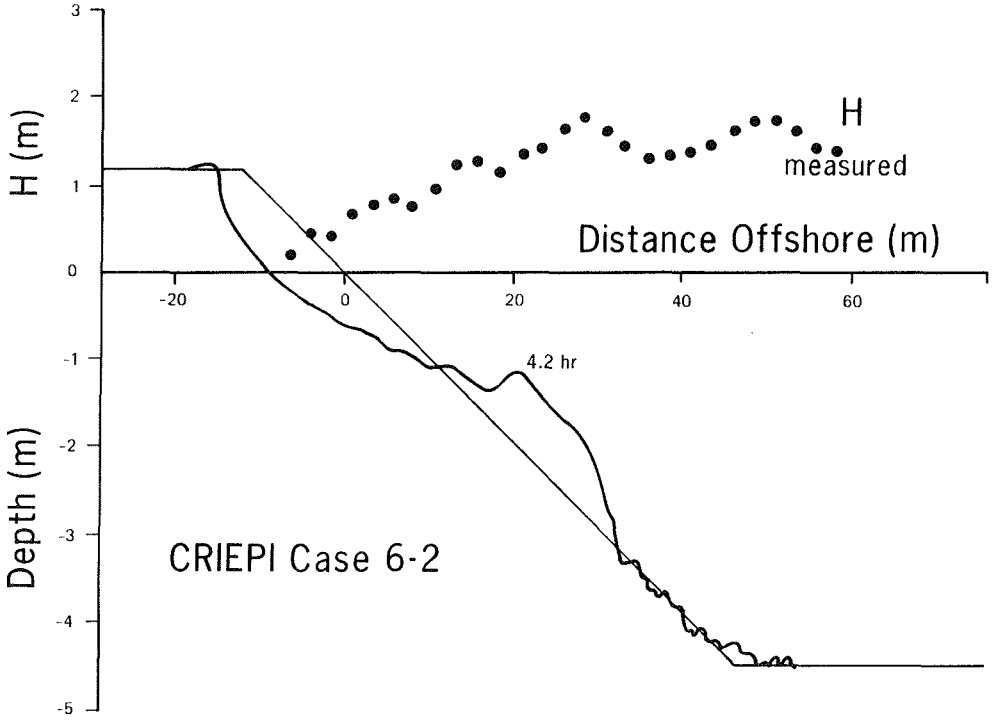

Figure 14. Profile measured after 4.2 hr together with the initial profile and wave height distribution

Actually, as the bar grew in size and the seaward slope became steeper, the bar should have promoted reflection, but it is surmised that the main effect

of reflection was to alter the breaking wave process somewhat since there is no evident feature in the surf zone profile attributable to reflected waves.

Equilibrium bar volume

239. As a bar moves offshore, it increases in volume to approach an equilibrium size. Figure 15 shows bar volume for the main breakpoint bar as a function of time for the CE and CRIEPI experiments, respectively. Some of the cases were not run sufficiently long to attain the equilibrium volume. The approach to equilibrium is typically smooth. If a breakpoint bar formed on a profile where onshore transport (accretion) dominated, equilibrium volume was reached rapidly and was relatively small. Examples are Cases 101, 301, and 801 from the CE data, and Case 2-3 from the CRIEPI data. Bar volume changed abruptly if the smaller seaward breakpoint bar merged with the main breakpoint bar. Often, further growth of the main breakpoint bar was hindered by this coalescence of bars, as shown in Case 300 (occurs at 15.0 hr). Profiles having only one bar showed a more regular development in time toward an apparent equilibrium volume.

240. Since equilibrium bar volume was not entirely reached in some cases, and in order to obtain an objective method for determining equilibrium bar volume, a simple expression of exponential type was least-square fitted to the data for each case. The chosen expression is often encountered in growth problems where an equilibrium state exists. The same expression was used by Kriebel and Dean (1985a) to characterize dune erosion. The bar volume V is assumed to grow toward the equilibrium volume V_{eq} according to

$$V = V_{eq} \left(1 - e^{-\alpha t}\right) \tag{7}$$

where t is time, and α is an empirical temporal rate coefficient. Correlation analysis (25 cases evaluated) involving pertinent wave and beach profile parameters showed that equilibrium bar volume was most closely related to deepwater wave height, sand fall speed (or grain size), and initial beach slope, although the correlation coefficients (see Appendix A) were not high (0.6-0.7). A larger wave height implied a larger bar volume, a greater fall speed (or larger grain size) implied a smaller bar volume, and an initially steeper slope also produced a larger bar volume for a given grain size. Fall

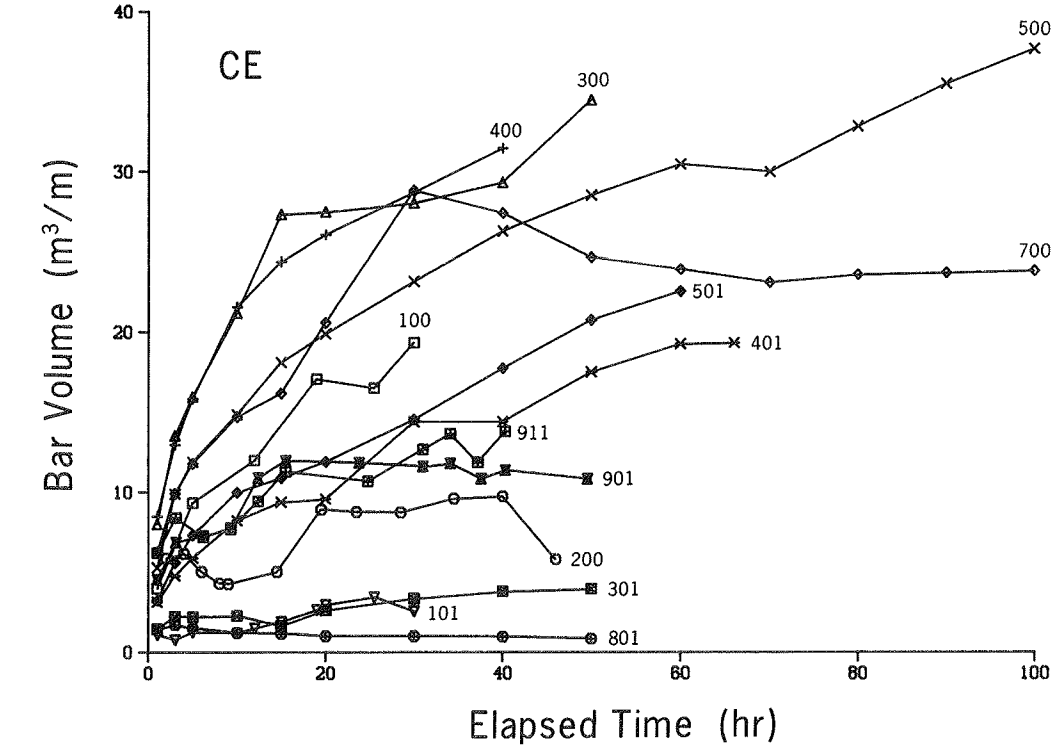

a. CE data

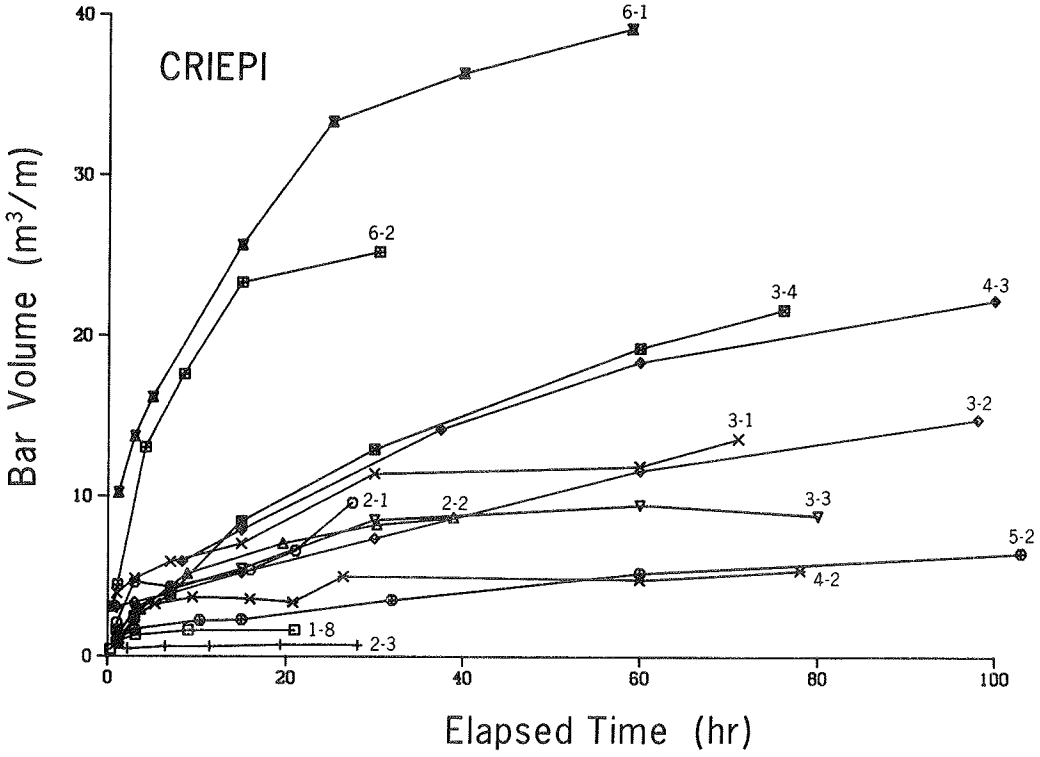

b. CRIEPI data

Figure 15. Growth of bar volume with elapsed time

speeds were calculated from an expression given by Hallermeier (1981) for the CRIEPI data, and in the CE cases fall speeds determined by Seelig (1983) were used. Fall speed depended on water temperature in the tank (Kajima et al. 1983b, Kraus and Larson 1988a). Under nonextreme water temperatures such as considered here, the fall speed is almost linearly dependent on grain size, resulting in similar correlation values for quantities expressed in terms of either the grain size or fall speed.

241. A stepwise regression analysis incorporating the aforementioned factors explained 70 percent of the variation in the data. Wave height was most important, accounting for 35 percent, followed by the fall speed which explained 30 percent. Wave period and initial beach slope together accounted for only 5 percent. If only bars formed on a profile which mainly experienced erosion (transport directed offshore), the explained variation increased to 80 percent, with the wave height and fall speed being most important. The dimensional regression relationship involving equilibrium bar volume V_{eq}, deepwater wave height, sand fall speed, and wave period for bars formed on erosional profiles is

$$V_{eq} = 0.088\ H_o^{2.26}\ w^{-1.36}\ T^{0.55} \tag{8}$$

242. It is desirable to use nondimensional quantities to obtain general relationships relating morphologic features to wave and sand parameters. From the regression equation describing equilibrium bar volumes on erosional profiles (Equation 8) dimensionless parameters were identified by dividing by the wave period raised to a suitable power. Equilibrium bar volume was normalized by the deepwater wavelength squared, and the independent parameters emerged as dimensionless fall speed and deepwater wave steepness. The coefficient of determination r^2 (see Appendix A), defined as the percentage of the sum of squares explained by the regression equation, will increase by incorporating the wave period in the parameters (from 75 percent without beach slope incorporated to 90 percent). The resultant regression equation is

$$\frac{V_{eq}}{L_o^2} = 0.028 \left[\frac{H_o}{wT}\right]^{1.32} \left[\frac{H_o}{L_o}\right]^{1.05} \tag{9}$$

243. Equation 9 is an inferior predictor of equilibrium bar volume compared with the original regression equation (r^2 decreased from 75 to 70 percent) formed by dimensional variables, since the least-square estimate will be more influenced by wave period which was found to be less important for determining equilibrium bar volume than wave height and sand fall speed. Thus, the advantage of nondimensional quantities is gained somewhat at the expense of predictability but will give a more general and physically-based relationship. Figure 16 displays a comparison between the predicted equilibrium volume according to Equation 9 and equilibrium volumes extrapolated from the measurements with Equation 7.

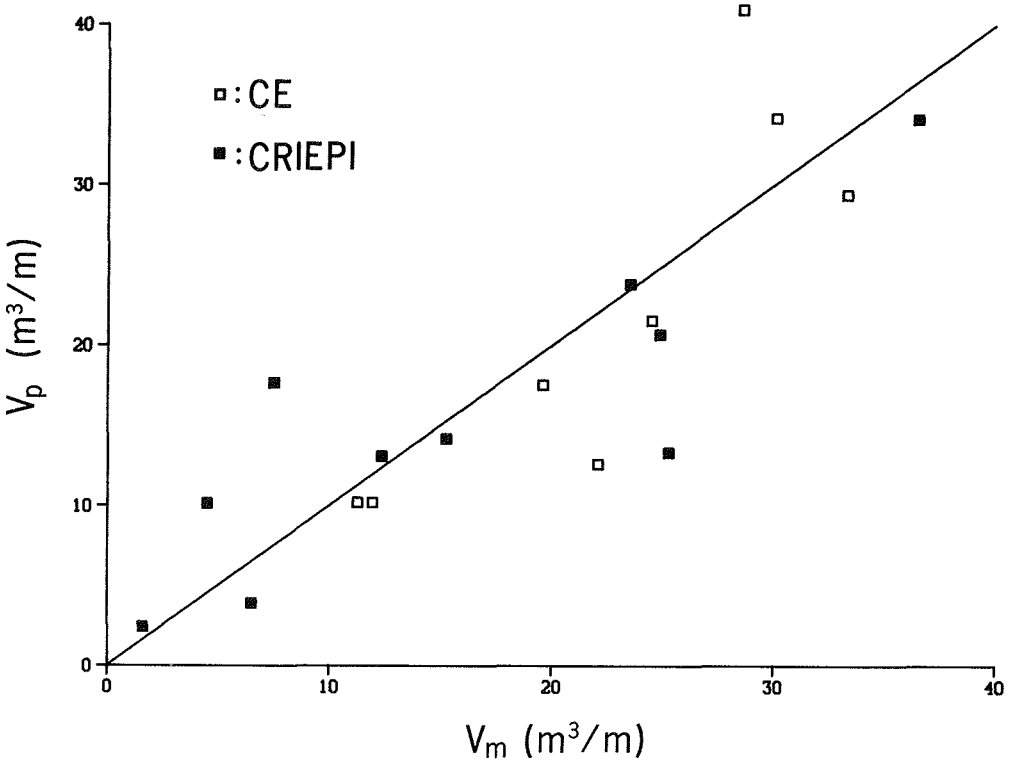

Figure 16. Measured equilibrium bar volume V_m and empirical prediction V_p

244. The temporal rate coefficient α in Equation 7 controls the speed at which equilibrium bar volume is attained. Correlation between α and wave and beach profile properties was in general low (correlation coefficients less than 0.5). Qualitatively, α increased with fall speed (or grain size) and decreased with wave height and wave period. A large α-value produces a rapid

response toward equilibrium. For larger wave heights, more wave energy is dissipated along the beach profile; that is, the bar becomes larger and forms farther offshore, causing more material to be moved before the equilibrium shape is reached (lower α-values). Furthermore, greater wave energy is required to move larger (heavier) sediment particles, implying more rapid attainment of equilibrium (higher α-values) for larger grain-size beaches.

Depth-to-bar crest

245. As a bar moved offshore, its height increased so that the depth to the crest h_c was roughly constant during a run (except perhaps, at the very first profile surveys) (cf. Birkemeier 1985a, Dette and Uliczka 1987). In Figure 17(a and b), the minimum depth on the bar, called the crest depth, is plotted as a function of time for the CE and CRIEPI data. For some cases in which a bar formed on an accretionary profile, the bar remained stationary, or even moved slightly onshore, causing the crest depth to decrease. Also, if two bars joined together, the crest depth changed abruptly since the inner bar crest was located in more shallow water.

246. A comparison between Cases 901 and 911 shows that even though the equilibrium bar volume was almost the same (11.3 and 12.0 m^3/m, respectively), Case 911 experienced a considerably larger fluctuation in depth at the bar crest. Wave parameters and beach properties were identical for these two cases, the only difference being a stepwise sinusoidal water level change imposed in Case 911 to simulate a tide. Consequently, during cycles of increased water level in Case 911, the depth at the bar crest increased and the bar grew closer to the initial still-water (reference) level. During cycles of lower water level, the depth at the crest decreased and a portion of the bar eroded, causing the bar crest to move away from the initial location of the still-water level. There was no significant time lag between water level change and change in depth at the bar crest (see also Shepard 1950).

247. The average depth at the bar crest was calculated for all profiles comprising an individual case. This average was closely related to the breaking wave height and showed little dependence on wave period and grain size. If an inshore bar grew together with the main breakpoint bar, the most seaward bar crest was used in determining the depth at the bar crest. The

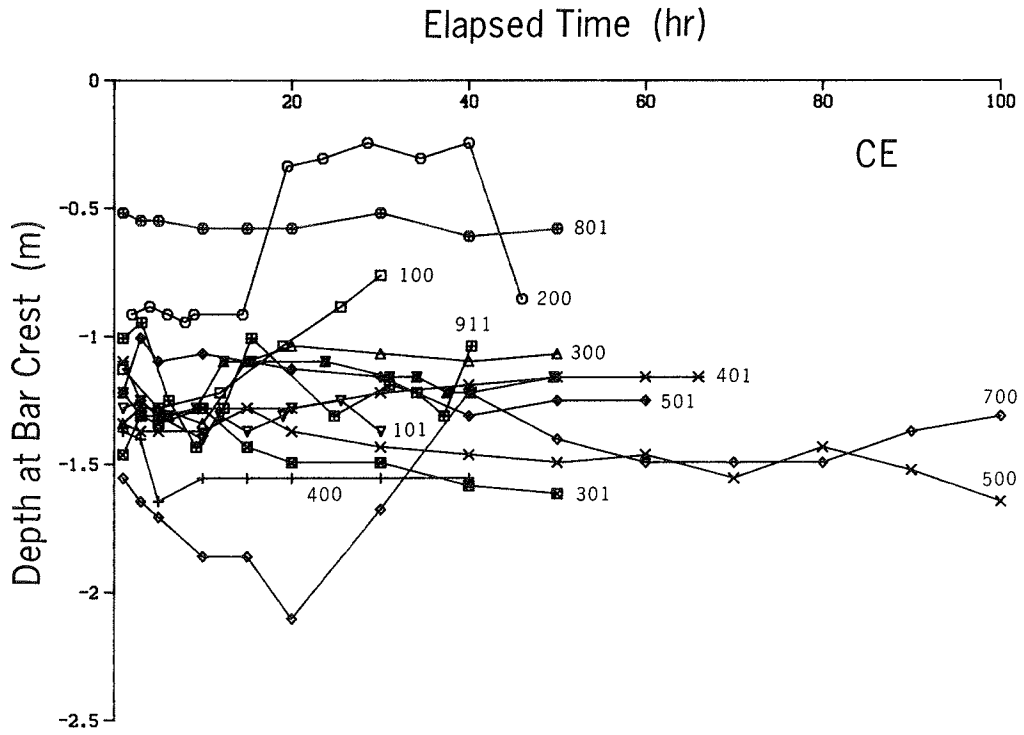

a. CE data

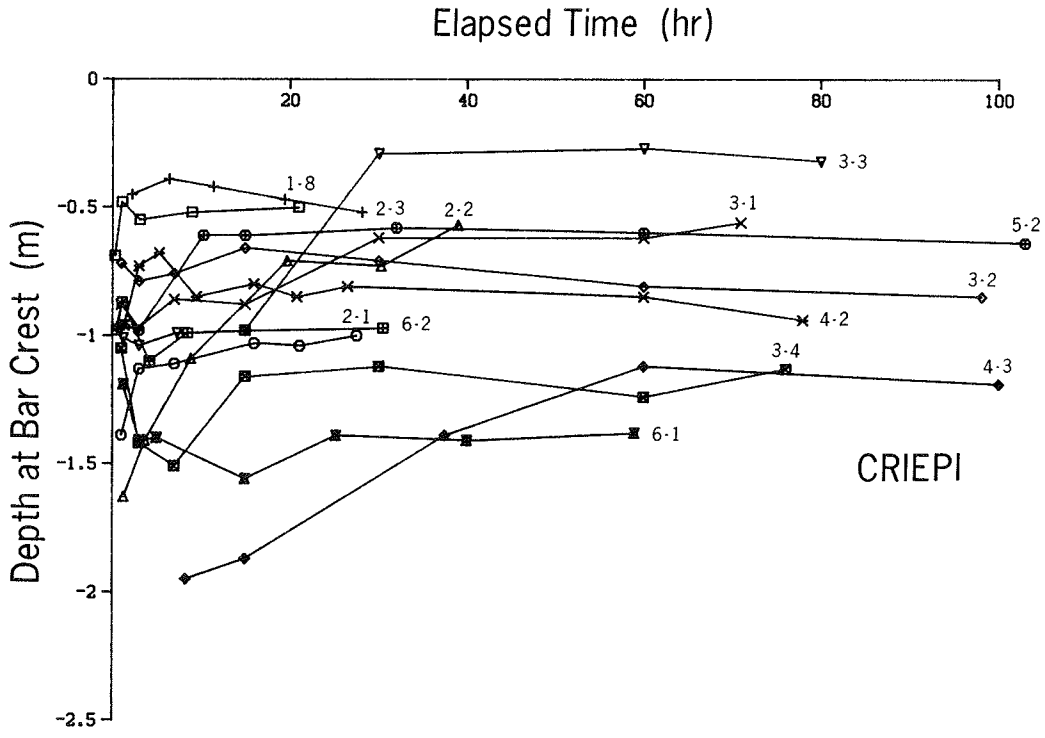

b. CRIEPI data

Figure 17. Evolution of depth-to-bar crest

following relationship with the breaking wave height was obtained:

$$h_c = 0.66\ H_b \tag{10}$$

Equation 10 is plotted in Figure 18. The coefficient of determination of the regression line was 70 percent.

248. For the cases where a small bar formed on an accretionary profile, the crest depth had a tendency to decrease slightly with time if onshore bar movement occurred, which contributed to the scatter in the data. Sunamura (in press) found a coefficient of 0.59 as opposed to 0.66 in Equation 10, based on small-scale laboratory wave tank data and some CRIEPI data.

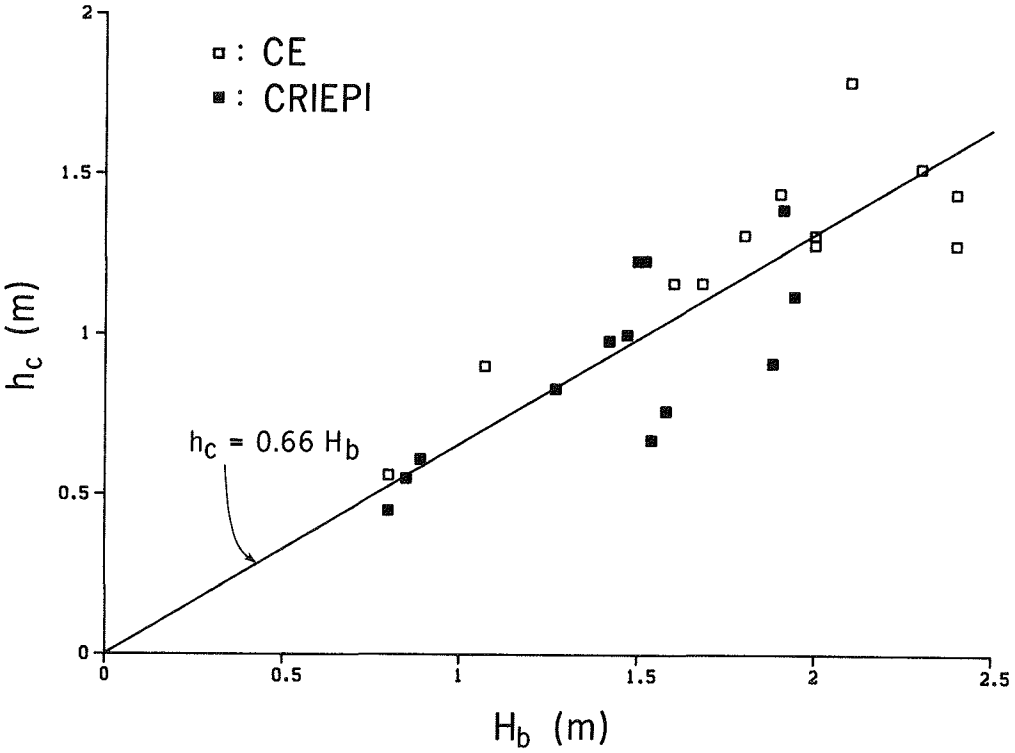

Figure 18. Depth-to-bar crest h_c versus breaking wave height H_b

Ratio of trough depth to crest depth

249. The maximum depth occurring immediately shoreward of the bar was taken as the trough bottom in the analysis. This was considered as a natural and objective definition of trough position, although a trough was sometimes located in an area where material accreted with respect to the initial

profile. Keulegan (1945) studied the ratio of trough depth h_t to bar crest depth h_c. He found an average value for h_t/h_c of 1.69 for laboratory beaches and 1.65 for field beaches. Shepard (1950) found much lower ratios at the Scripps pier, with a mean value of 1.16 (referenced to mean sea level). The smaller value determined by Shepard is expected, since the tidal range is relatively large (order of 2 m) along the southern coast of California. Changing water level, combined with random and longer period waves in the southern California Bight, would act to smooth the profile.

250. In the present study, this ratio was calculated for 26 CE and CRIEPI cases and ranged between 1.26 to 2.16, with an average of 1.74 and standard deviation of 0.26. The ratio was calculated as an average for all profiles surveyed during a case and showed little change in time for most cases. However, for some cases the very first profile survey showed a markedly different value of h_t/h_c, typically much lower than the average, and these spurious values were excluded from the calculation of the average.

251. The ratio of trough depth to crest depth showed an inverse dependence on the wave period, as illustrated in Figure 19. The wave period accounted for 60 percent of the variation in the data using a regression relationship between h_t/h_c and the wave period. Expressed as an empirical power law in terms of wave steepness, regression analysis gave

$$\frac{h_t}{h_c} = 2.50 \left[\frac{H_o}{L_o}\right]^{0.092} \tag{11}$$

252. Equation 11 had a coefficient of determination of 55 percent, slightly less than that found using only the wave period, but from a general point of view it is more attractive to use as a predictive relationship. Keulegan (1948) did not report a dependence on wave steepness.

253. Qualitative examination of the scattered data indicated that the ratio h_t/h_c tended to increase with grain size for bars formed on erosional profiles, but decreased with grain size for bars formed on accretionary profiles. In erosional cases in general the profile for coarser grain sizes showed a steeper shoreward bar slope, allowing for a larger vertical distance between the bar crest and trough bottom. The breakpoint bar formed on an

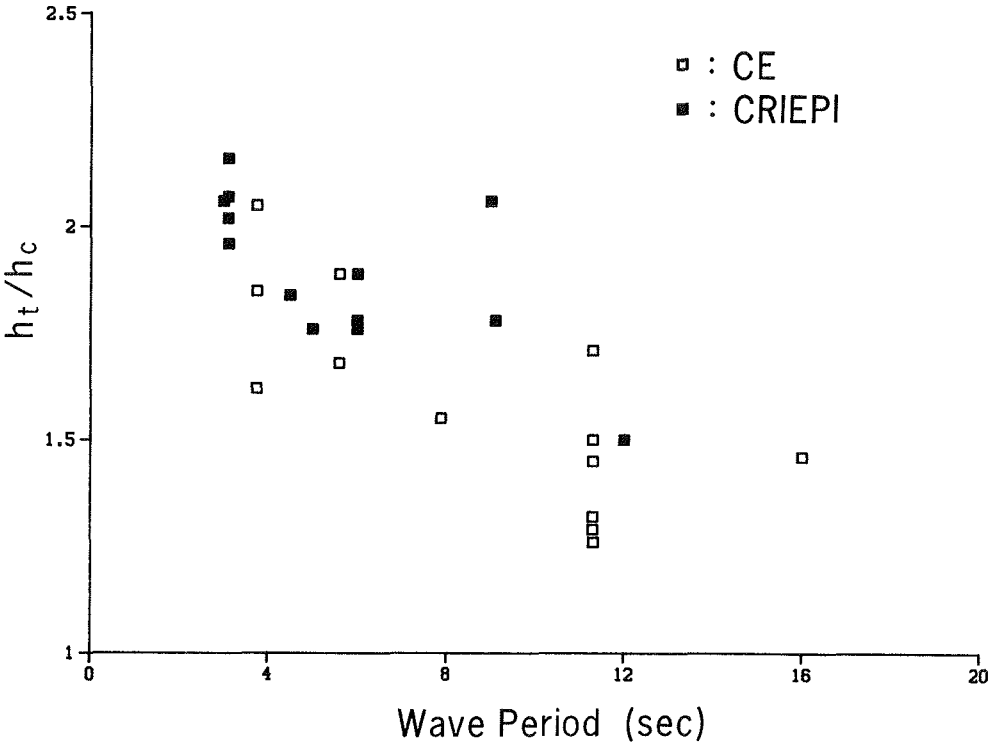

Figure 19. Ratio of depth-to-trough bottom and depth-to-bar crest h_t/h_c as a function of wave period

accretionary profile was normally small, and its size decreased with increasing grain size, making the bar flatter with a smaller value of h_t/h_c .

Maximum bar height

254. As a bar moved offshore, its maximum height defined with respect to the initial profile increased to approach an equilibrium value. Figure 20(a and b) shows maximum bar height Z_B as a function of time for the CE and CRIEPI experiments. Bars formed on an accretionary profile achieved equilibrium height very rapidly, often during the first hour of the run (see Cases 101, 801, 2-3, 3-3). A coarser grain size produced a smaller equilibrium bar height for the same wave parameters, and a larger wave height produced a larger equilibrium bar height for fixed wave period and initial profile slope. The curves displayed in Figure 20(a and b) are readily approximated by an expression similar in form to Equation 7. (Some cases where a bar formed on an accretionary profile showed an almost constant bar height in time and thus were not used in the analysis.) Maximum bar height for all cases was esti-

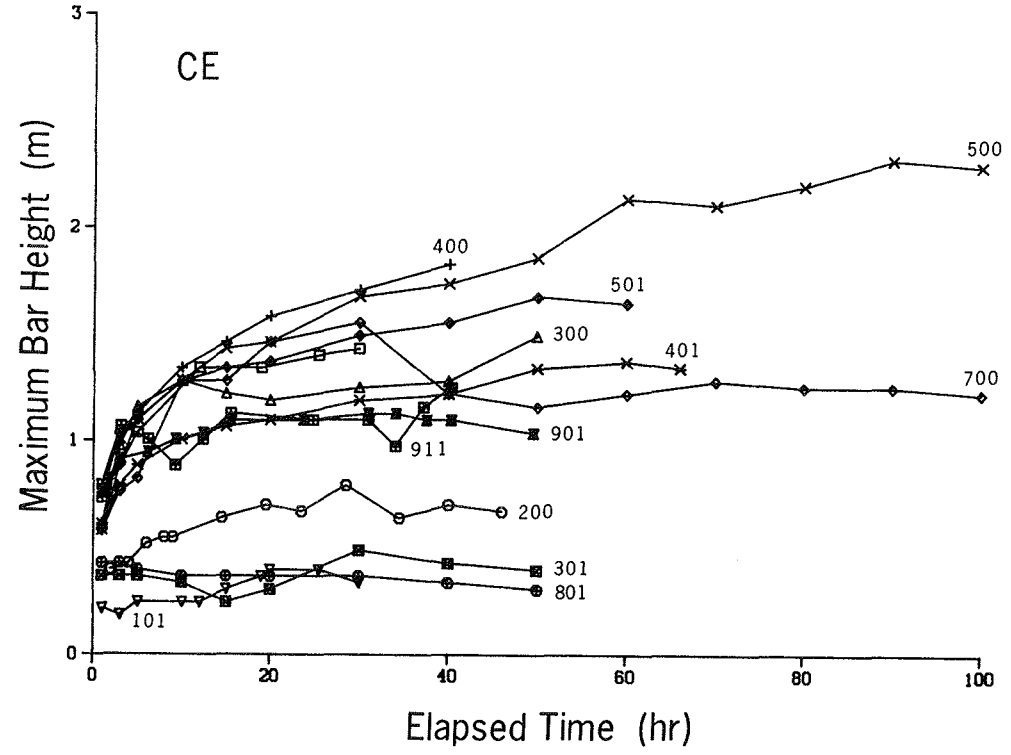

a. CE data

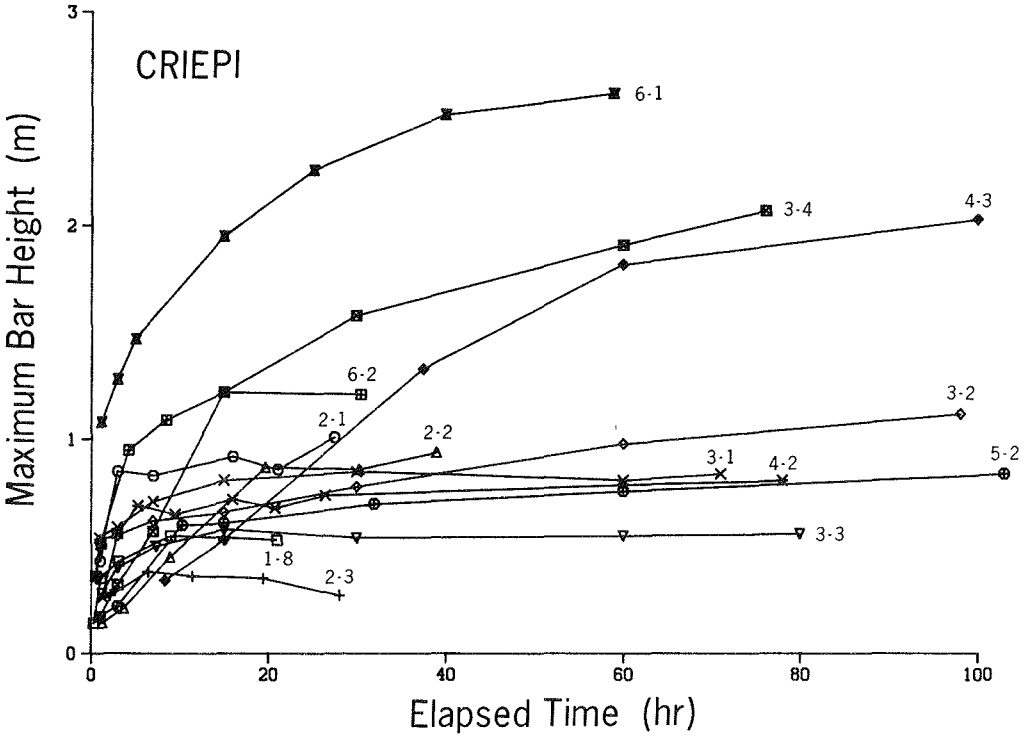

b. CRIEPI data

Figure 20. Evolution of maximum bar height

mated by least-square fitting of the data to an expression similar to that in Equation 7. Correlation analysis performed on the 24 values showed that the equilibrium bar height was most closely related to deepwater wave height and sand fall speed. If the wave height increased, the bar height increased, whereas a greater fall speed implied a smaller bar height. Equilibrium bar height was only weakly related to wave period, for which a longer period tended to produce a smaller bar height.

255. Regression analysis between the maximum equilibrium bar height and basic wave and beach parameters, preserving dimensions, accounted for 65 percent of the variation in the data. The deepwater wave height and the sand fall speed together accounted for 60 percent. If only bars that formed on erosional profiles were considered (19 values), the coefficient of determination increased considerably (80 percent), for which deepwater wave height and fall speed accounted for 75 percent. The dimensional regression equation for the erosional cases is

$$Z_B = 0.128\ H_o^{1.36}\ w^{-0.58} \tag{12}$$

256. From the regression relationship derived with dimensional quantities (Equation 12) it was possible to form nondimensional parameters by division with the wave period raised to a suitably chosen power. The maximum equilibrium bar height divided by the wavelength is a function of dimensionless fall speed and deepwater wave steepness. Wave period had little effect on bar height and, as mentioned previously, inclusion of the wave period may increase the coefficient of determination but not the predictability of the maximum equilibrium bar height. The regression equation is written

$$\frac{Z_B}{L_o} = 0.122 \left[\frac{H_o}{wT} \right]^{0.59} \left[\frac{H_o}{L_o} \right]^{0.73} \tag{13}$$

257. Use of nondimensional quantities in this case did not lower the coefficient of determination notably (from 80 percent to 75 percent) for predicting the maximum equilibrium bar height. Figure 21 shows a comparison

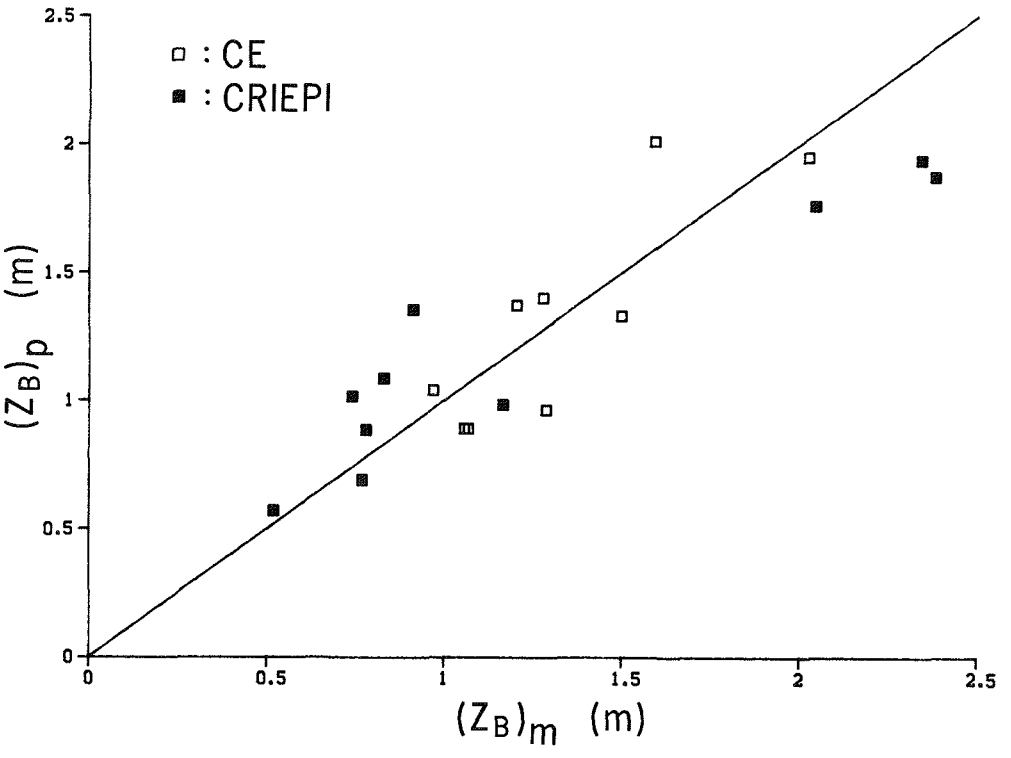

Figure 21. Comparison of measured equilibrium bar height $(Z_B)_m$ and empirical prediction $(Z_B)_p$

between the equilibrium bar height predicted by the regression model (Equation 13) and the measurements.

258. The temporal rate coefficients governing growth toward the maximum equilibrium bar height for bars formed on erosional profiles had highest correlation with sand fall speed. Similar to the situation for the rate coefficient governing bar volume growth, correlation coefficients were small (less than 0.5). However, a regression relationship between the rate coefficient and wave period, deepwater wave height, and sand fall speed gave a relatively high coefficient of determination of 70 percent. This relationship was considerably larger than any obtained for the rate coefficient pertaining to bar volume growth. The sand fall speed and deepwater wave height accounted for 60 percent of the variation in the data, giving

$$\alpha = 34.1\ H_o^{-1.43}\ w^{1.98}\ T^{1.23} \qquad (14)$$

259. From the dimensional regression equation, Equation 14, the dimensionless fall speed was identified as an important quantity. By normalizing with wave period, the quantity thus obtained was related to the dimensionless fall speed according to

$$\alpha T = 117 \left[\frac{H_o}{wT} \right]^{-2.30} \tag{15}$$

260. The coefficient of determination was only 55 percent, but Case 700 contributed to more than half of the sum of the residuals. The reason is probably due to a decrease in wave height that occurred between 20-30 hr during the run, strongly affecting buildup of the bar.

Bar location and speed of movement

261. Movement of a bar during wave action is perhaps most accurately characterized by its center of mass x_{CM}. The bar crest, which is the most convenient measure of bar location, especially in the field, is not as accurate a measure since the shape of the bar changes during the course of its growth, influencing the location of the crest more than the center of mass. In general, the mass center of the bar moved offshore on an erosional profile unless a more shoreward bar grew together with the main breakpoint bar. Actually, if a secondary bar merged with the main bar, further clear movement of the bar conglomerate was absent. On an accretionary profile, the small bar that formed moved somewhat onshore or was stationary.

262. In Figure 22(a and b), the horizontal location of the mass center is shown as a function of time for the CE and CRIEPI experiments. Distance was measured from the intersection of the initial profile and the still-water level. Bars formed on a beach composed of coarser grains in general moved less than those on beaches composed of finer grains under the same wave conditions (compare Cases 400-401 and 500-501). Case 911, which involved a sinusoidally varying water level, showed back-and-forth movement of the bar in response to the change in water level, an effect not observed in control Case 901 (fixed water level).

263. It was difficult to detect trends in the movement of the vertical position of the bar center of mass. For bars formed on accretionary profiles,

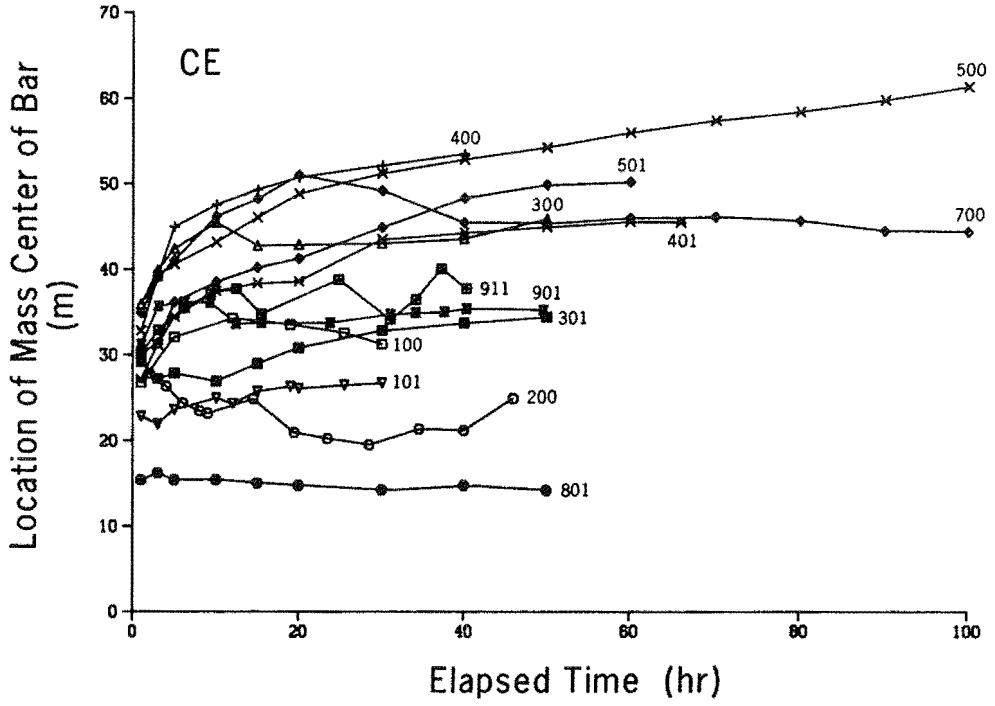

a. CE data

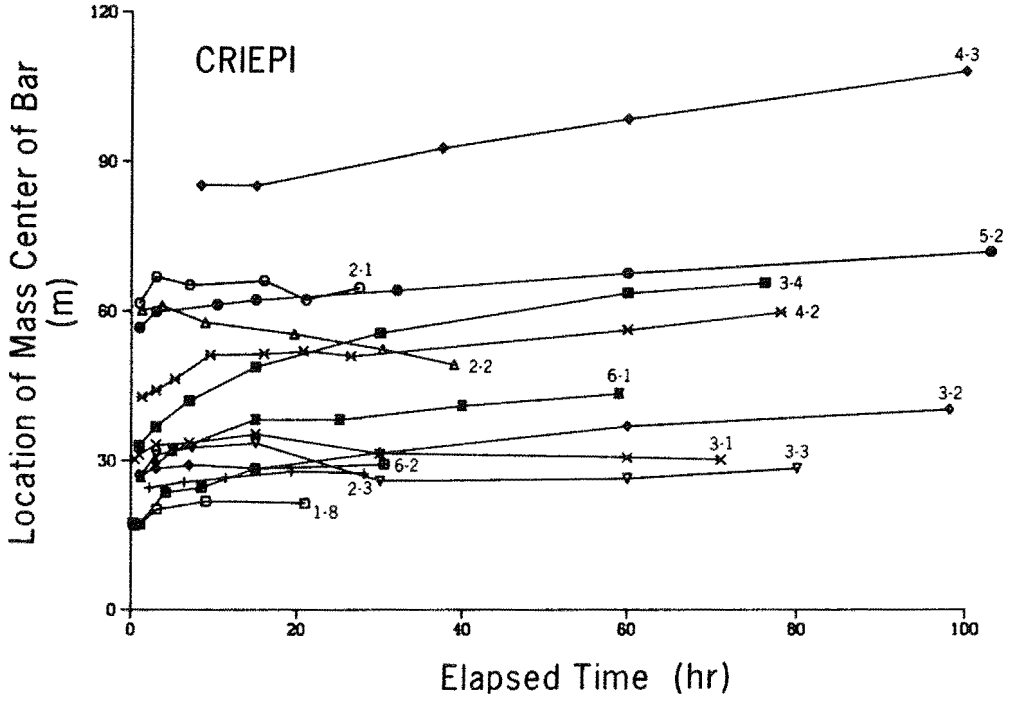

b. CRIEPI data

Figure 22. Horizontal movement of bar center of mass

vertical position of the mass center was relatively constant since the equilibrium bar volume was attained rapidly, and horizontal movement of the bar was limited. However, the overall trend for bars formed on erosional beach profiles was for the vertical distance to the bar mass center to increase with time.

264. As expected, bars appeared to be initiated at the same location along the profile for the same wave conditions and initial beach slope, irrespective of beach grain size. However, the bar center of mass at later times was usually located farther offshore and in deeper water for finer grain-sized beaches.

265. The locations of both the bar crest and the bar center of mass were used as reference points to calculate the speed of bar migration. Evolution of bar speed had the same characteristic features for both references. Only bars formed on erosional profiles were included in analysis of migration speed, since bars on accretionary profiles were almost stationary (see Figure 22). Furthermore, if an inner bar grew together with the main breakpoint bar, only the seaward portion of the bar conglomerate was considered to eliminate spurious instantaneous shoreward displacements of the center of mass resulting from coalescence of the bars. Figure 23(a-d) displays speed of bar migration. Positive speeds of bar migration indicate movement directed offshore. The main trend was similar for all cases and independent of definition (reference point), exhibiting a high initial speed of bar migration which slowed as the profile approached the equilibrium shape.

266. Case with a simulated tide. Case 911 from the CE experiment, which had a cyclical variation in water level, showed cyclical onshore and offshore bar movement, i.e., negative bar speeds as the water level dropped. The main purpose of Case 911 was to demonstrate that a variation in water level would produce a more gently sloping bar*. A negative speed of bar migration also occurred if bar shape changed considerably during a run, particularly if the location of the crest were used as the reference point. For example, Case 100 showed a negative bar speed after about 20 hr, as the

---

* Personal Communication, Thorndike Saville, Former Technical Director, Coastal Engineering Research Center, Ft. Belvoir, VA.

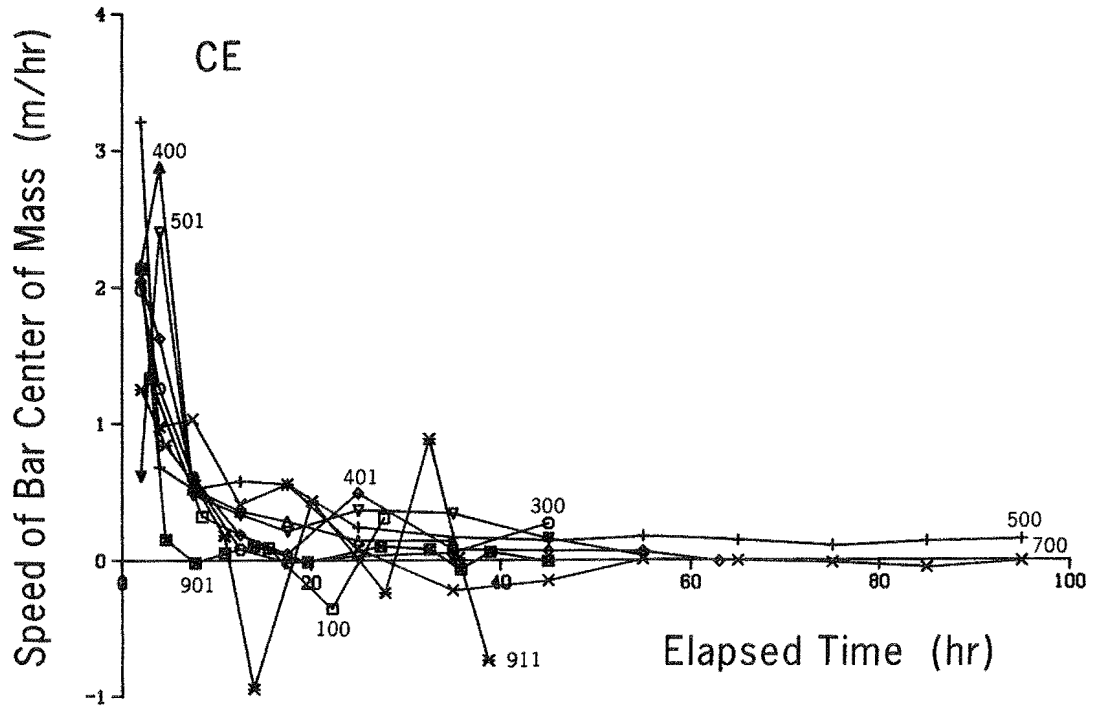

a. CE data, bar center of mass

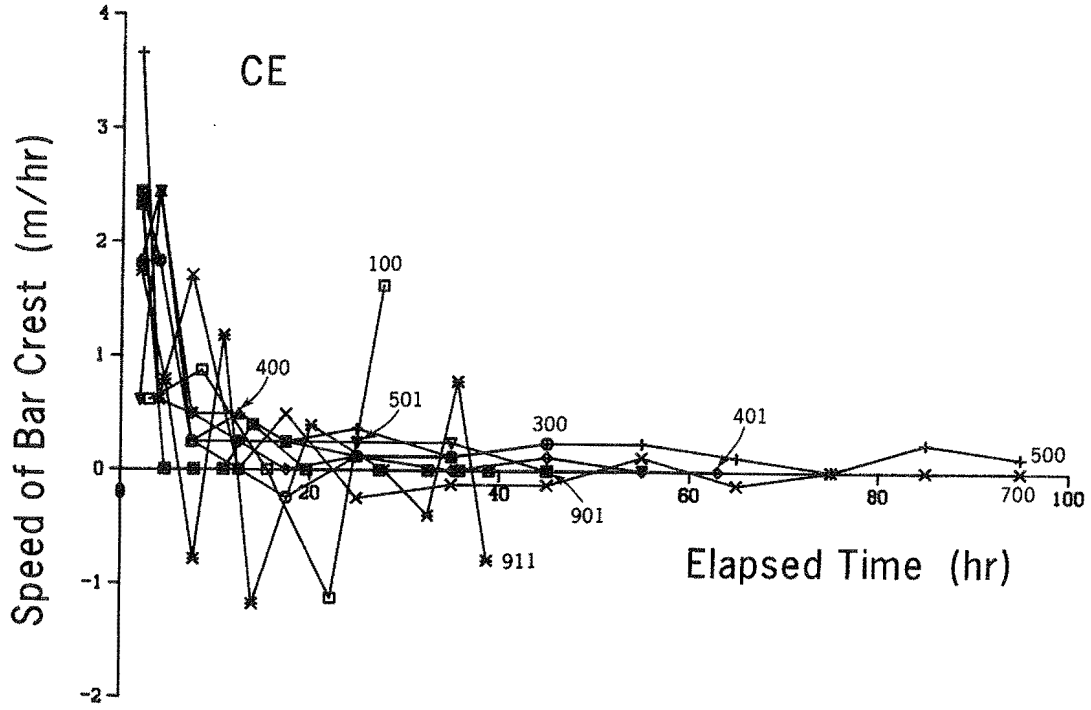

b. CE data, bar crest

Figure 23. Speed of bar movement with elapsed time (Continued)

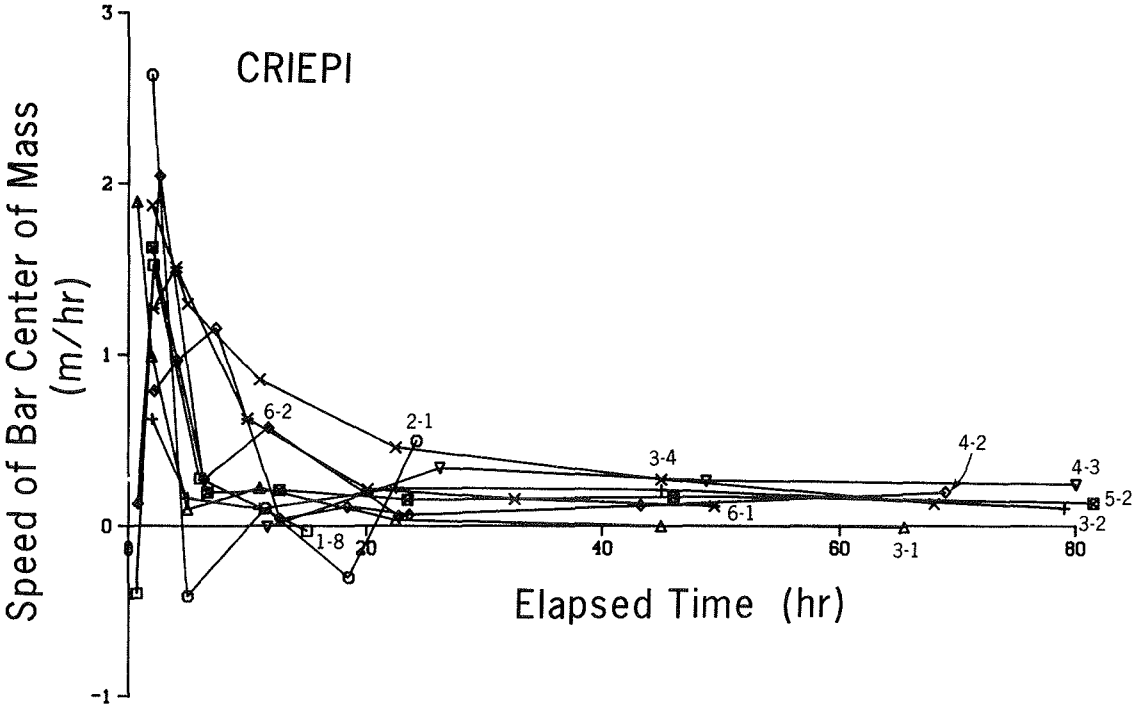

c. CRIEPI data, bar center of mass

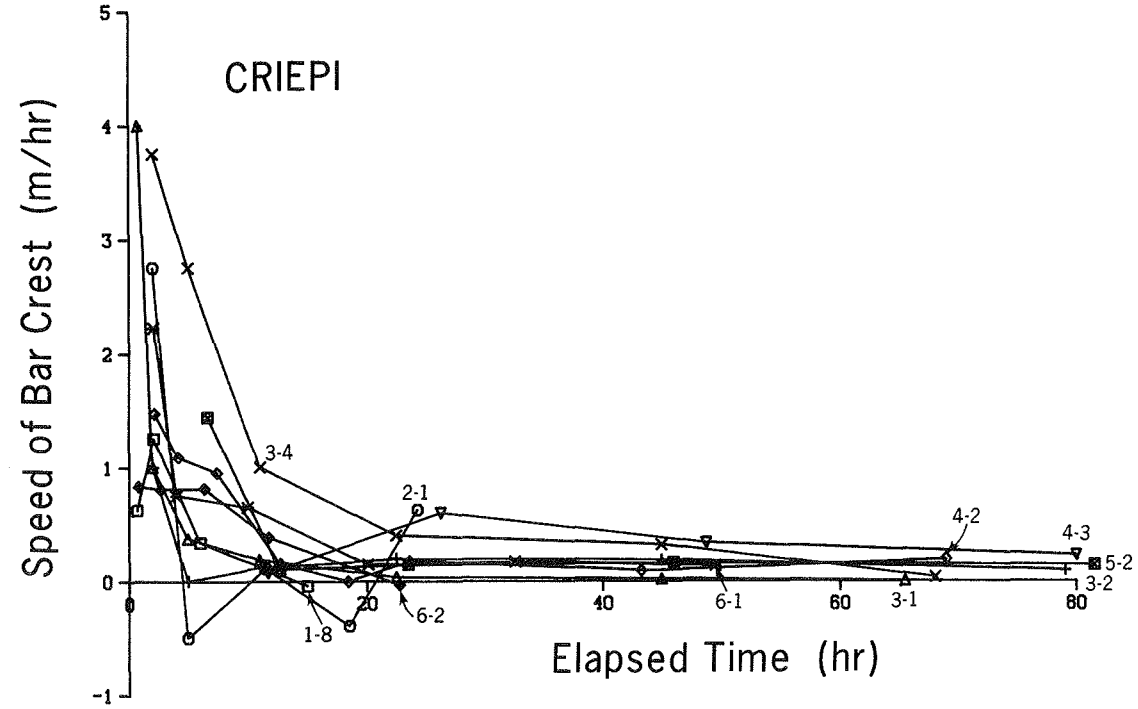

d. CRIEPI data, bar crest

Figure 23. Concluded

beach eroded back to the end of the tank and marked reflection started to occur, influencing bar shape.

267. Comparison with a field measurement. Initial speeds of bar movement in the LWTs had the same magnitude as observed in the field measurements of Sallenger, Holman, and Birkemeier (1985) made during a storm at CERC's FRF at Duck, North Carolina. In general, morphologic features of the profile in the field showed rapid response to changing wave conditions, in qualitative agreement with profile response generated in the LWTs. The bar crest at Duck had an average offshore speed of 2.2 m/hr during the initial phase of one storm (6-hr average) and a speed of 1.4 m/hr for another storm which had smaller waves. Migration speeds measured by Sallenger, Holman, and Birkemeier (1985) were close to those obtained in the CE and CRIEPI studies for the cases showing strong erosion (Figures 23b and 23d).

268. The distance between the location of the maximum trough depth and the bar crest was approximately constant during cases with a well-developed trough. Coarser grained beaches tended to have greater distances between trough bottom and bar crest. Larger waves also caused the distance from the bar crest to the trough bottom to increase for a specific grain size. For a typical unibarred profile, the vertical distance between maximum trough bottom and bar crest appeared to increase slightly with time up to the equilibrium value.

Distance from break point to trough bottom

269. According to the (small-scale) wave tank results of Miller (1976), the trough located shoreward of a breakpoint bar is initiated where the breaking waves completely disintegrate. Sunamura (in press) made the observation that this process is valid not only for plunging breakers but also for spilling breakers, although the trough is not so marked and takes longer to form under spilling breakers. The distance between break point and plunge point may thus be generalized to include both plunging and spilling breakers to yield a plunge distance. Galvin (1969) noted through small-scale and prototype-scale experiments that this distance was equal to about $4H_b$. For the CRIEPI data, Sunamura (in press) related the distance between trough bottom and break point to bottom slope and wave steepness at breaking. In the relationship, distance was normalized by deepwater wavelength, which gives the

impression of a stronger correlation between parameters than is the case.

270. In the present study, the CRIEPI data set, which contains comprehensive wave information, was used to determine the distance ℓ_{tc} between the break point and the maximum trough depth normalized by the deepwater wavelength. This quantity was best correlated with the ratio of the breaking wave height to the deepwater wave height and to the local slope just prior to breaking. Evaluation of the slope was somewhat subjective, and it was defined as the average for the region of approximately one-half the local wavelength seaward of the break point. Consideration was also given to characteristics of the cross-shore distribution of wave height to determine the region of considerable shoaling and thus where wave properties were greatly influenced by profile shape. The regression relationship derived is

$$\frac{\ell_{tc}}{L_o} = 0.12\ (\tan\beta)^{-0.44} \left[\frac{H_b}{H_o}\right]^{-2.36} \tag{16}$$

271. The coefficient of determination for Equation 16 is 65 percent for 110 values. Only profiles having a distinct trough were used in the analysis. Figure 24 displays predicted normalized plunge point distances (subscript p) and measurements (subscript m). The location of the maximum trough depth was inferred to be closely related to the location of the maximum cross-shore transport rate. A bar typically formed immediately seaward of the trough as an accretionary feature resulting from the seaward decrease in cross-shore transport rate.

Bar slopes

272. The growth of a bar is ultimately restricted by the maximum slope that sand grains can maintain without moving under the action of gravity. If this limiting slope is exceeded, avalanching will occur and the sand will be redistributed to attain a more gentle slope which is stable. Allen (1970) recognized these two different slopes and called them the angle of initial yield and residual angle after shearing, respectively. From his experiments with natural sand (diameters ranging from 0.27 to 3.17 mm in the experiments), he obtained an angle of about 48 deg to cause avalanching and an angle of about 33 deg as the stable slope after avalanching had ceased.

273. In the LWT experiments, as a bar approached equilibrium, its shoreward face appeared to approach the angle of initial yield, followed at later profile survey times by intermediate lower values. This alternating behavior in bar angle supports the concept of a continuous steepening of the

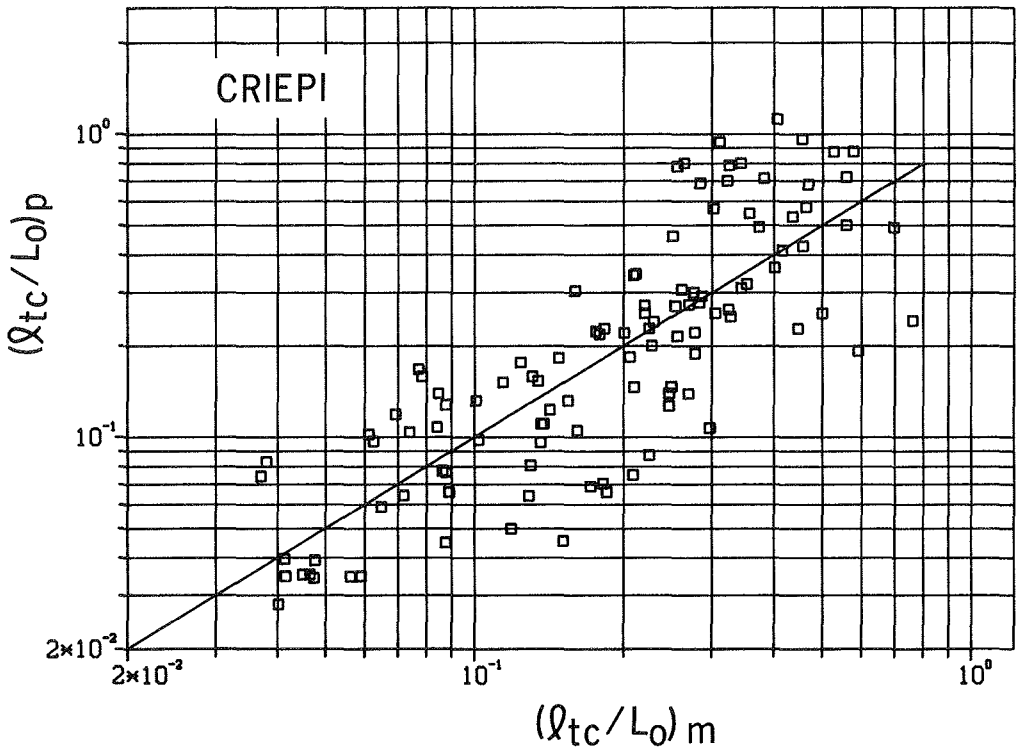

Figure 24. Comparison of measured and predicted nondimensional horizontal distance between break point and trough bottom

shoreward slope to a limiting angle followed by avalanching which adjusts the slope to a lower value. Figure 25 shows the behavior of the average shoreward slope of a bar β_3 with time for Cases 401 and 501, increasing at first and then having smaller values after a certain initial maximum slope was reached. However, the number of profile surveys is too small to obtain reliable information about the avalanching process apart from circumstantial evidence that it appeared to occur.

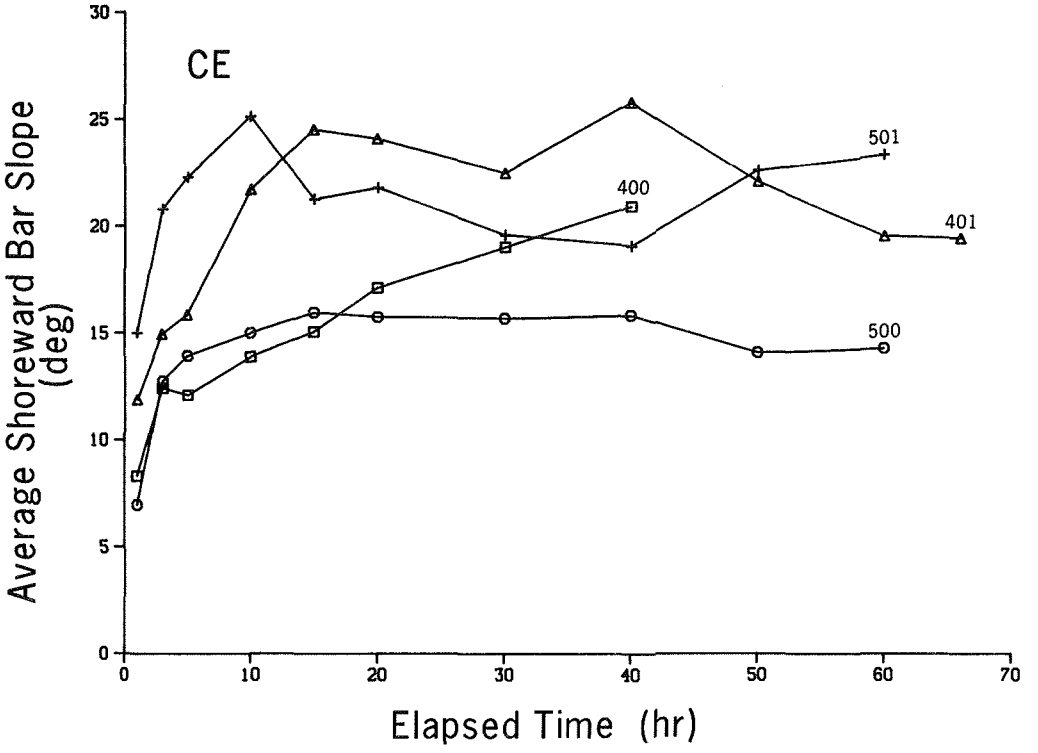

Figure 25. Evolution of shoreward slope of main breakpoint bars

274. In general, the average shoreward bar face slope generated in the LWT experiments increased with time, and the angle of initial yield was apparently not achieved (see Cases 400 and 500 in Figure 25). In particular, for the finer grain sizes, steepening of the shoreward face slope appeared to be slower even though the angle of initial yield should be approximately independent of grain size for the range of material studied.

275. If a second bar formed immediately shoreward of a main breakpoint bar, steepening of the shoreward slope of the main bar was usually hindered, and the slope sometimes decreased. The maximum bar face slope on the shoreward side of a bar was 35 deg (Case 4-3), which is considerably less than Allen's (1970) limiting value. A smaller maximum slope under wave action is logical because of the turbulent fluid environment existing in the surf zone, which is considerably different from the laminar flow conditions under which Allen performed his experiments. The expected result of turbulent flow is increased destabilization of the sand grains, thus lowering the maximum stable slope, which is in agreement with the trend of the observations. Evaluation

of the 14 cases where the angle of initial yield appeared to have been attained indicated that the maximum slope on the shoreward bar face was in the range of 20-35 deg, with an average of 28 deg. In each of the cases, the angle of initial yield should be somewhat larger than the value determined as the maximum slope. An estimate of bar face slope after avalanching occurred may be obtained by examining the minimum shoreward bar face slope after the angle of initial yield had apparently been exceeded. The slope thus calculated (10 cases showing clear minima) was in the range of 20-25 deg, with an average of 22 deg. These values should be somewhat higher than the actual residual angle after shearing since some steepening of the slope probably occurred between the times of avalanching and the profile survey.

276. The average seaward bar face slope was fairly constant through time, sometimes exhibiting a slight increase during the first hours of the run. Figure 26 shows the seaward bar face slope as a function of time for representative cases. The average slope was typically in the range of 8-12 deg, although local slopes reached 20 deg. The variation in average seaward bar face slope was small and appeared to be independent of grain size, but weakly related to wave period, with longer periods giving a more gentle slope.

277. The seaward face of the bar was in many cases well approximated by two or three planes having distinctly different slopes. The upper part of the bar face seaward from the crest had a slope β_2 ranging from 4-8 deg, whereas the slope of the lower part of the bar β_1 was in the range of 8-18 deg. In some cases, the very end of the bar could be approximated by a third line of constant slope, often with a magnitude smaller than that of the two shoreward slopes. The location of the intersection between the upper and lower seaward face slopes approximately coincided with the location of the break point in many cases (see Figure 14). This triplaned nature of bars formed under regular waves does not seem to have been noted before. Although such a configuration would probably not be exhibited in the field because of varying waves and water level, its manifestation under regular waves indicates the existence of a small and subtle regime of hydrodynamic forces in the region under prebreaking waves which acts on a wave-by-wave basis whether or not it is observed in macroscale profile surveys in the field.

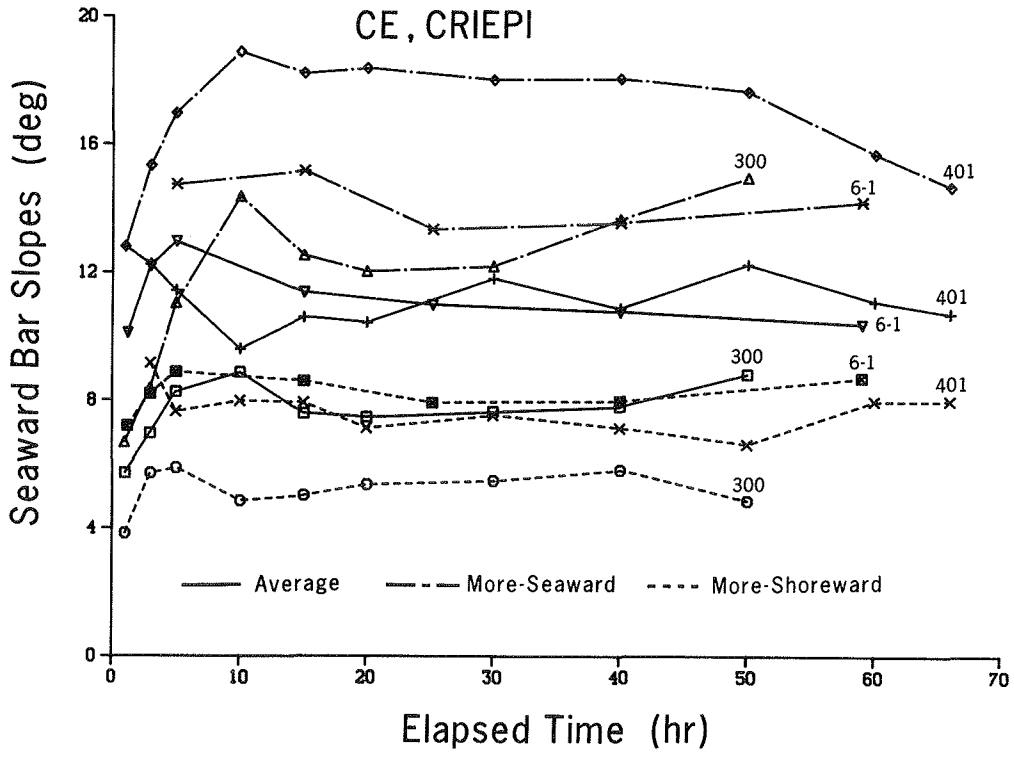

Figure 26. Evolution of seaward slopes of main breakpoint bars

278. Since average shoreward and seaward bar face slopes were considerably different, the bars were asymmetric in shape. The average shoreward bar slope was always steeper than the corresponding average seaward slope, making the bar positively skewed.

279. Bar face slopes encountered in the field are, in general, milder than slopes in the CE, CRIEPI, and other tank studies involving regular waves and constant water levels. Under laboratory situations, the smoothing effect on the profile of random waves and varying water level which normally exist in nature (e.g., Keulegan 1948) is absent. For example, Hands (1976) found that maximum bottom slope was less than 10 deg for numerous measurements of Lake Michigan bars (varying waves but constant water level). On the basis of frequent and repetitive high-accuracy surveys on an Atlantic Ocean beach over 5 years, Birkemeier* found that steepest shoreward bar slopes of approximately

* Personal Communication, 1987, William Birkemeier, Hydraulic Engineer, Coastal Engineering Research Center, Vicksburg, MS.

10 deg occurred when bars moved onshore during the profile recovery process after a high wave event, not when bars moved offshore. Seaward bar faces rarely exceeded 10 deg.

280. Within the context of this study, the difference between present and field results for bar face slopes can be attributed in great part to the action of random waves and varying water level, which would widen the breaker zone and smooth profile features in the field. Another factor is that steady wave conditions are usually not of sufficient duration in the field for bars to reach equilibrium form.

Step and terrace slope

281. In the LWT experiments, when erosion occurred the beach profile retreated to produce a characteristic scarp or step immediately landward of the still-water level. This scarp developed concurrently with a gentle terrace slope that was milder than the slope of the initial profile. The slope of the step increased with time and sometimes reached the angle of initial yield, exhibiting the same tendency of alternating maxima and minima, similar to the behavior of the shoreward slope of breakpoint bars as discussed above. If the initial slope was mild, the retreat of the shoreline was small; and the shoreline sometimes advanced somewhat even if a breakpoint bar formed offshore. In this latter case most of the material in the bar was taken from the surf zone rather than from the foreshore. If the waves were not too severe (erosive) in these cases, the bar may have also received a net contribution of material by onshore transport from the area located seaward of it. However, if the waves were severe, a step formed even if the slope were relatively gentle since the surf zone was not wide enough to dissipate all of the incident wave energy, thereby resulting in strong wave attack and erosion of the foreshore.

282. Figure 27 illustrates the average slope of the step β_5 as a function of time for selected cases in which considerable erosion of the foreshore took place. Time development of the average terrace slope β_4 immediately seaward of the step is also presented. For a coarser grain size, steepening of the step slope proceeded more slowly (Case 401) and may have achieved an equilibrium value before the angle of initial yield was reached. The slower response of the coarser grains is probably due to their greater

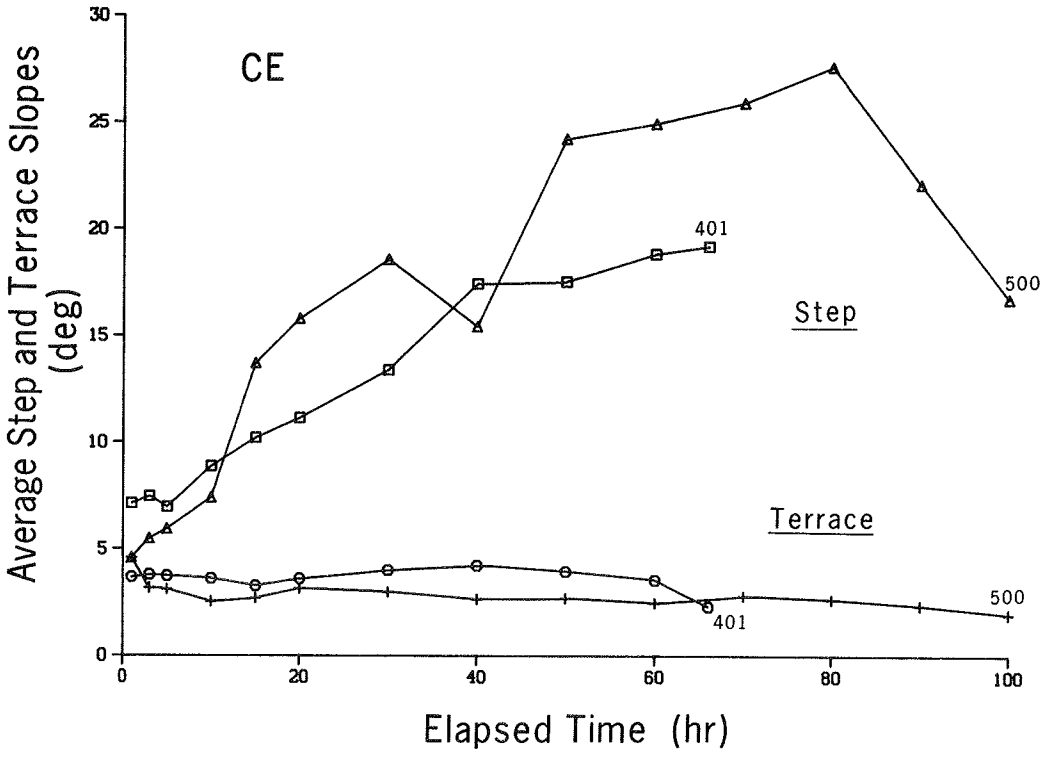

Figure 27. Evolution of representative step and terrace slopes

stability against dislodgement and transport by the bore. The terrace slope was more gentle than the initial slope and appeared to be almost independent of grain size, with finer grain sizes showing a slight tendency to form gentler slopes.

Form and Movement of Berms

Berm genesis

283. As wave steepness becomes smaller (e.g., as a storm wanes and the wave height decreases), the transport direction changes from offshore to onshore and material builds up on the foreshore, a process documented by Hayes and Boothroyd (1969), Sonu (1970), and Kriebel (1987). A berm forms which is a function of local wave and water level movement on the foreshore and sediment properties. In this study, the berm was defined as the volume of material accreted on the foreshore with reference to the initial plane slope (Figure 4b). This is a natural definition since a berm is intuitively thought

of as an accretionary feature. The berm typically forms above the still-water level but may extend below the water surface and move the shoreline position slightly seaward as it grows with time. The vertical extent of the berm is closely related to the runup limit, whereas its shoreward extent in the equilibrium state is mainly determined by how the grains move under gravitational force. The point on the foreshore where berm formation is initiated mainly depends on the runup limit where a larger runup implies berm initiation further shoreward. Runup is essentially a function of local beach slope, wave period, and breaking wave height for both regular waves in the laboratory (Hunt 1959, Savage 1959) and irregular waves in the field (Holman and Sallenger 1985).

284. No information about runup was available from the CRIEPI experiments and only little information from the CE experiments. In the CE experiments, runup was measured in most cases, typically for the first 10-20 waves (Kraus and Larson 1988a). There were only five CE cases which had berm build-up and measurement of runup. However, an indication of the relationship between berm formation and runup may be obtained by viewing Figure 28 where the distance to the mass center of the berm is plotted as a function of the runup length ℓ_r, all quantities referenced to the initial still-water level. The runup length is the average of all runup measurements, and the first profile survey (typically performed after about 1 hr of wave action) was used to calculate the distance to the berm center of mass. The distance to the center of mass was roughly half the runup length which, if the berm is considered to be approximately symmetrical, indicates that the runup length was close to the shoreward end of the berm, as would be expected. All berms in the previously-mentioned five cases were formed on profiles showing a strong tendency for onshore transport during the full duration of the run, although a small breakpoint bar may have been present.

285. In cases where a berm was present but the transport rate was more variable in direction both along the profile and in time, the berm was often small and sometimes formed with its center of mass below the still-water level. Equilibrium properties of the berm on such profiles (berm volume, maximum berm height) were reached very rapidly, typically prior to the time of the first profile survey.

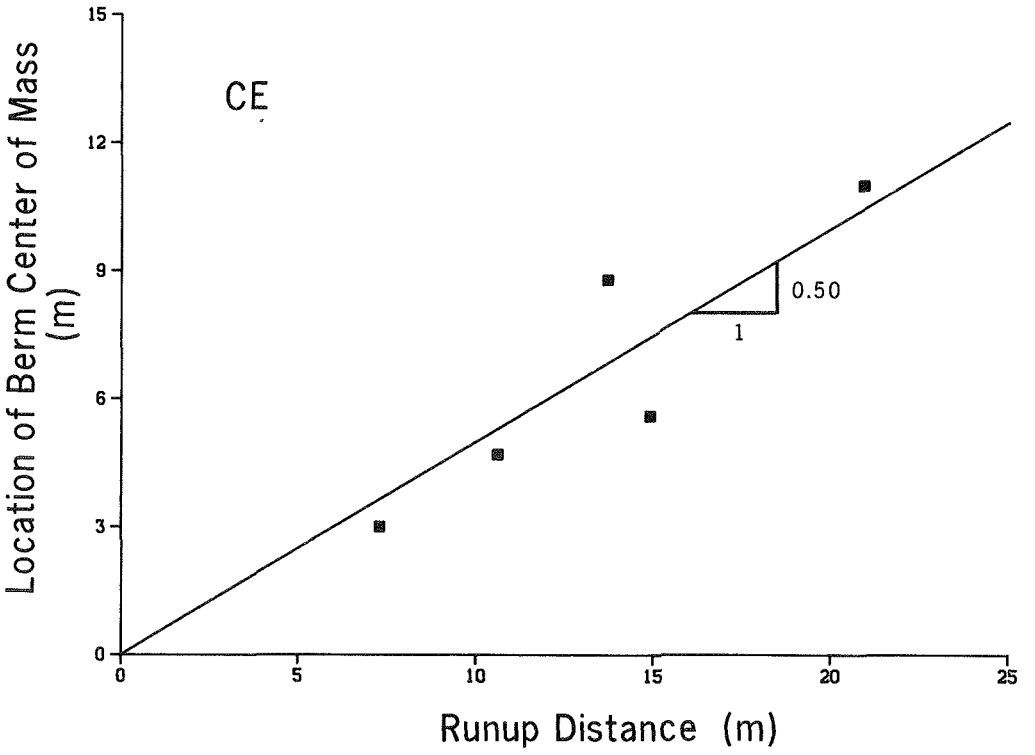

Figure 28. Relation between berm center of mass and wave runup

286. For most berms, the horizontal movement of their center of mass was small, indicating that the berm grew uniformly in time over its length. If the berm showed a net movement of its center of mass, it was always in the shoreward direction. The length of the berm at equilibrium appeared to depend mainly on breaking wave height and little on wave period (Bagnold 1940, Sunamura 1975, Takeda 1984).

Active profile height

287. A quantity Z_R was defined as the maximum subaerial elevation of the active profile above still-water level for either bar or berm profiles (Figure 4b). An empirical equation was obtained from the LWT data by relating this quantity to the surf similarity parameter, $\tan\beta/(H_o/L_o)^{1/2}$ (Battjes 1975). The surf similarity parameter was evaluated using the initial beach slope, resulting in the empirical equation

$$\frac{Z_R}{H_o} = 1.47\left[\frac{\tan\beta}{\sqrt{H_o/L_o}}\right]^{0.79} \qquad (17)$$

The coefficient of determination was 75 percent for 32 cases for which the height of the active profile could be distinguished.

Equilibrium berm volume

288. In the LWT experiments, volume of the berm increased with time to approach an equilibrium value attained when the profile was in balance with the incident waves, thereby dissipating wave energy without significant changes in shape. Seventeen cases exhibiting some kind of foreshore buildup were identified in the CE and CRIEPI data sets. However, only eight of these cases showed strong berm buildup with onshore transport occurring during most of the run. In some CRIEPI cases, accretion on the foreshore started to occur only at the very last few profile surveys, and equilibrium was reached almost immediately (for example, Cases 4-2 and 5-2). Profiles of this type were erosional, but these cases had a moderate wave climate and a gentler initial slope, allowing for a small amount of onshore transport on the foreshore as the breakpoint bar system approached equilibrium. In Figure 29(a and b), the berm volume as a function of time is displayed for the CE and CRIEPI experiments.

289. To estimate equilibrium berm volume, an expression similar to Equation 7 was least-squares fitted to the data for the eight cases. The number of cases was too small to derive reliable empirical relationships between berm volume and wave characteristics and beach profile properties. Some tendencies noted may be of interest for indicating which factors appear to control equilibrium berm volume. Berm volume showed the greatest dependence on sand fall speed, with a greater fall speed implying a larger berm volume. This phenomenon seems reasonable because the tendency for onshore transport increases with greater fall speed for the same deepwater wave steepness (Figure 6). Within the range of grain sizes used in the experiments, coarser material often experienced more marked onshore transport than the finer material. In contrast, the finer material, for the cases where berm buildup occurred, had a less dominant transport direction, thus resulting in

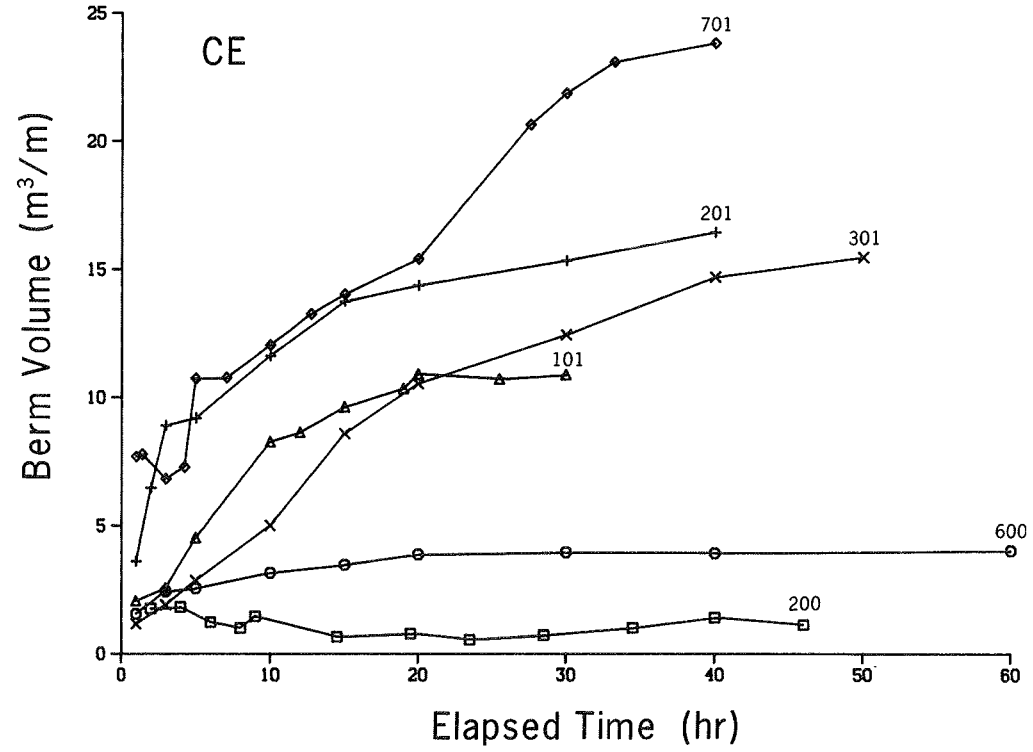

a. CE data

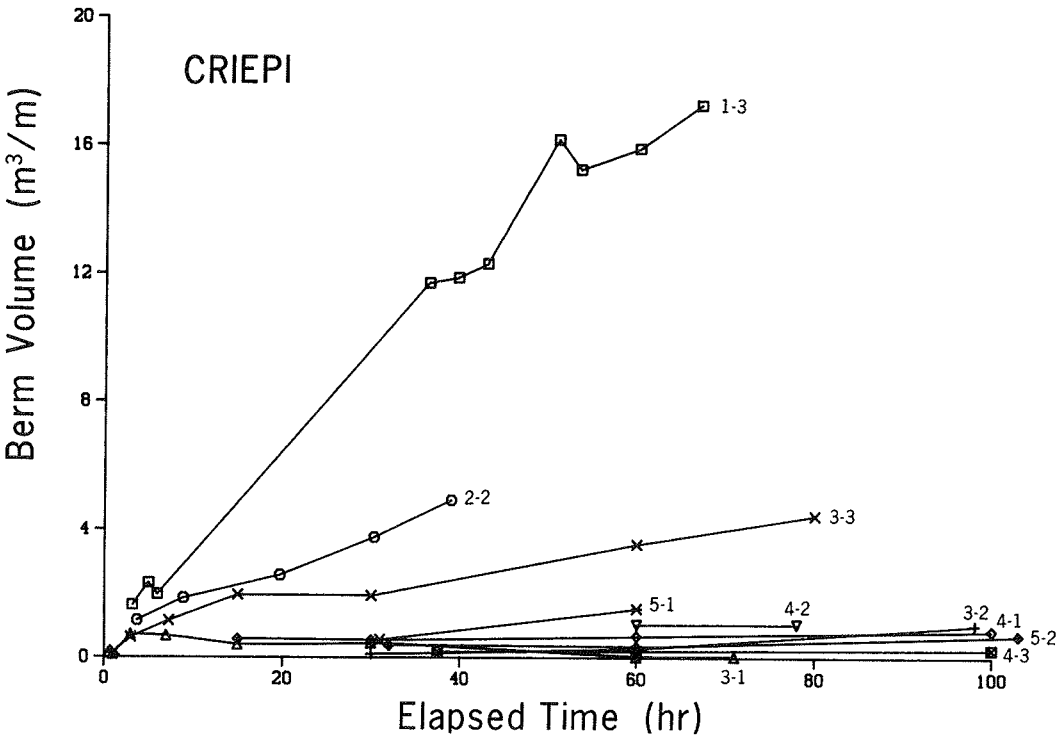

b. CRIEPI data

Figure 29. Growth of berm volume with elapsed time

smaller equilibrium berm volumes. An increase in wave height produced a larger berm volume, whereas wave period seemed to be a negligible factor. However, wave period influenced the rate at which equilibrium berm volume was reached, with a longer wave period producing more rapid berm buildup.

Maximum berm height

290. Maximum berm height Z_b defined with respect to the initial profile showed development with time similar to berm volume. Figure 30(a and b) shows the growth of maximum berm height as a function of time. If accretion on the foreshore occurred in cases with predominant offshore transport, equilibrium berm height was attained quickly, as seen in Cases 200, 3-1, and 4-2. Equilibrium maximum berm height was estimated from a least-squares fit of the data from each case (eight cases used in total), with an expression of the form of Equation 7. Grain size emerged as an important variable for the same reasons as discussed for equilibrium berm volume. Breaking wave height appeared as a considerably more decisive factor than deepwater wave height, probably because runup is more closely related to breaking wave height. The ratio between maximum equilibrium berm height and breaking wave height had a relatively small range. The average value of the ratio was 0.5, ranging from 0.3 to 0.8 for the eight cases analyzed. The standard deviation was 0.16.

291. Berm height, normalized by some appropriate length scale (wave height or wavelength), showed no correlation with dimensionless sand fall speed. This occurrence is not surprising since this quantity is generally believed to characterize suspended transport which is not the dominant transport mode on the foreshore. For a specific grain size, berm height divided by breaking wave height was found to be weakly dependent on the surf similarity parameter, but a clear overall relationship could not be obtained. Runup height is usually expressed in terms of the surf similarity parameter (see Hunt 1959), so this dependence is expected; however, the present data sets on berm growth are too limited to conclusively verify such a relationship.

Berm slopes

292. If a berm formed on the foreshore, its seaward face slope steepened and a positive slope developed on its shoreward face. Average seaward berm face slope was relatively constant, with a slight tendency to increase

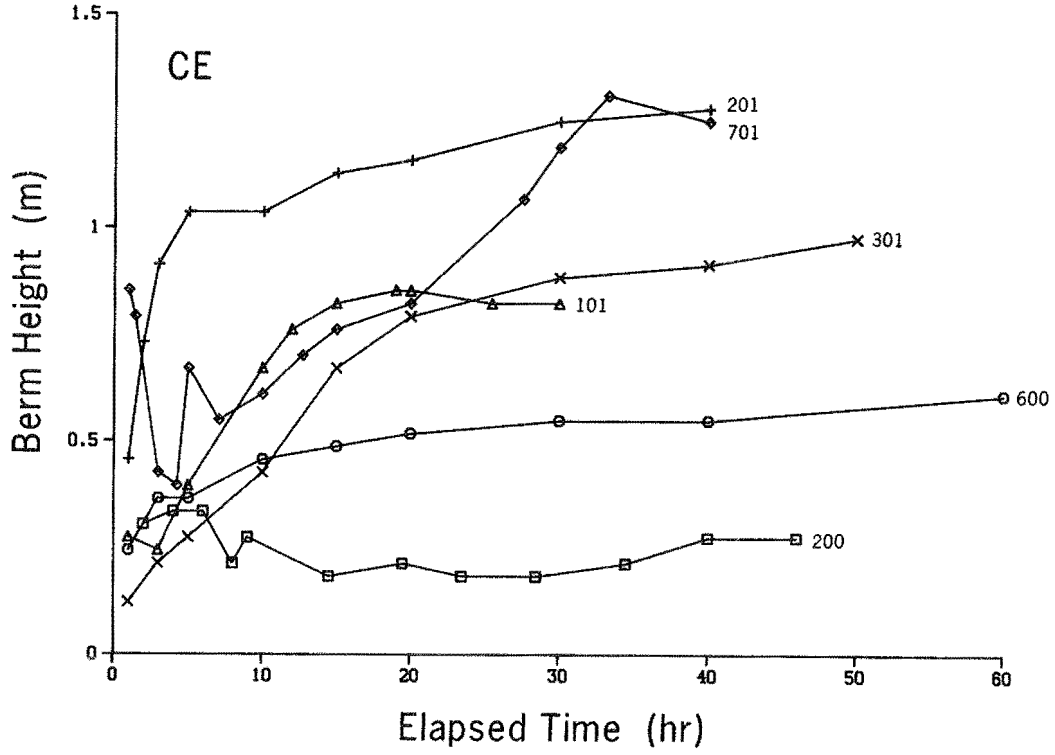

a. CE data

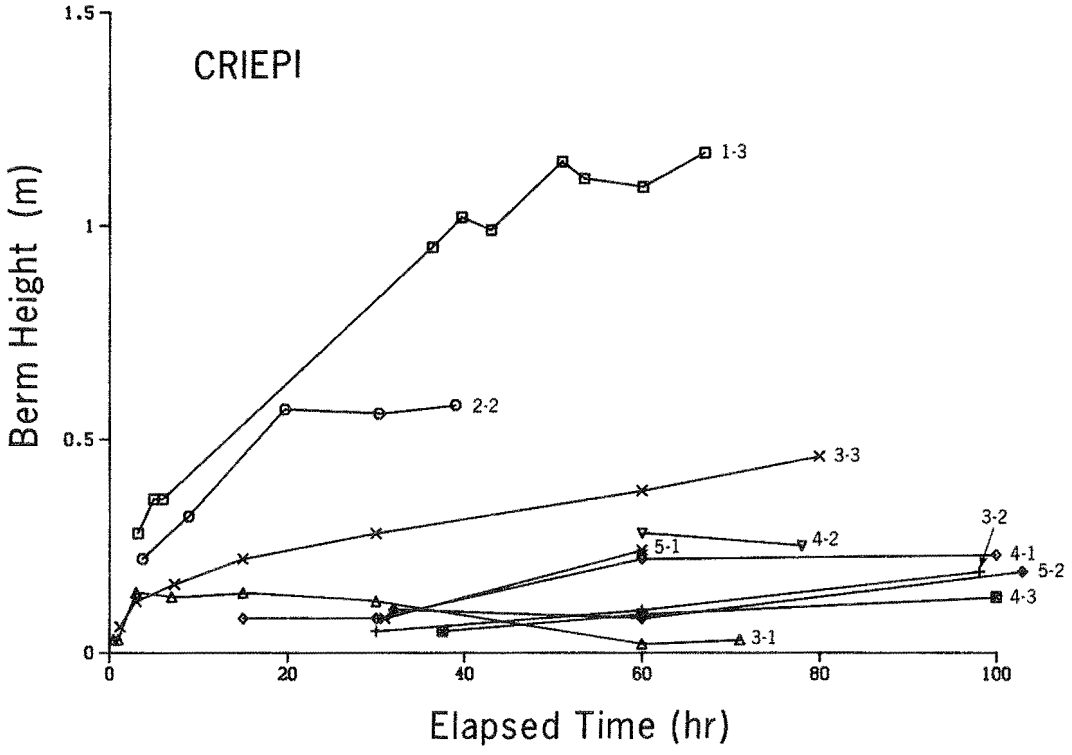

b. CRIEPI data

Figure 30. Growth of maximum berm height with elapsed time

with time. Figure 31 shows the time change of the average shoreward berm face slope ϕ_1 and seaward slope ϕ_2 changed during two typical cases (Cases 300 and 1-3) with berm buildup. The seaward berm slope was approximately independent of grain size and ranged between 6-8 deg.

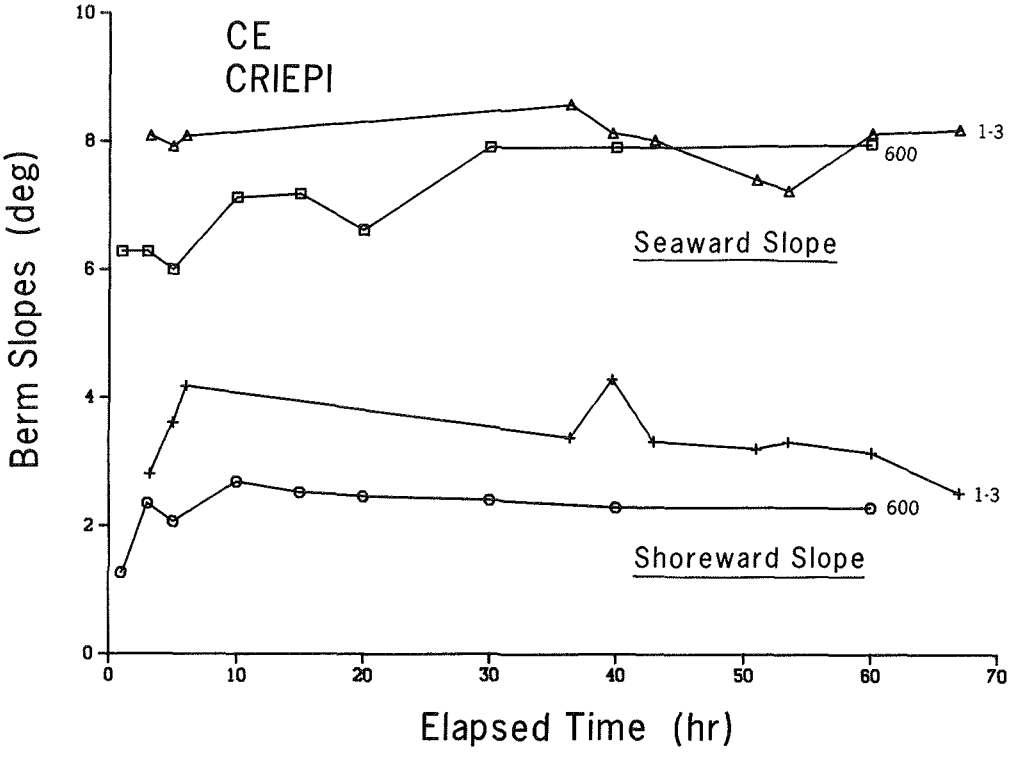

Figure 31. Growth of representative berm slopes with elapsed time

293. If a well-developed shoreward berm face slope was present, it was considerably more gentle than the seaward face slope. Typical values of the average shoreward berm face slope were 2-4 deg, although steeper slopes occurred. The average shoreward berm face slope also appeared to be independent of grain size and constant in time, except for one case (Case 201) which showed an increase with time toward an equilibrium value of about 15 deg. In this case the grain size was coarse, and the wave height and wave steepness were relatively small. The waves were probably breaking very close to the shoreline, one of the few cases where no breakpoint bar appeared along the profile, strongly affecting the shape of the berm.

Summary

294. Numerous morphologic features of beach profiles generated under breaking waves in large wave tanks were quantitatively described in this chapter. Selected morphologic parameters are presented in Tables 4 and 5, together with the breaking wave height. Under steady, regular waves and constant or slowly varying water level, the evolution of bars and berms was found to be regular, exhibiting clear growth and equilibrium properties that were readily described by simple regression expressions. The dimensionless sand fall speed H_o/wT emerged as an important parameter in predicting both profile response and geometric properties of various major morphologic features. The strong relationship between wave and sand characteristics and morphologic features suggests the possibility of quantitatively predicting the evolution of macroscale features of the profile.

295. The effect of scale was made apparent through the different values of empirical coefficients in the criteria for erosion and accretion (bar/berm formation) for small-scale and prototype-scale wave and beach conditions. Interestingly, most criteria held for both small- and prototype-scale experiments provided that empirical coefficients were modified. It was found that use of mean wave height with field data allowed the same criterion to be used (Equation 2) as found for the LWT experiments involving regular waves, with no change of the empirical coefficient.

296. In general, profile response in the LWT experiments, apart from effects related to use of regular waves, was considerably in agreement with what is observed on a natural beach. Irregular waves as occur in the field are expected to give a smoother character and slower rate of change of morphologic features.

Table 4

CE Experiments: Values of Selected Quantities

	Bar				Berm		
Case No.	V_{eq} m^3/m	h_c m	$(h_t/h_c)_{avg}$	H_b m	V_{eq} m^3/m	Z_b m	Z_R m
100	18.5	1.16	1.45	1.68	----	----	----
200	8.2	0.90	1.50	1.07	----	----	0.89
300	30.1	1.31	1.71	2.00	----	----	1.56
400	28.6	1.52	1.68	2.30	----	----	1.50
500	33.3	1.44	1.84	1.90	----	----	1.05
600	----	----	----	1.15	3.8	0.53	0.88
700	24.5	1.79	1.46	2.10	----	----	1.81
101	3.7	1.31	1.26	1.80	11.7	0.88	1.29
201	----	1.18	1.32	1.90	14.9	1.17	1.45
301	2.9	1.44	1.29	2.40	18.3	1.01	1.36
401	19.6	1.28	1.89	2.40	----	----	1.48
501	22.1	1.16	2.05	1.60	----	----	0.72
701	----	----	----	1.95	23.1	1.14	2.56
801	----	0.56	1.62	0.76	----	----	0.47
901	11.3	1.28	1.55	2.00	----	----	0.97
911	12.0	----	----	----	----	----	1.26

Table 5

CRIEPI Experiments: Values of Selected Quantities

	Bar				Berm		
Case No.	V_{eq} m^3/m	h_c m	$(h_t/h_c)_{avg}$	H_b m	V_{eq} m^3/m	Z_b m	Z_R m
1-1	----	0.47	1.89	0.95	----	----	0.37
1-3	----	----	----	1.40	27.7	1.12	1.31
1-8	1.6	0.55	2.06	0.85	----	----	0.24
2-1	7.5	1.12	1.78	1.94	----	----	0.23
2-2	8.7	0.67	2.06	1.54	7.3	0.60	0.52
2-3	0.7	0.45	1.96	0.80	----	----	0.14
3-1	12.4	0.91	1.78	1.88	----	----	0.75
3-2	15.3	0.76	1.76	1.58	----	----	0.55
3-3	9.1	1.00	1.50	1.47	5.0	0.43	0.98
3-4	24.9	1.23	2.16	1.50	----	----	0.48
4-1	----	----	----	0.50	----	----	0.21
4-2	4.5	0.83	1.84	1.27	----	----	0.37
4-3	23.5	1.23	2.07	1.52	----	----	0.34
5-1	----	----	----	0.63	----	----	0.36
5-2	6.5	0.61	2.02	0.89	----	----	0.43
6-1	36.5	1.39	1.76	1.91	----	----	1.66
6-2	25.3	0.98	----	1.42	----	----	1.19

PART V: CROSS-SHORE TRANSPORT RATE

297. If a beach profile is not in equilibrium with the existing wave climate, sediment will be redistributed along it to produce an equilibrium profile shape in which state the incident wave energy will be dissipated without causing further significant net sediment movement. It has been established that as sediment is transported across the shore certain characteristic net transport rate distributions occur, and these distributions have specific properties in time and space. Regularity in transport rate distributions is anticipated since the previous chapter showed that the shape of the beach profile changed regularly through time.

298. The objective of this chapter is to describe properties of the cross-shore sand transport rate and relate them to wave parameters, sand characteristics, and beach profile shape. Quantitative knowledge of cross-shore transport provides the necessary foundation for the numerical modeling component of this investigation.

299. Keulegan (1948) appears to have been the first to measure cross-shore sand transport along the profile. He used traps mounted in a small wave tank and found that the maximum transport rate was located at the point of impending wave breaking where the front of the wave was almost vertical near the crest. He noted a correlation between the sand transport rate and total displacement of the water surface, and he recognized the existence of a critical wave height for sand transport to occur.

300. Several early papers concerned development of criteria for predicting the predominant direction of the transport (onshore or offshore). Rector (1954) used deepwater wave steepness and ratio between median grain size and deepwater wavelength. Ippen and Eagleson (1955) studied the movement of individual particles on a plane slope under shoaling waves and found net motion to result from inequality of hydrodynamic drag and particle weight. Their criterion for distinguishing between onshore and offshore motion contained three nondimensional parameters: wave steepness, ratio of wave height and water depth, and ratio of sediment fall speed and wave celerity.

301. Van Hijum (1975, 1977) determined the distribution of the cross-shore transport rate on a beach of coarse material by comparing consecutive

beach profiles in time. The equation of mass conservation was integrated from successive beach profile surveys, and an average net transport rate over the studied time interval was obtained. The technique of determining the distribution of the net cross-shore transport rate from consecutive profile surveys has been employed in other studies (for example, Hattori and Kawamata 1981; Watanabe, Riho, and Horikawa 1981; Shimizu et al. 1985). A classification of transport rate distributions for LWT results was proposed by Kajima et al. (1983a) based on a beach profile classification by Sunamura and Horikawa (1975) who used data from experiments with a small tank.

302. By determining the transport rate from profile change, an average net distribution of the cross-shore transport rate is obtained for the elapsed time between two surveys. An alternative method of acquiring information on the transport rate is measurement of the sediment concentration and fluid velocity field. Sawaragi and Deguchi (1981) and Deguchi and Sawaragi (1985) measured sediment concentrations in small-scale laboratory experiments and obtained concentration profiles at selected locations across the beach profile. Vellinga (1986) and Dette and Uliczka (1987b) made similar measurements of concentration profiles in experiments performed with large tanks and waves of prototype scale.

303. The average net cross-shore transport rate may be obtained by integrating the equation of mass conservation between two beach profiles in time. The transport rate $q(x)$ across the profile is thus calculated from the mass conservation equation written in difference form with respect to time as

$$q(x) = \frac{1}{t_2 - t_1} \int_{x_o}^{x} (h_2 - h_1)\, dx \tag{18}$$

where

t_1 , t_2 = times of profile surveys

x_o = shoreward location of no profile change, where $q(x_o) = 0$

h_1 , h_2 = profile depths at survey times 1 and 2

304. To evaluate the transport rate numerically, measured profiles used in this study where approximated by a set of cubic spline polynomials (see

Part IV). Subsequent calculations used in the analysis were carried out from a point on the shoreward end of the profile where no change occurred during the run to a seaward point where there was no movement of material (typically, to the horizontal part of the tank beyond the toe of the beach).

305. In Equation 18, sand porosity has been incorporated in q, the cross-shore transport rate, implying that the porosity is independent of time and space. Qualitatively, it was noted during the CE experiments that the foreshore sand tended to compact, whereas sand at the flanks of the breakpoint bar tended to be looser (Kraus and Larson 1988a). The error introduced by assuming constant porosity is believed to be negligible.

306. Errors may be introduced through limitations in accuracy of the profile surveys or due to long time interval between surveys. A small systematic error in profile depth measurements may give a finite contribution if summed over the profile length and could give rise to an apparent transport at the seaward boundary of the profile where no transport actually occurred. In particular, the CE surveys, having a 1.2-m (4-ft) spatial interval, were in some cases not taken frequently enough to indicate negligible transport at the seaward boundary. Therefore, in these cases, to proceed with the analysis, one of the profiles was displaced vertically to achieve the condition of zero transport at the boundary. The vertical displacement was in general small (less than 1 cm) and less than the measurement accuracy of the profile survey ($\pm$1.5 cm). A small displacement of one of the profiles exerts some influence on the magnitudes of maximum and minimum transport rates but only slightly changes the shape of the transport rate distribution.

General Features of Cross-Shore Transport

307. Distributions of the net cross-shore transport rate were determined for both the CE experiment (18 cases) and the CRIEPI experiment (24 cases). However, in most of the analyses a subset comprising 33 cases was used which encompassed those cases starting from an initial plane slope. Profile behavior was thereby more readily isolated, and the added complexity of an arbitrary initial profile shape avoided. Between 5 and 10 transport rate distributions were calculated for each case, depending on the number of

profiles surveyed. Information about the specific cases, such as wave conditions, sand grain size, and initial profile slope are summarized in Tables 1 and 2.

308. Figure 32 shows the beach profile at consecutive times for CE Case 300, which is an example of a bar profile with transport mainly directed offshore. Two bars appeared, and the shoreline receded considerably with a pronounced scarp or step formation. Seaward of the step, the foreshore eroded with a slope more gentle than the initial slope (1:15). In Figure 33 are shown the calculated distributions of the cross-shore sand transport rate associated with Case 300. Transport directed offshore has a positive sign; the coordinate system originates from the position of the initial still-water shoreline. Decay of the transport rate with time is clear from Figure 33, and the maximum transport rate calculated from the final two surveys is more than one order of magnitude smaller than the maximum from the first two surveys.

309. The peak in the transport rate distribution translated seaward with the break point, and thus the bar moved seaward. The first maximum in the transport rate occurred shoreward of the first break point, close to the plunge point and slightly seaward of the location of the trough bottom. Another, smaller maximum in the transport rate was present further inshore, and this maximum also moved slightly seaward with time. For the transport rate distributions at later times, the shape was flatter and no maxima were prominent, indicating that material was mainly conveyed from the inner to the outer part of the profile. Seaward of the first maximum, the transport rate decreased rapidly with an approximate exponential shape.

310. CE Case 101 is an example of a case of mainly onshore transport, resulting in deposition on the foreshore and creation of a berm. Figure 34 shows surveyed profiles at consecutive times, with an initial slope of 1:15. Although a large berm formed on the foreshore, a small bar was also present just shoreward of the break point. The bar was created mainly during the first hours of the run, and it rapidly reached an equilibrium volume. The trough shoreward of the bar became less pronounced as the berm grew.

311. In Figure 35 distributions of the transport rate pertaining to Case 101 are shown (negative transport rate implies onshore transport). The transport rate decreased with time as the profile approached equilibrium

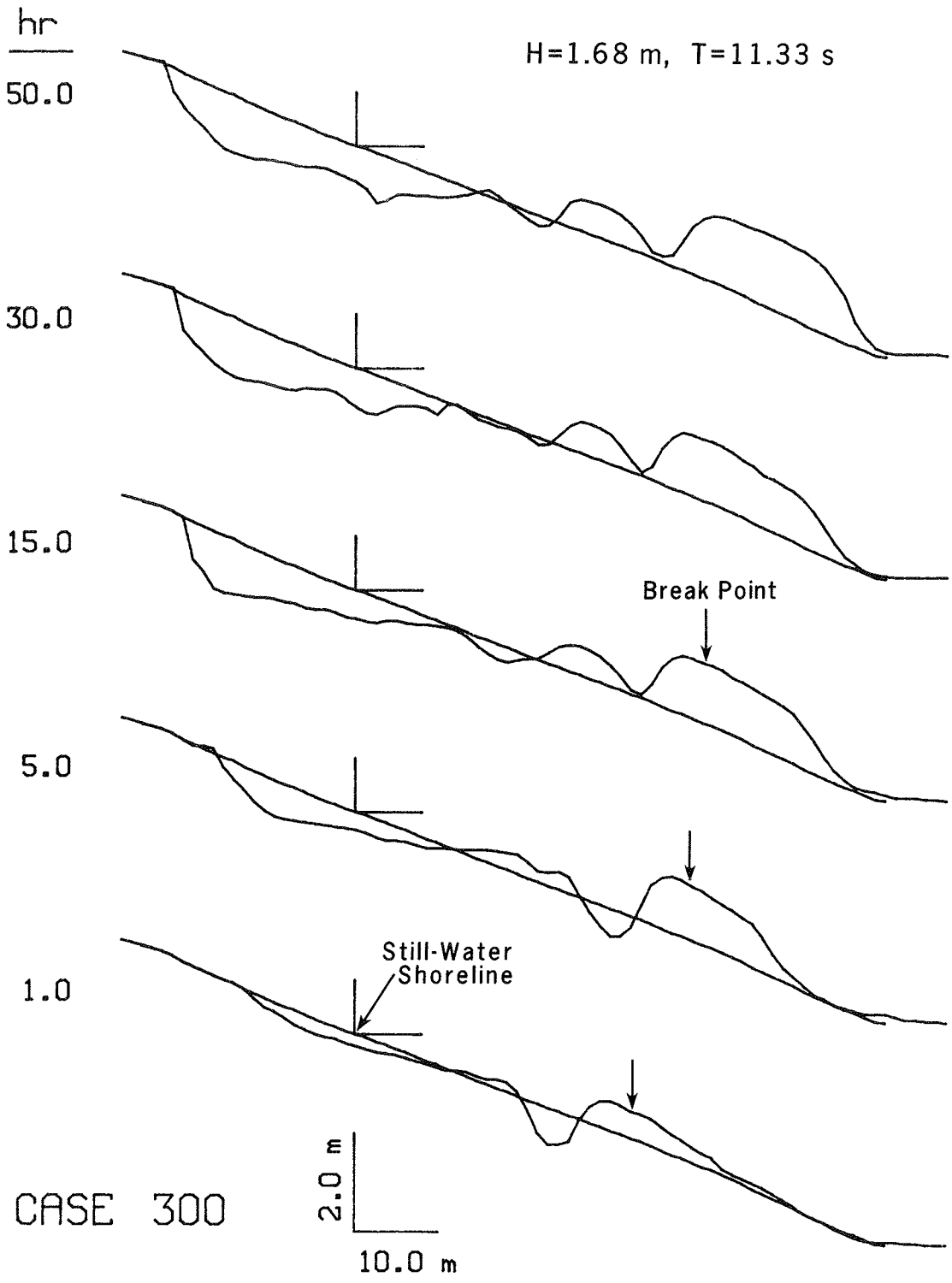

Figure 32. Evolution of beach profile under constant incident wave conditions for an erosional case (Case 300)

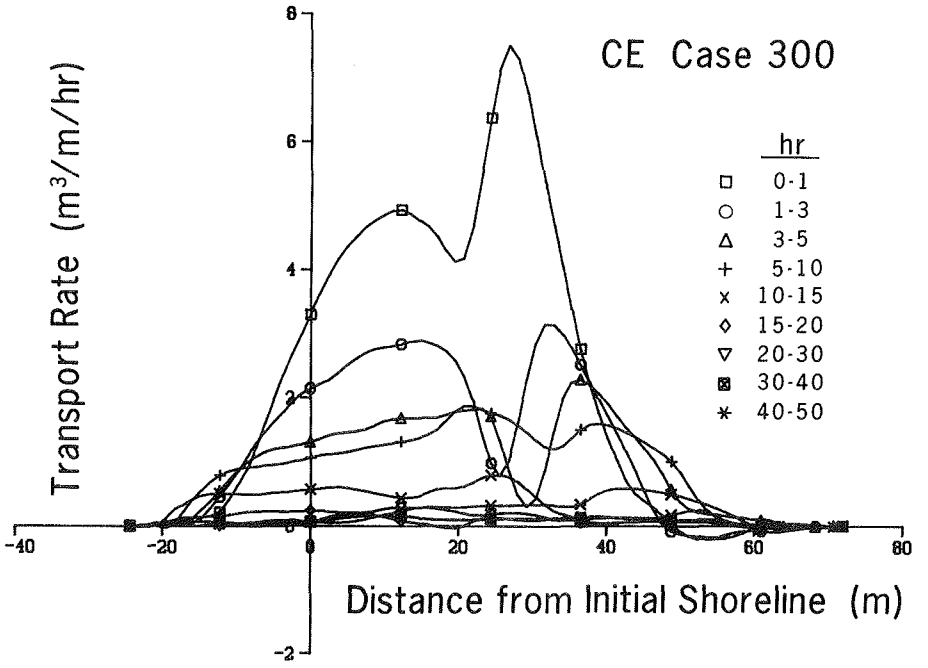

Figure 33. Calculated distributions of the net cross-shore sand transport rate for an erosional case (Case 300)

shape. Initially, the transport rate distribution showed a clear negative peak, but the shape of the distribution became smoother as the breakpoint bar approached equilibrium volume. Material was thus transported shoreward over the bar and deposited on the foreshore. The breakpoint bar was formed mainly by onshore transport and is seen as the minimum occurring in the first transport rate distribution. Similar to Case 300, the seaward part of the transport rate distribution may be well approximated with an exponential function decaying with distance in the offshore direction.

Classification of Transport Rate Distributions

312. Depending on wave conditions and sand size, the distribution of the cross-shore transport rate took a specific shape. Since the transport rate in this study is determined from consecutive profile surveys, calculated distributions represent an average net response of the profile and not the instantaneous transport rate. If the initial and final profiles from a

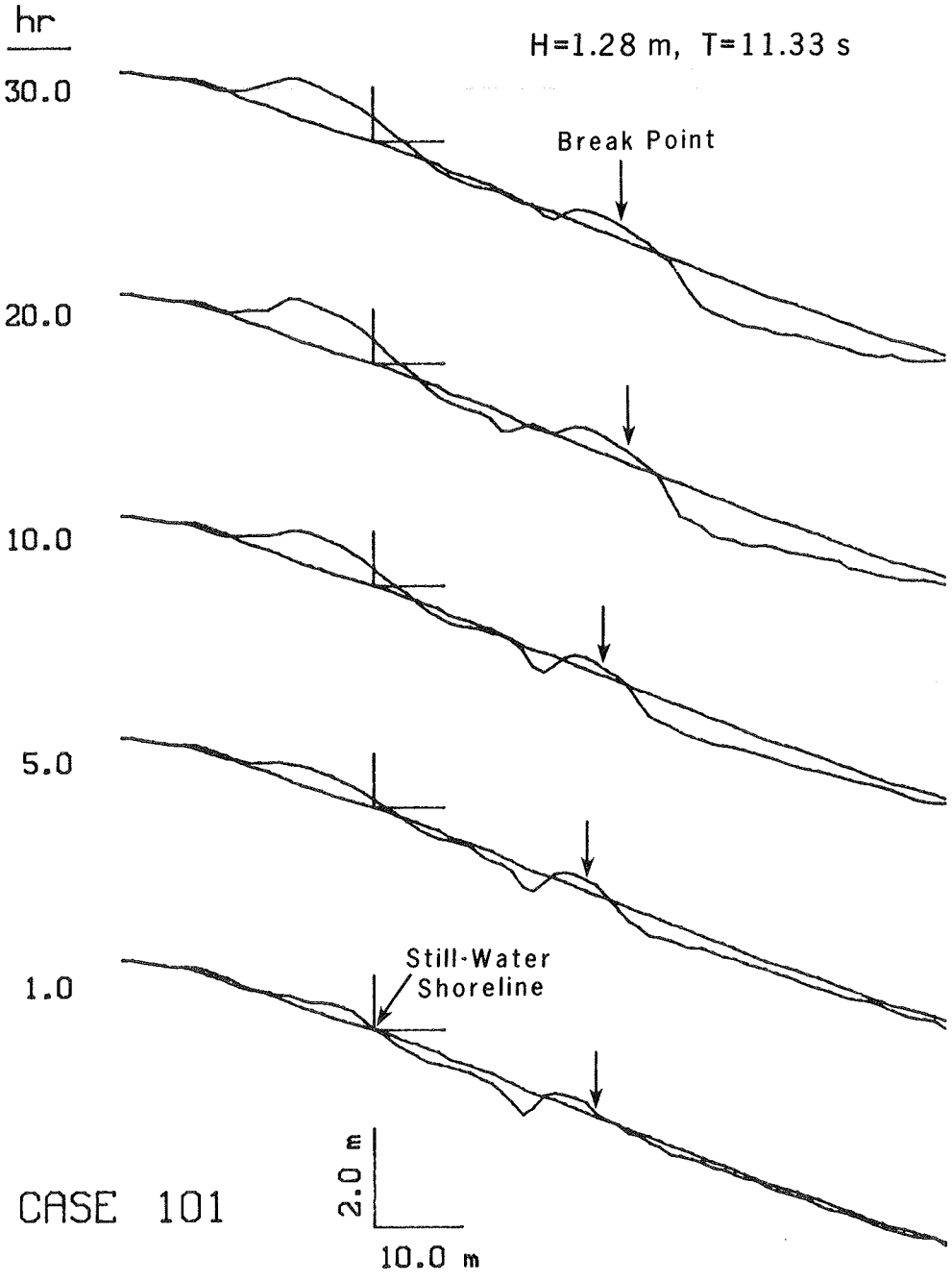

Figure 34. Evolution of beach profile under constant incident waves for an accretionary case (Case 101)

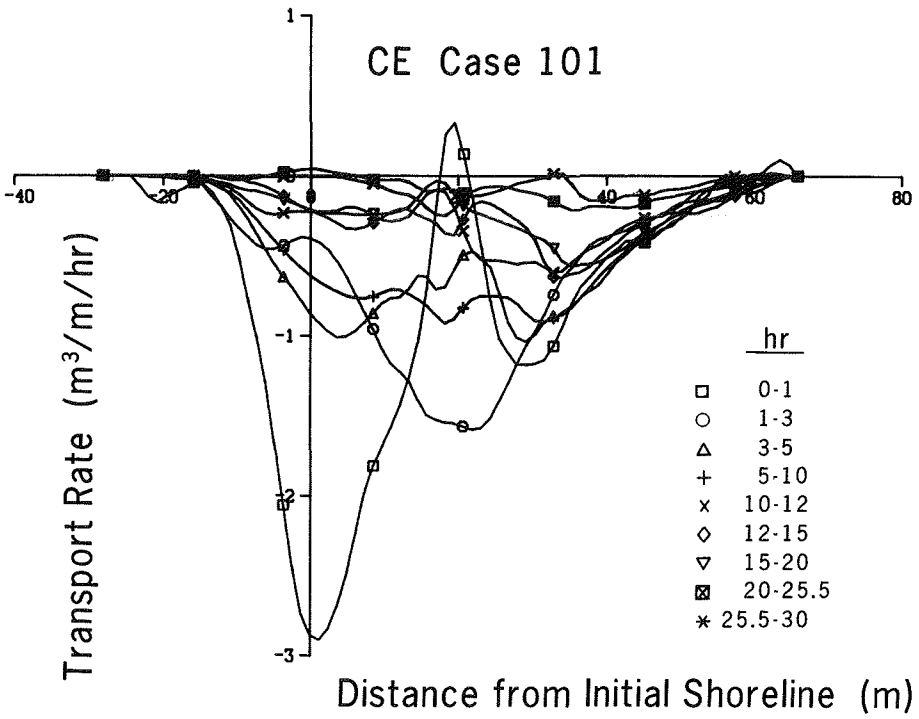

Figure 35. Calculated distributions of net cross-shore sand transport rate for an accretionary case (Case 101)

specific case are used to calculate the distribution of the transport rate, an overall picture of the profile response is obtained. The distribution determined from the initial and final profile surveys will be termed the "equilibrium distribution," although it is recognized that the final profile survey only approximates the actual equilibrium configuration and the time weightings are not equal between cases.

313. Based on this so-defined equilibrium distribution, a classification of net transport rate distribution shapes is more easily performed than if consecutive profiles in time are used. This description also indicates where the sand originated which supplied the bar and berm. For example, depending on the wave and sand properties, a bar may be formed from sand supplied from either its shoreward side or its seaward side or from both sides.

314. From the equilibrium transport rate distributions, three main shapes were identified, although general trends in the distributions often exhibited small perturbations. Figure 36(a-c) illustrates the three principal

distribution shapes calculated for three cases, CE Cases 300 and 101, and CRIEPI Case 3-2. Note that the cases shown from the CE data are identical to those presented in Figures 33 and 35, where the distributions of the net transport rates were given corresponding to consecutive survey times and not as equilibrium forms. The classification of transport rate distribution is closely related to criteria for distinguishing bar and berm formation (erosion and accretion). A barred profile is generally associated with erosive conditions, implying offshore transport, whereas a profile with berm buildup mainly experiences onshore transport. However, in some cases where a bar formed, even though much of the material composing the bar was eroded from the foreshore, onshore transport from the region seaward of the bar also contributed.

315. The equilibrium transport rate distribution, illustrated by Case 300, is called Type E (Erosional) and is characterized by transport in the offshore direction along the full extent of the active profile. A positive derivative in the transport rate with respect to the cross-shore coordinate indicates local erosion of the profile, whereas a negative derivative indicates local deposition. At locations where the derivative is zero, the depth was constant and material was simply conveyed through the point. A minimum or maximum in the equilibrium distribution of the transport rate pertains to a morphologic feature along the beach profile. Cases where the transport was directed offshore along the entire profile are by definition subject to strong erosion, giving rise to one or more breakpoint bars. For larger grain sizes, the width of the peak of the equilibrium transport rate distribution decreased for the same wave conditions, indicating that the major part of the sand movement was concentrated in a narrow portion of the profile. This concentration is caused by the requirement for greater energy dissipation to achieve the equivalent transport condition for beaches composed of larger sand grains.

316. For the second main type of equilibrium transport rate distribution, exemplified by Case 101 and called Type A (Accretionary), transport is directed onshore along the full extent of the active profile. The distribution is in essence the mirror image, through the cross-shore coordinate axis, of the Type-E distribution. In general, however, any secondary minimum in the

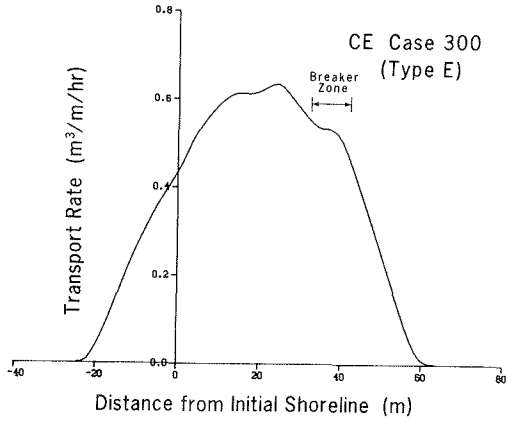

a. Type E, Erosional

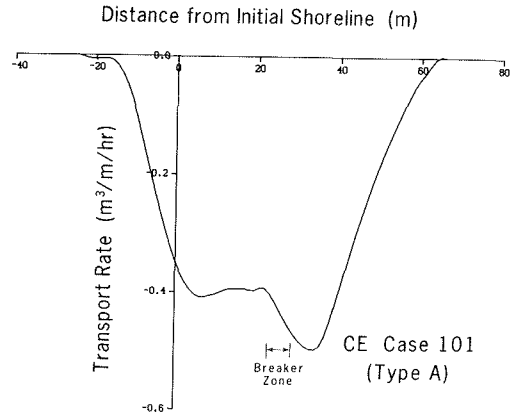

b. Type A, Accretionary

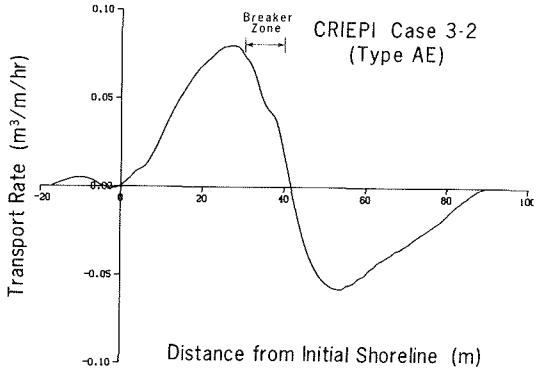

c. Type AE, Mixed Accretionary and Erosional

Figure 36. Net cross-shore sand transport rate distributions

transport rate distribution is more pronounced than for Type E, related to the small bar frequently present and located slightly shoreward of the break point on accretionary profiles. The onshore-directed transport gives rise to a berm on the foreshore.

317. The third main type of equilibrium transport rate distribution, Type AE, and typified by Case 3-2, is characterized by one peak with offshore-directed transport occurring on the foreshore and another peak with onshore-directed transport located seaward of the break point. Thus, the bar receives contributions of material from both offshore- and onshore-directed transport. The Type-AE equilibrium transport rate distribution is characteristic of bar profiles which were closer to the dividing line between bar/berm profiles than profiles associated with Type-E distributions. Figure 37 illustrates profile evolution for CRIEPI Case 3-2, which is a typical example resulting from mixed accretionary and erosional (Type AE) transport distributions.

318. Of the 33 cases examined, 29 were easily classified as having Type A, E, or AE equilibrium transport rate distributions (15 E-type, 10 A-type, and 4 AE-type). In some cases, particularly when the change in beach profile was small (i.e., the beach profile almost stable under the incident waves), the distributions take on a more complex form with multiple peaks for onshore- and offshore-directed transport appearing along the profile. If the beach profile is close to an equilibrium shape under the incident waves, it is expected that the transport rate distribution will not show such a strong net overall trend as compared to a profile that is far from equilibrium with the imposed waves. Distributions rarely occurred having a peak for onshore-directed transport on the foreshore and a peak for offshore-directed transport located more seaward, and then only if minor changes in the profile occurred.

319. Kajima et al. (1983a) proposed a classification, similar to that developed in this study, in which three basic distribution types and two subdivisions were defined. One of their main distributions differs from that presented here. Their distribution corresponding to Type AE has a peak with onshore-directed transport located shoreward of the peak with offshore-directed transport which is opposite to the present classification. The two subdivisions each contain three peaks, varying in direction onshore and offshore. Sawaragi and Deguchi (1981) derived distribution shapes from

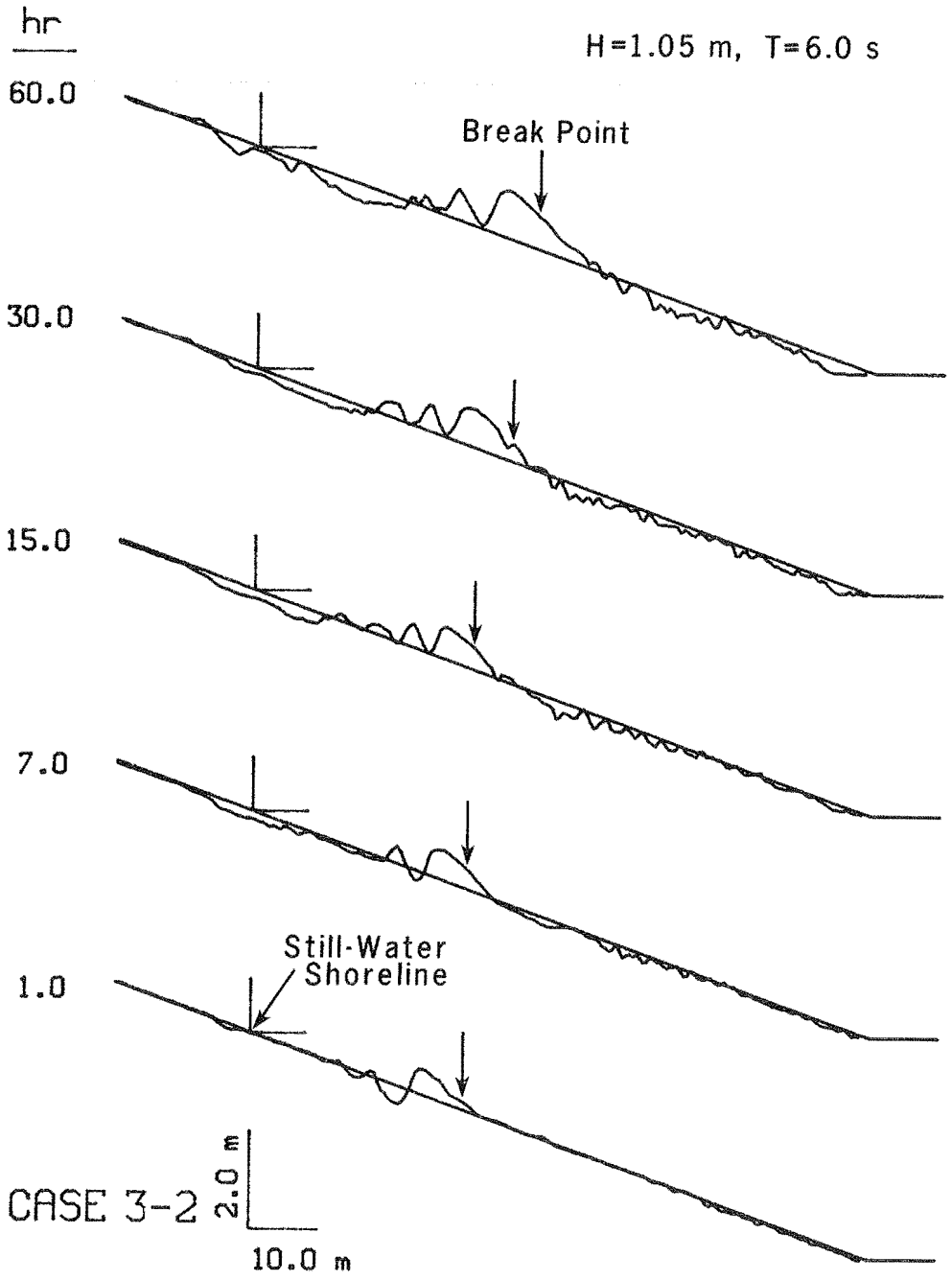

Figure 37. Evolution of beach profile under constant incident wave conditions for a mixed accretionary and erosional case (Case 3-2)

schematic profile shapes identified by Sunamura and Horikawa (1975). Their classification is also similar to the two mentioned above.

320. A factor that may influence profile development and net transport rate distribution is the limited depth in the horizontal section of the tanks in the CE and CRIEPI experiments. The effect is judged to be relatively minor since the depth in the horizontal section was at least 2-3 times the wave height in that part of the tank. Nevertheless, it is probable that some amount of onshore transport would have occurred if the depth and movable bottom had not been limited for those cases having transport distribution Type E. In any case, such a contribution would probably be small compared to the amount of material eroded from the foreshore.

321. Aubrey (1979) studied long-term exchange of material across the profile in the field. He applied empirical eigenfunction analysis to determine characteristic bar and berm profiles (prevalent during the winter and summer, respectively) and discovered two pivotal points where the profile depth was effectively constant. One pivotal point occurred for the studied beach at 2 to 3-m depth and the second one at 6-m depth below mean sea level. The seasonal volume exchange over the two pivotal points had a relation of 1 to 5, with the largest exchange taking place over the pivotal point closest to shore. This occurrence indicates that, in a long-term perspective during which weak onshore movement of sand may give a finite contribution, material exchange in deeper water is much less than that in the nearshore. For a single storm event giving rise to bar formation simulated in the LWT experiments, the ratio between the sand transport rate from the seaward and shoreward sides of the bar should be small.

Approach to Equilibrium

322. As a beach profile approaches an equilibrium shape dictated by the incident waves, the net cross-shore transport rate decreases to approach zero at all points along the profile. By studying a relevant quantity related to the transport rate distribution at consecutive times, a picture of the approach to equilibrium can be attained. The peak onshore or offshore transport rate along the profile is a candidate quantity which might be

considered for examining the decay of the transport rate distribution with time. However, since the shape of the transport rate distribution also varies with time, a peak transport rate may not be the best overall indicator. Instead, the average absolute transport rate Q_A along the profile was used since it provided a better measure of all transport activity along the profile. The average absolute transport rate was calculated as

$$Q_A = \frac{1}{x_1 - x_o} \int_{x_o}^{x_1} |q| \, dx \tag{19}$$

where x_1 is the seaward limit of profile change.

323. Figure 38(a and b) shows the decay of Q_A with time for the CE and CRIEPI experiments. The general trend was for rapid decay during the first 10 hr, followed by a slower decrease with elapsed time. The approach to zero transport was slow at longer elapsed time since small adjustments in the profile occurred even if the profile had attained a near-equilibrium shape.

324. In many of the CRIEPI cases, Q_A was small from the beginning of the run, since the initial beach profile was close to the equilibrium shape. The maximum occurring for one of the CE cases (Case 700), just before 20 hr, approximately coincided with a decrease in wave height that took place during the experiment (Kraus and Larson 1988a), forcing the profile toward another equilibrium condition. The general conclusion made based on Figure 38(a and b) is that the equilibrium concept is valid and that a numerical model developed for simulating realistic beach profile change must include this property.

Peak offshore transport

325. To quantify the time decay of the transport rate distribution as a function of wave parameters and sand size, the peak onshore or offshore transport rate is a good target quantity since the peak rate has a clear physical meaning. Figure 39 plots the peak transport rate as a function of time for 16 of the CE cases. For cases with strong erosion, decay with time of the peak offshore transport rate was much more pronounced than for cases with mainly accretion on the foreshore. If onshore transport prevailed, the